Doctor Thesis

Evaluation of Atmospheric Corrosion in Steels for Corrosion Mapping in Asia

(アジアにおける腐食環境マップ作成に向けた鋼の大気腐食評価に関する研究)

Graduate School of Engineering

Yokohama National University

Dara TO

September 2017

PREFACE

This dissertation is submitted in partial fulfillment of the requirements for the degree of Doctor of Engineering, in the graduate school of engineering, Yokohama National University. The research described the behaviors of atmospheric corrosion under the title of "*Evaluation of Atmospheric Corrosion in Steels for Corrosion Mapping in Asia*".

The dissertation introduces a new method to predict corrosion kinetic through Atmospheric Corrosion Monitoring (ACM) sensors based on galvanic cell technique. The most valuable output of this research is the classification of corrosivity categories and the exploration of atmospheric corrosion data mapping in Asia atmospheres. The mathematical models for corrosion estimation were also made in function of environmental parameters. The results of the research are the great references, which provides necessary information for material selection and protective method against atmospheric corrosion in the stage of design and construction; and particularly, leading to service life prediction of metal structures and equipment.

Some parts of this work have been presented in the following publications:

- Dara To, Tadashi Shinohara, Osamu Umezawa, International Journal of Research in Engineering and Technology, Vol. 5, Issue 8, pp. 382-387, (2016.8).
- Dara To, Tadashi Shinohara, Osamu Umezawa, ECS Transactions, Vol. 75, Issue 29, pp. 1-10, (2017.1.20), doi:10.1149/07529.0001ecst, Eds. A. Nishikata, M. Sakairi, I. S. Cole, C. Leygraf, R. Srinivasan, E. Tada, H. Katayama, M. Itagaki, PRiME 2016, (2016.10).
- Dara To, Tadashi Shinohara, Osamu Umezawa, ISSN 0892-4228.Corrosion Engineering, Vol. 66, No. 2, pp. 39-42, (2017).
- Dara To, Tadashi Shinohara, Osamu Umezawa, 材料と環境 (ZAIRYO-TO-KANKYO), Vol. 66, No. 4, pp. 131-135, (2017.4).

Dara To
Graduate School of Engineering, Yokohama National University
2014 ~ 2017

ACKNOWLEDGEMENTS

First of all, I am very grateful to my supervisor, Prof. Osamu Umezawa, for his best attempt, kindly help, warm observing, and especially a very high supporting effort to qualify the requirement for my Ph.D. graduation at the Yokohama National University. I would like to express my sincere gratitude to my research project leader, Dr. Tadashi Shinohara, National Institute for Material Science (NIMS), for his valuable guidelines, encouragement, and commitment. I greatly appreciate his effort for supporting me during three years of my study in NIMS. He truly exemplifies the merit of technical excellence and academic wisdom. I also thank Professors: Shoichi Hirosawa, Wataru Nakao and Makoto Hasegawa for their advice.

I wish to acknowledge Dr. Norimitsu Koga, for his cooperation and useful information concerning the academic issue. I would like to pass my gratefully acknowledgement to the experts who were involved in the validation research project (*Corrosion Mapping of Structural Materials in Asian Area with Understanding Effects of Environmental Factors)*: Dr. Tadashi Shinohara (Group leader), Dr. Hong Lien Le (Researcher, Institute of Materials Science, Vietnam), and Dr. Amnuaysak Chianpairot (Researcher, National Metal and Materials Technology Center, Thailand). Without their passionate participation and input, the validation survey could not have been successfully conducted.

Finally, I would like to offer my special thanks to the supporting Japanese government, Ministry of Education, Culture, Sports, Science, and Technology, for the valuable scholarship for studying and living in Japan. I also wish to thank all Yokohama National University officers and International Student Support Section for their cooperation in the academic organization and living consultant.

Dara To
Graduate School of Engineering, Yokohama National University
2014 ~ 2017

ABSTRACT

Abundant information on the atmospheric corrosion of metal, in both long-term and short-term exposure tests, have been published in the scientific literature. Those corrosions data were evaluated and bounded as ISO standards. Since those standards were made based on the European atmospheres, they might not be applicable for Asia atmospheres. To rectify such unfortunate situation the atmospheric corrosion mapping of structural materials in Asia area has been conducted under "E-Asia project"; It is the research cooperation between Japan (16 exposure test sites), Vietnam (14 exposure test sites), and Thailand (7 exposure test sites), which is supported by Japan Science and Technology Agency (JST). The environmental parameters such as Relative Humidity (RH), Time-Of-Wetness (TOW), Temperature (T), and chemical substances (SO_2 and Cl) were taken into account. The Atmospheric Corrosion Monitoring (ACM) sensors were also used to investigate the atmospheric corrosion behaviors for most of the exposure test sites. The artificial rainfall equipment was also developed and used to study the effect of chemical species and its concentration on the ACM sensors outputs and corrosion mass loss. The morphologies of corrosion product layers were also investigated by Scanning Electron Microscopy (SEM), X-Ray Diffraction (XRD), and Energy Dispersive Spectroscopy (EDS). The results revealed that the atmospheric corrosion behaviors in Asia region are somewhat different from the ISO standards. It was found that the critical temperature for the maximum corrosion attack is about 20 ^{o}C, while the ISO 9223 suggested 10 ^{o}C is the critical temperature. Moreover, there was a mismatch between the Corrosion Rate (CR) measured from the actual exposure test sites and the CR calculated based on the mathematical formula, called "*Dose-response functions*", suggested by ISO 9223. In this research, a new mathematical formula for calculating CR in Asia region was proposed based on the environmental parameters, and the actual CRs investigated in Asia environment. And the corrosivity category classification was also made for each environment of each country.

Keywords: *Atmospheric corrosion, corrosivity category classification, corrosion rate, corrosion product, air pollution, chemical species, Atmospheric Corrosion Monitoring (ACM) sensor, surface roughness.*

TABLE OF CONTENTS

LIST OF FIGURES

LIST OF TABLES

LIST OF SYMBOLS AND ABBREVIATIONS

- b: Constant coefficient that characterizes the protective property of corrosion products.
- c: Molar concentration (mol/L)
- COR: Total corrosion loss (mm or g/cm^2)
- CR: Corrosion Rate (mm/y or g/cm^{2}d)
- D: the corrosion loss of metal (mass loss per unit area or thickness loss)
- I: Sensor output (μA)
- Ku: Kurtosis of profile
- m: mean line profile
- Pr: Annual precipitation rate (mm/y)
- Ra: Arithmetic mean values
- r_{corr}: a constant coefficient of initial corrosion loss over the first year of exposure time (mm/y)
- RH: Relative Humidity (%)
- Rq: root mean square of profile
- Sk: Skewness of profile
- Sa: Surface root mean square
- Ssk: Surface Skewness
- Sku: Surface kurtosis
- TOS: Annual time of sunshine (h/y)
- TOW: Time of wetness (h)
- t: the exposure time
- σ: standard deviation or variance
- σ: Electrical conductivity (μs/cm)

CHAPTER 1

Chapter 1: Introduction to the Atmospheric Corrosion

1.1 Cost of Atmospheric Corrosion

Metal, especially steel, has been widely used for structural construction and equipment due to their cost, strength, facility, and recyclability. Most of the steel productions are subjected to the outdoor used, often in the highly polluted atmosphere where corrosion is much more severe than those in the rural or clean environment. Corrosion is the degradation of a material's properties or mass over time due to environmental effects. It is calcified as one of the most costly problems in societies, especially in the industrial and infrastructure sector. The serious consequences of the atmospheric corrosion have become a problem of worldwide significance. In our everyday life, corrosion causes plant shutdowns, waste of valuable resources, and reduces performance efficiency, costly maintenance, and expensive overdesign. In some countries where corrosion loss has been surveyed, the economic loss was about 1-5% of GNP (Gross National Product) [1], [2]. According to the first report of the cost of corrosion in Japan, which has been published in 1977, the economic loss caused by corrosion, which did not include the indirect loss, was about 1-2 percent of GNP. About two decades later, in 1997, a Survey of Corrosion Cost in Japan was conducted; based on the In/Out method the total corrosion loss (direct + indirect) was accounting for 3-4 percent of GNP [3]. Since then, the atmospheric corrosion issue has been becoming an important topic, which was brought to public attention concerning with the stages of design, construction, and maintenance process of metal structures.

1.2 Catastrophic of Corrosion Damage

In general, the problems of corrosion of metal structures are the uniform corrosion (for carbon steel), pitting corrosion (for steel), stress corrosion cracking (for high-strength material), corrosion fatigue (high-strength material)…etc. Frequently these problems can result in some portion of plants stop working or even shutdown of the

entire structure because of unexpected corrosion failure. The failure can also lead to human injury or even loss of life. The followings are the corrosion failures of metal structures recorded in the corrosion histories:

- *Leakage of Radioactive Liquid at the Fukushima Nuclear Power Plant:* The failure of Fukushima nuclear power plant on March 11, 2011, was a huge industry lost. The 9.0 magnitude earthquake and tsunami caused a meltdown of nuclear power plan. Four nuclear reactors were emitting radiation. The Tokyo Electric Power Co. (Tepco), the company that owns the plant, injects water to keep them cool. In August 2013, 300 tons of radioactive liquids leaked from a storage tank. The Nuclear Regulation Authority considered the leakage as the worst accident at Fukushima since the earthquake and tsunami in 2011 caused reactors to melt. The Tepco concluded that the tank leak was probably caused by corrosion around faulty seals [4].

- *The Collapse of the Silver Bridge (Point Pleasant, West Virginia, US)*: On December 15, 1967, a steel structure bridge, called the Silver Bridge, collapsed into the Ohio River while it was full of rush-hour traffic, and resulting in the deaths of 46 people. The collapse of the entire structure was due to a defect in a single link, eye-bar 330, of suspension chain structure as saw in Fig. 1. The eye-bars were made of heat treated medium-high carbon steel which usually strong but brittle; it is acceptable to crack from atmospheric corrosion. A small crack was formed on the eye-bar during casting. Over the years, stress corrosion and corrosion fatigue allowed the crack to grow in that corrosive environment. The crack was only about 0.1 inches (2.5mm) deep when it went critical, and it broke in a brittle fashion [5][6].

- *Sewers explosion in Guadalajara 1992, Mexico:* A series of explosions, happened on April 22, 1992, in Guadalajara, Mexico, killed over 200 people and damaged about 1,000 buildings along 8 kilometers of Gante Street. The estimation of monetary loss, caused by this catastrophe ranged between $300 million and $1 billion. The explosions were due to gas leakage resulting from corrosion damage of the underground gasoline pipeline [7]. A subsequent investigation found that the new water pipeline, made of zinc-coated iron, was built too close to an existing steel

gas pipeline as seen in Fig. 2. Underground humidity caused these materials to create an electrolytic reaction leading the pipelines to corrode, creating a hole in the pipeline that permitted gas to leak into the ground and the main sewer pipe.

- *The Aloha airline accident record:* On April 28, 1988, 19 years old Boeing 737, operated by Aloha airline had an accident. A portion of the tore loose and caused an explosive decompression of the aircraft at the first-class ceiling, in full flight at 24,000ft [8][9] as seen in Fig. 3. The National Transportation Safety Board attributed the incident was caused by the failure of the operator's maintenance program to detect corrosion damage at the lab joints of the aircraft skins, leading to corrosion-accelerated fatigue [10]. However, the flight landed safely, but several passengers received serious injuries.

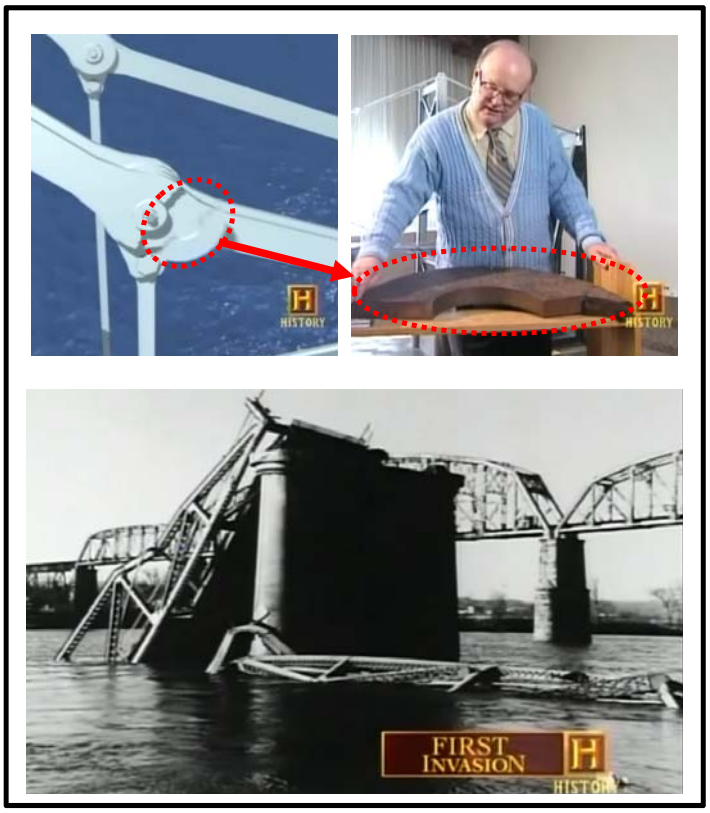

Fig. 1- Collapse of the Silver Bridge caused by of atmospheric corrosion [6].

Fig. 2- Explosion in Guadalajara caused by corrosion of gasoline pipeline [11].

(a) Failure of Boeing 737 at the upper fuselage *(b) Lab joints upper fuselage*

Fig. 3 - Corrosion failure of Boeing 737 on April 28, 1988 [8].

1.3 Forms of Corrosion

The corrosion failures have been increasingly important in this modern society with the growing of metal structure constructions. The failure analysis process is needed for observing the cause of the problems. In general, forms of corrosion failure are the essential aspect of a comprehensive investigation.

The commonly known of eight basic forms of corrosion was established by Fontana [12]. The forms of corrosion representing the corrosion phenomena categorized based on their appearances as shown in Fig. 4.

- ***Uniform Corrosion:*** The uniform corrosion, or general corrosion (Fig. 3 (a)), is the most common form of corrosion that typically proceeds uniformly over the entire expose the surface of the metal, especially carbon steel. The uniform corrosion attacks a metal structure by decreasing metal surface until failure. However, uniform corrosion is relatively easy to measure and predict, making sudden failure very rare.
- ***Pitting Corrosion:*** Pitting is a form of extremely localized corrosion attack that results in cavities or holes on the surface of the material(Fig. 3 (b)). The attacks can proceed rapidly and deeply at some tiny spots, while the vast area of the metal surface remains free from corrosion. Pitting is one of the most destructive attacks and more dangerous than uniform corrosion because it is difficult to observe and predict since the corrosion product often covers the pits. Pitting corrosion occurs when discrete areas of a material undergo rapid attacks while most of the adjacent surface remains virtually unaffected [13].
- ***Crevice Corrosion****:* Crevice corrosion refers to the corrosion occurring in confined spaces where the access of working fluid from the environment is very limited (Fig. 3(c)). It is usually associated with a stagnant solution, on the microenvironmental level. The stagnant tend to occur in a crevice or shielded areas like those formed under gasket, washer, insulation material, fastener head, disbonded coating, threads…etc. Because the oxygen diffusion into the crevice is limited, the differential aeration cell tends to be set up between crevice (microenvironment) and the external surface (bulk environment). And thus the anodic reaction proceeds in a concentration cell, leading to the high-localized attack. The failure of aircraft skins at lab-joints, as shown in section 1.2 (Fig. 3), is an example of the crevice corrosion attack.
- ***Galvanic Corrosion:*** Galvanic corrosion, sometimes called be metallic corrosion, refers to the corrosion damage induces when two dissimilar metallic materials are brought into contact in the presence of electrolyte; thus, electrochemical corrosion cell is set up (Fig. 3(d)). When a galvanic couple forms, one of the metals in the couple becomes the anode, and it will

corrode faster than it would be all by itself, while the other becomes the cathode and corrodes slower than it would alone.

- ***Erosion Corrosion:*** Erosion corrosion is the cumulative attack induced by electrochemical reactions and mechanical effects from relative motion between the electrolyte and the corroding face (Fig. 3(e)). Erosion corrosion is defined as accelerated degradation in the presence of this relative motion. Erosion corrosion is found in systems such as piping, elbows, joints, valves, pumps, nozzles, heat exchangers, turbine blades, baffles…etc.
- ***Selective Leaching:*** Selective leaching refers to the removal of one element from a solid alloy by corrosion processes (Fig. 3(f)). A typical example is the selective removal of zinc in brass alloys (dezincification). It can occur with other alloys in which aluminum, iron, cobalt, chromium and other elements are removed.
- ***Intergranular Corrosion:*** The microstructure of metallic materials is made up of grains, separated by grain boundaries. Intergranular corrosion is localized attack along the grain boundaries, while the bulk area of the grains remains unaffected (Fig. 3(g)). The situation can happen when the grain boundaries are depleted. For stainless steels, the intergranular attack is usually the result of chromium carbide precipitation at grain boundaries, which produce a narrow zone of chromium depletion at the boundaries due to heat treatment or welding.
- ***Stress Corrosion Cracking (SCC):*** SCC is the combined interaction of mechanical stress (above the critical value), and corrosion reaction in the corrosive environment; which leads to form a micro-crack then propagate (Fig. 3(h)). The SCC can proceed unexpectedly and rapidly, leading to catastrophic failure. To control SCC is to select a material with a proper service environment. Normally, high strength steel is susceptible to hydrogen, stainless steel susceptible to chloride, and brass susceptible to ammonia.

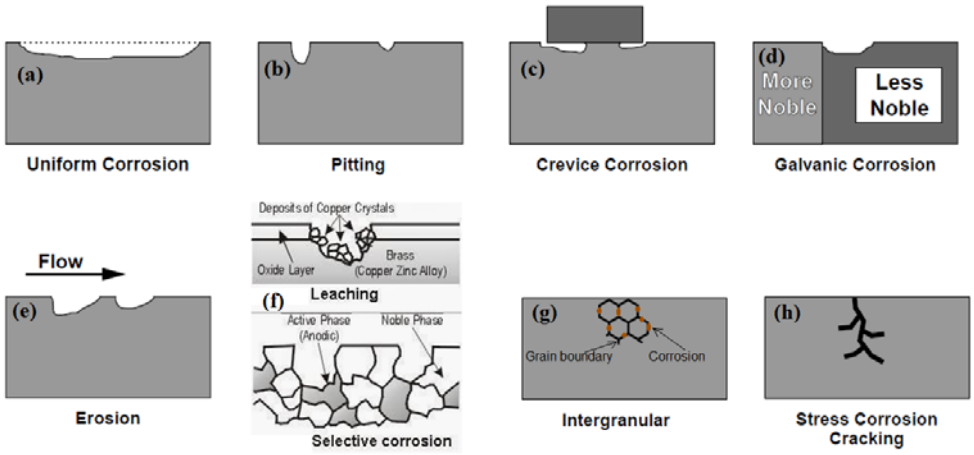

Fig. 4 - Eight form of corrosion [13].

1.4 Atmospheric Corrosion Behaviors

1.4.1 Corrosion Mechanism

Most of commonly used of metals are unstable in the atmosphere, except gold and platinum that are already in their metallic stable state. These unstable material's compositional elements have natural tendency to return to their most thermodynamically stable state by atmospheric corrosion reactions while they are exposed to the atmosphere. The word atmospheric corrosion stands for material or metal deterioration or surface damage in an aggressive outdoor-environment. It is a very complicated process caused by a chemical or electrochemical reaction between a metal and its environment. In general, atmospheric corrosion initiates and develops under the presence of water films formed by fog, dew, or raindrop. The films are considered as surface electrolyte layer since they have their own conductivity for electrons to transfer. An electrolyte is a conductive solution, which contains positively and negatively charged ions called cations and anions, respectively. An ion is an atom that has lost or gained an electron and carries an electrical charge. Thus, the corrosion process can be chemical in nature or electrochemical due to current flow, which requires at least two reactions, called anodic and cathodic reactions, to occur in a corrosive environment. The reactions of atmospheric corrosion of a metal *M* in aqueous media are presented as below:

Anodic reason: $M \rightarrow M^{z+} + ze^{-}$ (1)

Cathodic reaction: $\frac{z}{4} O_2 + \frac{z}{2} H_2O + ze^- \rightarrow zOH^-$ (2)

These equations indicate that an anodic reaction, known as oxidation, loss metal electrons while the cathodic reaction accepts or gains electrons, known as reduction. Consequently, both anodic and cathodic are dependent reactions in a corrosion process.

In the case of steel or iron in contact with an electrolyte solution, the oxidation and reduction reactions are written as below:

Anodic reason: $Fe \rightarrow Fe^{2+} + 2e^-$ (Oxidation) (3)

Cathodic reaction: $\frac{1}{2} O_2 + H_2O + 2e^- \rightarrow 2\,OH^-$ (Reduction) (4)

In the anodic reaction, each Fe atom loses two electrons, which are occurring at the metal/solution interface as saw in the Fig. 5. A positive ion, called cation (Fe^{2+}), is ejected from the metal surface and goes to the electrolyte solution at the anodic site, while the two liberated electrons remain in the metal. Because H^+ has a natural tendency to accept an electron from the metallic iron, the cathodic reaction occurs. And those two reactions, anodic and cathodic reactions, occur spontaneously.

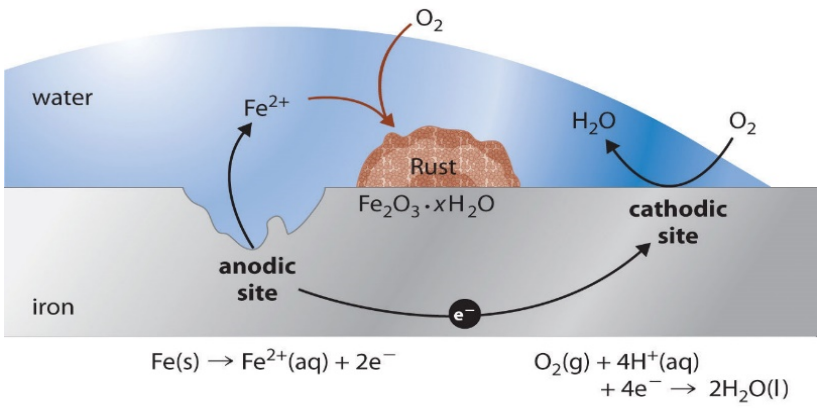

Fig. 5 - Schematic illustration of corrosion mechanism [14].

1.4.2 Atmospheric Corrosion Parameters

It is well known that atmospheric corrosion is an electrochemical process, which can only proceed in the presence of an electrolyte, or aqueous solution. Pure water

is not very corrosive to most of the metals. Generally, the presence of dissolved ions can make the environment more reactive, causing atmospheric corrosion more severe by chemical attack. Thus, time of wetness, TOW, and chemical composition of surface electrolytes is the main factors affecting the corrosion kinetic.

- ***Time of Wetness, Tw:*** Time of wetness is the duration in which the metal surface is covered by the aqueous film, making corrosion happen. Rain, dew, fog, the temperature of the air and metal, and other factors affect the time of wetness. The T_w can be calculated based on the meteorological data, RH $\geq$ 80% and T$\geq$ 0 ^oC, where located near the atmospheric corrosion test station. However, this method might not achieve the exact time making corrosion possible since it also depends on the metal and environmental properties. The new and reliable method for measuring T_w is using an electrochemical device known as galvanic sensing probe such as atmospheric corrosion monitoring (ACM) sensor. These electrochemical devices produce the signal output only when sufficient electrolyte layer covers the electrodes to products corrosion current. The duration of this event is taken as T_w.
- ***Pollutants and Composition of Surface Electrolyte:*** The chemical species deposited from the atmosphere into the surface electrolyte is of great importance in determining Corrosion Rate (CR). Oxygen, sulfur dioxide, NO_x, and Cl^- are the corrosive ions that normally taken into account for atmospheric corrosion investigation.
- ***Oxygen:*** The penetration of oxygen from the air into the electrolyte layer increases the cathodic reaction, as seen in Eq (2). The thin electrolyte layer covering the metal surface saturated with O_2 resulting in high cathodic reaction rate, leading to high corrosion attack. And it has been proofed by many authors that the corrosion rates reach the maximum when the electrolyte layer becomes very thin (1 to 100 μm) [15]-[18].
- ***Pollutant Substances:*** The chemical substances like sulfur dioxide, and airborne salinity, Cl^-, are considered as the most aggressive species causing the breakdown of the passive oxide film and leading to corrosion initiation

and progression. Sulfur dioxide, a product of the combustion of sulfur, containing fossil fuels, plays a significant role in atmospheric corrosion in urban and industrial atmospheres. With moisture or aqueous media, the SO_2 is usually oxidized to form H_2SO_4 and results in acid rain or acid fog making the environment more aggressive, especially the regions close to the industrial zone. In the marine atmosphere, especially the region close to the shore, the Cl^- deposition is prominent, and it decreases with increasing distance from the shore.

1.5 Atmospheric Corrosion Prediction and Stage of Maintenance

Material and environmental parameters are the primary critical variables for corrosion prediction and maintenance process of the metal structure exposed to an outdoor environment. The performance of the structural concerns with the material selection process, which must be done in the primary stage of design based on the understanding of environmental parameters, and the appropriate maintenance process during service life. Even the best designs may not be supposed to anticipate all problems that may occur during the service life of a system. For this reason, an extensive task must be performed in corrosion control at the design stage and also in the operational phase.

1.5.1 Atmospheric Corrosion Prediction

For most of the structural materials, especially steel, the corrosion kinetic decrease with increasing exposure time as seen in Fig. 6. Several methods have been suggested to estimate the corrosion thickness reduction of metals and alloys. The methods are made based on the outdoor exposure test, mathematical model, and galvanic cell technique. These methods allow predicting the average thickness loss or mass reductions over time and thus giving an advantage to the primary step of service life estimation.

The most reliable method for atmospheric corrosion thickness loss is the long-term outdoor exposure test under the natural environment, which can be found in numerous textbooks and research publications, but this approach is time-consuming

and costly. Many efforts in long-term corrosion test have been made to develop and prove the mathematical model of corrosion kinetics in various types of atmosphere [2], [19]-[25]. The model is presented by the power function below:

$$D = r_{corr}\, t^{b} \quad (5)$$

Where:

- D: is the corrosion loss of metal (mass loss per unit area, (g/m^2), or thickness loss, (μ).
- t: is the exposure time, expressed year.
- r_{corr}: is a constant coefficient of initial corrosion loss over the first year, expressed in grams per square meter per year ($g/m^2.y$), or micrometers per year (μ/y).
- b: is the metal-environment-specific time exponent.

➢ ***The Initial Corrosion Rate (r_{corro})***

As stated by the ISO 9224 [23], the corrosion rates over the first year, r_{corro}, are the guiding values for atmospheric corrosivity categories classification. And those values can be calculated by the mathematical model, called *Dose-respond functions (ISO 9223*[26]), or measured from actual exposure test (1-year outdoor corrosion test) which is considered as the most reliable technique. These two techniques are applied in this research, and it will be discussed in detail in the chapter 4.

➢ ***Metal-environment-specific time exponent***

The exponent b depends on the metal and its environment where it is exposed to, usually less than 1. In case the long-term corrosion loss data are available, b value can be calculated from the data. In case the long-term corrosion loss data are not available, the b value can be selected from tables of ISO 9224. In a real application where the detail compositions of commercial material are not known, select B1 from the table of Appendix I. These B1 values were taken as the average time exponent from long-term corrosion test (IOS CORRAG atmospheric corrosion test program [26]). In safety reason, it is important to estimate conservative upper limit of corrosion thickness loss; the exponent b values used in the Eq (5) should be

increased to account uncertain data distribution. Thus standard deviation is added to the average values to obtain 95 % of confidence level [23]. The B2 values include two standard deviation addition for the upper limit of corrosion attack estimation. The B1 and B2 values are shown in Table II-1 (Appendix I). These are the *b* values to be used in Eq (5). Table II-2 provides the values of the function, t^b, up to 100 years for four types of metal.

The power function is, however, recommended to be used for estimating the thickness reduction that refers to the uniform corrosion. It is important to stress that the failure of metallic structures may be caused by another form of corrosion like pitting corrosion, bimetallic corrosion, or stress corrosion cracking…etc. These forms of corrosion are very complicated to estimate and predicted since the rust layer covers the surface crack. Thus the qualify maintenance should be taken into account during a lifetime in service.

1.5.2 Stages of Maintenance

Maintenance costs are a significant part of the total operating expenses of all manufacturing or production plants. The level of maintenance will vary greatly with the severity of the operating environment and the criticality of the engineering system. A proper maintenance procedure must be made to ensure the reliability of the metal structure throughout their entire life. There are three stages of maintenance needed for operating any structure or component: Preventive maintenance, Corrective maintenance, and Predictive maintenance.

- *Preventive maintenance* is referred to the regular checkup of the structure or equipment to prevent failure. For atmospheric corrosion prevention, the preventive maintenance must be performed on the initial stage of structural design including the material selection, corrosion passivation methods (painting, coating, galvanizing…etc), maintenance facility and schedule…etc.
- *Corrective maintenance* is a maintenance effort performed to identify or rectify the failure of elements of a structure so that the system can be returned to operational condition. For most of the engineering metals

structures, the failures of the elements are mostly caused by pitting corrosion, galvanic corrosion, and stress corrosion cracking (SCC), while that caused by the uniform corrosion is very rare since it is easy to detect and requires a simple method to observe.

- *Predictive maintenance* is made for the purpose of maintaining equipment in satisfactory operating condition by providing systematic inspection, detection, and correction of the incipient problems to prevent catastrophic failure. Inspection and detection technique for the measurement of corrosion ranges from simple visual examination to nondestructive evaluation. Compare to preventive and corrective maintenance; the predictive maintenance is very complicated that need the qualifying effort and technique; since the corrosion pits or cracks are usually invisible due to the formation of corrosion product layers covering the metal surface. Significant technological advances have been made for corrosion detection. For instance, the combined use of acoustic emission (AE) and ultrasonic (UT) allows inspecting an entire structure.

1.6 Research Literature

The atmospheric corrosion problems have been investigated since the last several decades. Due to the modern science and technology with a fast development and industrial growth; the atmospheric corrosion topic has been increasingly important and greatly impact on society.

There are various kinds of metals and alloys have been manufactured to be utilized for different purposes. For engineering metal structure, like carbon steels and alloy steels, chemical compositions are the notable difference that results in various mechanical strengths, its appearances, and corrosion resistances. The mechanical strengths and its appearances can be improved by various methods in the stage of structural design, but corrosion attacks cannot be avoided, just more or less. In the reason of improving the corrosion resistance of the material, its chemical compositions are crucial for research and investigation.

In 1910, it was found that alloy steel with 0.07% of Cu, manufactured by US steel, showed 1.5-2% greater atmospheric corrosion resistance than a conventional carbon steel [28]. In the following year, 1911, US steel started to manufacture steel sheet with a special focus on the Cu contain. The subsequent investigation showed that the Cu concentration in excess of 0.25% was insignificant in improving corrosion resistance. For most of the atmospheric corrosion test, the steels with 0.15% Cu provided similar results to those with 0.25% Cu [29]. Once the properties of copper steel become well known, further research on alloy steels started to expand, leading to develop and manufacture the weathering steel, known as Cor-Ten steel; the steels have high corrosion resistance (Cor) and tensile strength (Ten). The compositions of Cor-Ten steel are shown in *Table 1* [30]. According to the long-term exposure tests in an industrial atmosphere of Kearny, reported by Larrabee in 1961 [31], the corrosion resistance of weathering steel was much improved compare to Cu-bearing steel and plain carbon steel, as seen in Fig. 6. The corrosion thickness losses were very severe at the initial few years of exposure test; thereafter, it transited to reach a steady condition for all materials. The corrosion kinetic of weathering steel was seen to be very low in the steady condition, while that of Cu-bearing steel and plain carbon steel was relatively high. For long-term corrosion attack, the formation of rust layers can insulate the metals surfaces from its environment, leading to low corrosion attack, especially the rust form on weathering steel.

Table 1 – Chemical composition of weathering steel [30].

Grade	C	Si	Mn	P	S	Cr	Cu	V	Ni
Cor-Ten A	0.12	0.25-0.75	0.20-0.50	0.07-0.15	0.03	0.50-1.25	0.25-0.55		0.65
Cor-Ten B	0.16	0.30-0.50	0.80-1.25	0.03	0.03	0.40-0.65	0.25-0.40	0.02-0.10	0.4

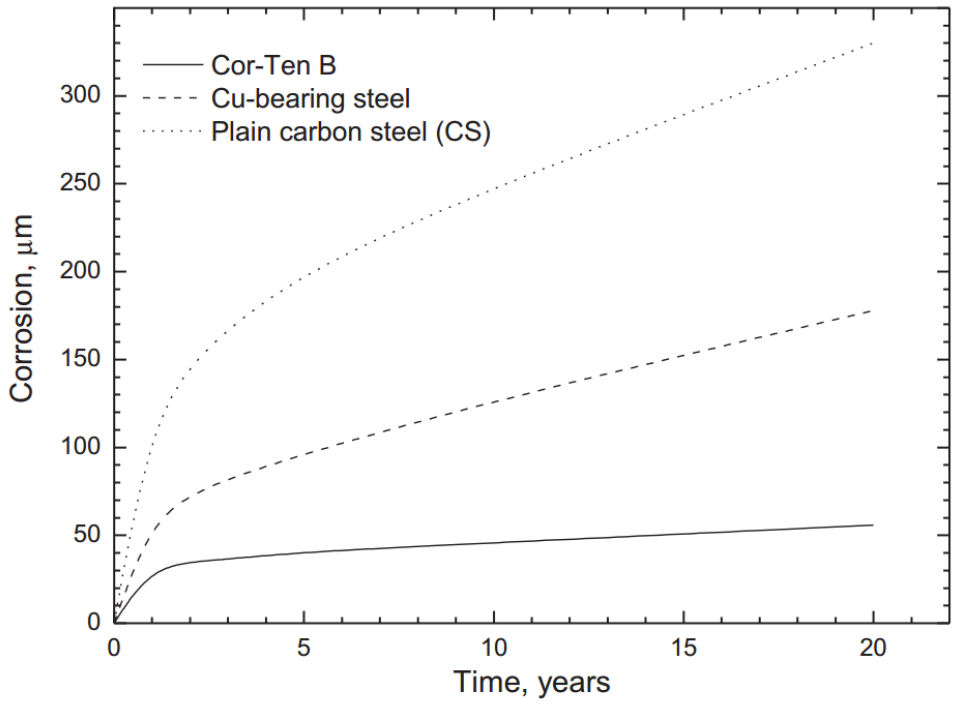

Fig. 6 - Comparison corrosion kinetics of weathering steel (Cor-Ten B), Cu-bearing steel, and carbon steel [31].

Since then, weathering steels have been recommended to be utilized in the weathers or outdoor atmospheres without any painting method is required, because the formation a compact and well-adhering of rust layer plays a role as corrosion resistance, known as patina [19]. However, the physical appearance of the patina layer is somewhat not preferable. In some application painting and galvanizing materials are needed. Thus, weathering steels, carbon steel, and other alloy steels are mostly used in engineering metal structures due to the cost, strength, appearance, and facilities in constructions. Accordingly, many types of research have been made to overcome the atmospheric corrosion problems for estimating the corrosion attack for various kinds of those materials. Lately, the great effort has been done to achieve the ISO standards for corrosion measurements, categories classification, and guiding for long-term corrosion estimation [26]-[34]. And these international standards have been widely used as research references.

Fuente, et al. investigated a long-term of atmospheric corrosion of mild steel exposed to rural, urban, industrial, and marine atmospheres in Spain for

characterizing the corrosion rust layer and corrosion rate. It was found that the crystal structures of corrosion products vary with atmospheres where it was exposed. Corrosion attacks were more severe in industrial and marine atmospheres, and less so in the urban and rural atmospheres. In all cases, the corrosion rates were considered to decrease with exposure time [20].

Hong Lien, et al. studied the atmospheric corrosion of carbon steels and zinc-galvanized steel at 6-8 testing stations in Vietnam for about 10-years exposure test (1995-2005). The study was carried out by taking a special focus on the effect of environmental parameters. The results revealed that the corrosion of carbon steels was dominated by the time of wetness, while that of zinc-galvanized steel strongly depended on the chloride ion concentration in the atmosphere. The corrosion rate (CR) of the zinc-galvanized steels was greatly lower than that of the carbon steel. For both metals, the corrosion losses decreased with increasing exposure time [21].

Morcillo, et al. made an extensive review of the atmospheric corrosion data of weathering steels which addressed on rust layer stabilization time, steady state of corrosion rates, and the effect of exposure condition [19]. The corrosion kinetic reached the stabilization time early in the corrosive atmospheres; but late in the less corrosive atmospheres. The steady state of corrosion rate increases with the corrosivity of atmospheres. Morcillo has also noted that the presence of atmospheric pollutants SO_2 and airborne salinity Cl^- has a rather considerable effect on weathering steel corrosion. There seems to be a critical level of SO_2 and Cl^- (SO_2 = 20mg /m^2 d and Cl^- = 3mg/ m^2 d), which the use of conventional unpainted weathering steel is not feasible.

Morales, et al. investigated the atmospheric corrosion of carbon steel, zinc, and copper sheets in subtropical areas (Canary Island, Spain) in marine atmospheres [35]. The 35 test stations were made to collect the environmental parameters and corrosion rate during 3-years of exposure test. It was frequently found that the corrosivity of some atmospheres exceeded those established by the standard ISO 9223 norm (exceeded C5 category [36]), especially copper and zinc as seen in Table 2. Thus, Morales proposed enlarging or to add a scale of corrosivity categories

classification in order to cover the atmospheric corrosion in coastal areas of tropical and subtropical regions.

According to the above research literature, in all case the corrosion rate of metal and alloys, exposed to the actual environment, is not constant; it decreases with exposure time because of the accumulation of rust layers on the surface of metal enhance corrosion resistance. And thus, it has been confirmed that the corrosion attack follows the power function as stated in ISO 9224 [32]. However, some researchers reported that the guiding value of ISO standards did not cover worldwide atmospheres [35]. And there were some doubts that, a higher concentration of SO_2 and Cl^- in the atmosphere lead to further corrosion phenomenon, which harmful for steel structure [19]. To rectify such unfortunate situations local atmospheric corrosion investigations are needed for classifying atmospheric corrosivity categories, and to guide for long-term atmospheric corrosion prediction.

1.7 Objective and Mechanism of Research

The aim of this research is to study the atmospheric corrosion behaviors and to explore the corrosion data mapping in Asia regions. To achieve these targets:

- The artificial rainfall equipment was developed for studying the effect of rain, chemical species, and its concentrations, on the corrosion rate and ACM sensors outputs.
- The outdoor exposure tests of carbon steels, weathering steels, galvanized steels, and 55% of Al-Zn coated steels were conducted for finding the actual corrosion rate (CR).
- The Atmospheric Corrosion Monitoring (ACM) sensors were also exposed nearby the metallic samples.
- The environmental parameters like Temperature (T), Relative Humidity (RH), time of wetness (TOW), SO_2 and Cl^- deposition rates were collected at most of the exposure test stations.

- The corrosion rates and environmental parameters were used to establish the corrosion data in Asia region and to verify the validation use of ISO standards in Asia atmospheres.

Table 2 - Corrosion rate of carbon steel, copper, and zinc test sheets. Classification of corrosion aggressiveness for the first year of exposure, according to the ISO 9223 [35].

Test sites		Carbon steel		Copper		Zinc	
		r_{corr} ($\mu m\,year^{-1}$)	Classification	r_{corr} ($\mu m\,year^{-1}$)	Classification	r_{corr} ($\mu m\,year^{-1}$)	Classification
Tenerife							
1	Meteorológico	15.7	C_2	3.73	C_5	1.02	C_3
2	Policía Local S/C	19.5	C_2	3.15	C_5	1.16	C_3
3	Oceanográfico	19.5	C_2	4.77	C_5	6.29	C_5
4	Montaña Ofra	28.5	C_3	4.87	C_5	3.29	C_4
5	Química	39.5	C_3	3.90	C_5	1.59	C_3
6	Pajalillos	17.3	C_2	3.26	C_5	1.55	C_3
7	Isamar	20.1	C_2	2.93	C_5	2.18	C_4
8	Garimba	44.7	C_3	3.48	C_5	2.25	C_4
9	Ayuntamiento Puerto Cruz	17.8	C_2	6.95	>C_5[a]	4.75	C_5
10	Botánico	20.9	C_2	2.56	C_4	0.99	C_3
11	Montañeta	19.2	C_2	1.68	C_4	1.03	C_3
12	Buenavista	24.1	C_2	4.91	C_5	2.89	C_4
13	El Palmar	22.7	C_2	3.61	C_5	1.68	C_3
14	Las Raíces	22.9	C_2	1.92	C_4	1.42	C_3
15	Izaña	3.8	C_2	1.33	C_4	0.77	C_3
16	Unelco Caletillas	35.9	C_3	6.03	>C_5	5.09	C_5
17	La Planta	24.2	C_2	5.73	>C_5	3.71	C_4
18	La Oficina	25.5	C_3	8.30	>C_5	5.32	C_5
19	El Bueno	25.6	C_3	3.24	C_5	1.68	C_3
20	Unelco Granadilla	94.5	C_5	14.28	>C_5	50.48	>C_5
21	Los Cristianos	17.7	C_2	13.28	>C_5	2.97	C_4
22	Vilaflor	–[b]	–	–	–	0.49	C_2
23	Cueva del Polvo	17.5	C_2	10.76	>C_5	3.48	C_4
24	Guía de Isora	17.3	C_2	3.93	C_5	1.49	C_3
La Gomera							
25	San Sebastián	25.1	C_3	3.93	C_5	2.58	C_4
26	Valle Gran Rey	31.2	C_3	17.11	>C_5	6.48	C_5
27	El Cedro	17.2	C_2	2.53	C_4	0.67	C_2
El Hierro							
28	Valverde	218.1	>C_5	6.14	>C_5	7.31	C_5
29	Arpto. El Hierro	263.2	>C_5	21.34	>C_5	223.9	>C_5
La Palma							
30	Arpto. La Palma	41.4	C_3	7.62	>C_5	11.78	>C_5
31	El Paso	15.2	C_2	2.80	C_4	5.07	C_5
32	Pto. Naos	16.6	C_2	7.84	>C_5	4.79	C_5
33	Los Llanos	12.5	C_2	3.48	C_5	2.13	C_4
34	Fuencaliente	21.3	C_2	5.86	>C_5	4.40	C_5
35	San Andrés y Sauces	19.3	C_2	5.01	C_5	1.80	C_3

[a] >C_5: Corrosion rate higher than the ones given by the ISO 9223 norm.
[b] Data not available.

1.8 Research Project Cooperation

The outdoor exposure tests were conducted by the E-Asia Joint Research Program under the research title of "***Corrosion Mapping of Structural Materials in Asian Area with Understanding Effects of Environmental Factors"*** It is the research cooperation between:

- Japan: National Institute for Material Science (NIMS), host institution.
- Vietnam: Institute of Material Science (IMS), Research member.
- Thailand: National Metal and Materials Technology Center (MTEC), Research member.

The research program started from October 1, 2012, to March 31, 2016. And 37 test stations were made for outdoor exposure tests: 16 sites in Japan, 14 sites in Vietnam, and 7-sites in Thailand. The organization of the research project is shown in Appendix II, and the detail of the research and results is emphasized in Chapter 4. The author has also been investigating the atmospheric corrosion behaviors of carbon steel exposed to rural, urban, and marine atmospheres in Cambodia since January 7, 2015. And the initial atmospheric corrosion behaviors in Cambodia will be discussed in detail in Chapter 3.

1.9 Scope of Research

The atmospheric corrosion test requires great effort with long-term investigation. This research is a good initiative for developing long-term atmospheric corrosion database. However, the thesis will address only on the initial stage of atmospheric corrosion of carbon steel mapping in Asia countries including Japan, Vietnam, Thailand, and Cambodia. The atmospheric corrosivity classifications, determinations, and recommendations will be made based on the first year corrosion tests results. The surface roughness evolution, corrosion morphologies, and crystal structures of corrosion products were also taken into account. The behaviors of ACM sensors outputs affected by chemical species and its concentrations were observed by artificial rainfall test, and the empirical data will be used to verify the actual atmospheric corrosion in the future research.

Some of the atmospheric corrosion databases are kept as a property of JST joint research program, which is not allowed to be explored in this thesis. The numerical data of environmental parameters, corrosion rates, and ACM sensors output of the outdoor exposure tests will be taken into account for future study. The study does not cover all aspects related to the corrosion fracture mechanism caused by stress corrosion cracking, creep corrosion, galvanic corrosion (bi-metallic), high-temperature corrosion…etc.

1.10 Thesis Organizations

The thesis is systematically organized into five chapters that describe overall work of the present research. The outline of the each chapter is illustrated as below:

- Chapter 1: The background of atmospheric corrosion and its problems, research literature, objective and the mechanism of the research, research project collaboration, and the scope of work are depicted. This chapter aims to explore the atmospheric corrosion problems, leading to study and investigate in the following chapters.

- Chapter 2: It is the early stage for observing the behaviors of ACM sensors outputs and corrosion rates, affected by environmental parameters like various types of chemical species and its concentration, under the artificial rainfall test. The results in this chapter guide to estimate and evaluate the corrosion phenomenon in the actual environment.

- Chapter 3: The initial stage of atmospheric corrosion of carbon steel will be elaborated in detail through the 1-year corrosion test in urban and marine atmospheres in Cambodia. The corrosion morphology, crystal structure, composition corrosion product, and the texture of the rust layer in micro-aspect will be demonstrated. The surface roughness evolution of carbon steel subject to corrosion will also be explored in this chapter.

- Chapter 4: In this chapter, the procedures of exposure tests and the results of atmospheric corrosion mapping in Asia regions, which have been done under E-Asia research project, will be emphasized. The evaluation, corrosivity categories classifications, and recommendation guiding for regional used of atmospheric corrosion data were made. And the effect of environmental parameters on corrosion behaviors will be indicated and verified to that elaborated by the ISO standards.

- Chapter 5: This chapter summarizes and concludes the overall outcomes of the research work. And the recommendation will be made, guiding to hint the future research of atmospheric corrosion in the Asia regions.

CHAPTER 2

Chapter 2: The Corrosivity of Chemical Substances Estimated by the Atmospheric Corrosion Monitoring (ACM) under Artificial Rainfall Test

2.1 Introduction

With the influence of human activities and especially the industrial grow gas emissions which contain most of the pollutant substances are continuously increased, and it results in acid rain and acid fog, which considered as the most corrosive media that effectively enhance the atmospheric corrosion kinetic. To define the atmospheric corrosion behaviors of metallic material affected by environmental parameters, investigations are often made by laboratory observation [37]-[41], and field exposure test with considering the type of atmospheres, namely: rural, urban, industrial, and marine atmospheres [21],[22],[42]. Those atmospheres usually content different corrosion parameters such as relative humidity (RH), time of wetness, and especially the pollutant substances. The substances like SO_2 and Cl are found to be a major corrosive species in the industrial and marine atmosphere, respectively. According to ISO 9223 [35], the SO_2 deposition rate, chloride deposition rate, temperature, and relative humidity are the main parameters of *Dose-response functions* for calculating the first-year corrosion loss of metallic structure [26].

In the modern science and technology, the corrosion parameters have been investigated in detail, and some technical investigation methods have been proposed. In general, the electrochemical method cannot be utilized to monitor the corrosion in a micro cell under a very thin aqueous layer. Recently, it was found that the galvanic cell technique is an essential method, which has been used to predict the corrosion tendency and corrosion kinetic [43]. The galvanic pair-sensing probe, known as Atmospheric Corrosion Monitoring (ACM) sensors, is the application of galvanic cell method. By using this type of sensor, Oshikawa et al.,

[44] suggested that 20% of ACM sensor output in rain period is effective to estimate corrosion rate (CR) of carbon steel exposed to Choshi, Nishihara, and Miyakojima, as severe marine atmospheres with a large amount of airborne sea salt. Nakano and Oshikawa compared corrosion behaviors of carbon steel in salt spray test (SST), by NaCl solutions >0.003%, to that in the actual rain during Typhoon in Okinawa area [45]. On the other hand, Shinohara [46] suggested that the CR of carbon steel during rain period is constant (CR= 0.061μm/h) at mild exposure test sites, Shimizu and Tsukuba. However, those were estimated and evaluated by analyzing the actual exposure test results of CR and Fe-Ag galvanic couple of ACM sensor output; the detailed studies of corrosion and others galvanic couples of ACM sensors output affected by various chemical substances during rain period were not conducted.

With the aim of contributing to clarify this matter, the research in this chapter is to identify the phenomenon of corrosion affected by numerous chemical species by using artificial rainfall equipment. Four types of ACM sensors were also used to investigate the corrosivity of rainfall solution through the sensors outputs. The sensible characteristic of ACM sensors will be defined and recommended for the reliable used.

2.2 Atmospheric Corrosion Monitoring (ACM) sensors

It has been known that galvanic couple sensing probe was used for dew detector [47] time-of-wetness meter [48], or moisture sensor [49]. Further integrations and applications of this type of sensor, called Atmospheric Corrosion Monitoring (ACM) sensors, have been used to predict the atmospheric corrosion behaviors [50]. The schematic illustration of ACM sensor, which consists of the Fe-Ag couple, is presented in the Fig. 7. The signal output, known as galvanic current, range between nanoampere to milliampere, depends mainly on the electrical conductivity of aqueous film formed by dew or raindrop on the striped surface of the sensors. And the signal outputs of the sensors are recorded and collected every minute by 16 CH data logger SYRINX SAXM-50F. In this research, four types of ACM sensors, Fe-Ag, Zn-Ag, Al-Ag, and Cu-Ag, were used to investigate the phenomenon of corrosion through the signal output of ACM censors.

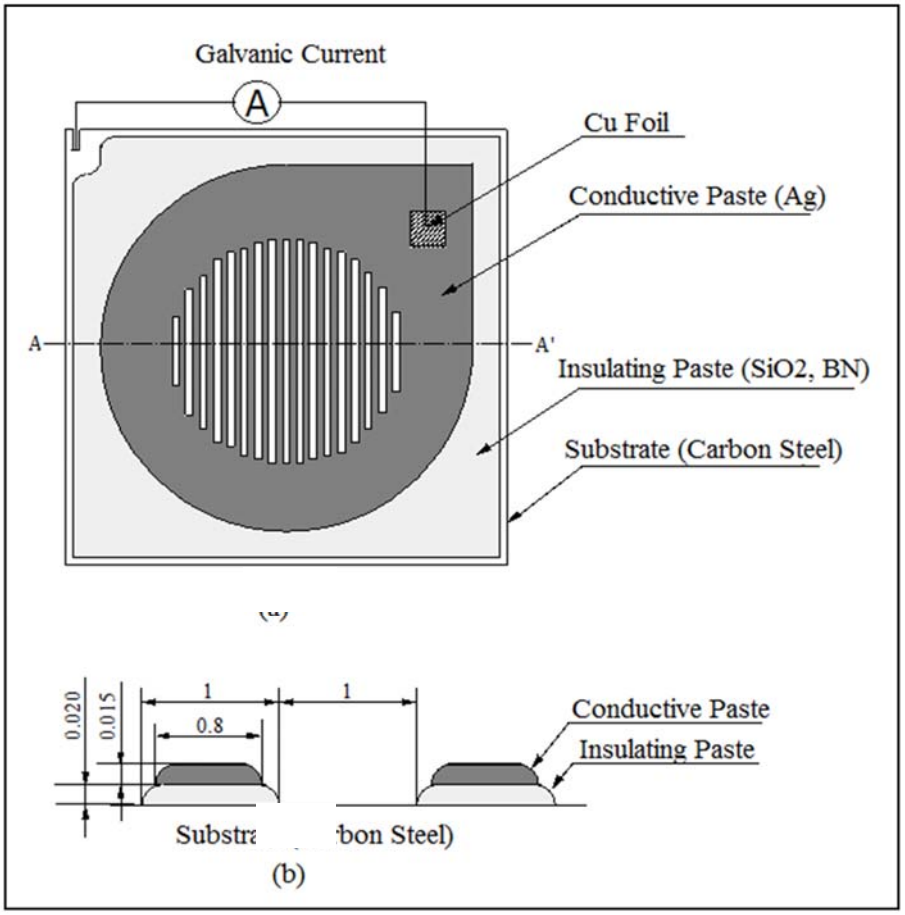

(a) Schematic illustration of ACM sensor (Fe-Ag couple) [50].

(b) Over view the 4-types of ACM sensors

Fig. 7 - Atmospheric Corrosion Monitoring (ACM) sensors.

2.3 Development of Artificial Rainfall Equipment

The author has developed an artificial rainfall equipment [51] to investigate the effects of rainfall on the corrosion behaviors of metallic material. The rainfall equipment, as seen in *Fig. 8*, is composed of a chamber with orifices array at the bottom, a water reservoir, an air mixer ($N_2$80% and $O_2$20%), and a nozzle connected by two inlet pipes (water and air). The *internal-mix two-fluid* nozzles type has been used to assure the uniform distribution of rainfall, and to make a wide range of water spray states such as rain, shower, and dew. The states depend mainly on the pressure of both air pressure and water pressure inlet pipes. Fig. 9 (a) and (b) below show the rainfall distribution and precipitation rate, *H (mm/h)*, in relation to the air pressure and water pressure. To find the level of rainfall distributions and their defects, 9-beakers were rectangularly arrayed on the bottom of the chamber in order to receive water droplets and to measure the water levels that highly depend on both air and water pressure. The results revealed that the minimum and maximum defects of rainfall distributions in 9 beakers were about ±10% and ±25% respectively, compared to the mean value of rainfall levels (as seen in *Fig. 9* (c)).

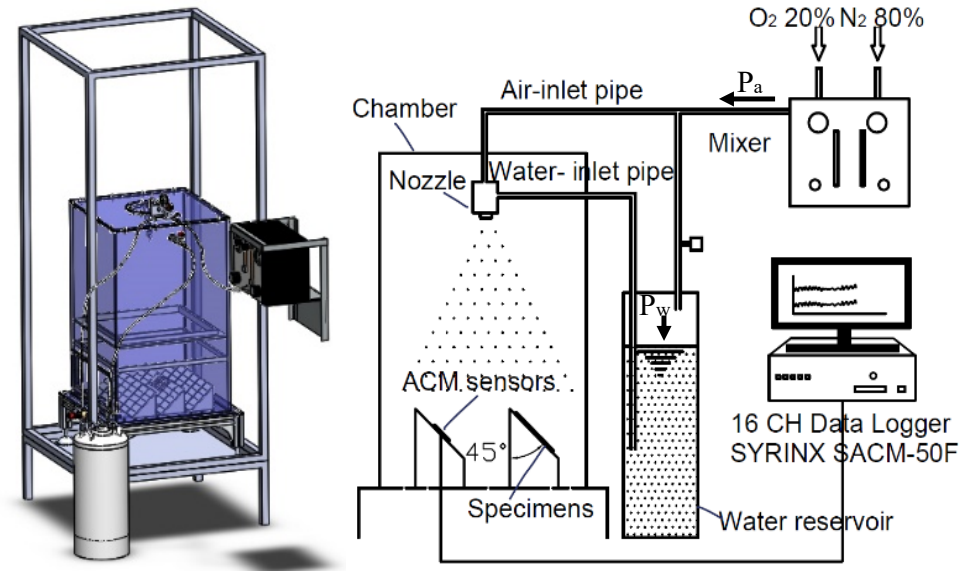

(a) 3D representation. *(b) Schematic representation.*

Fig. 8 - Artificial rainfall equipment [51].

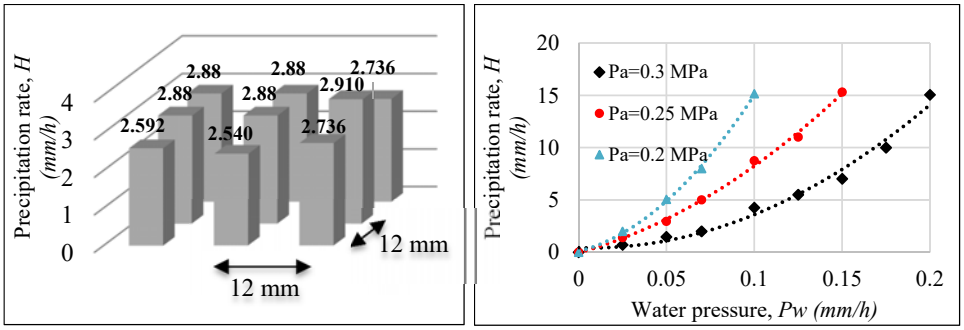

(a) Rainfall distribution in 9 beaker (Pw = 0.075, Pa=0.03 MPa).

(b) The effect of air pressure, Pa, and water pressure, Pw, on the precipitation rate

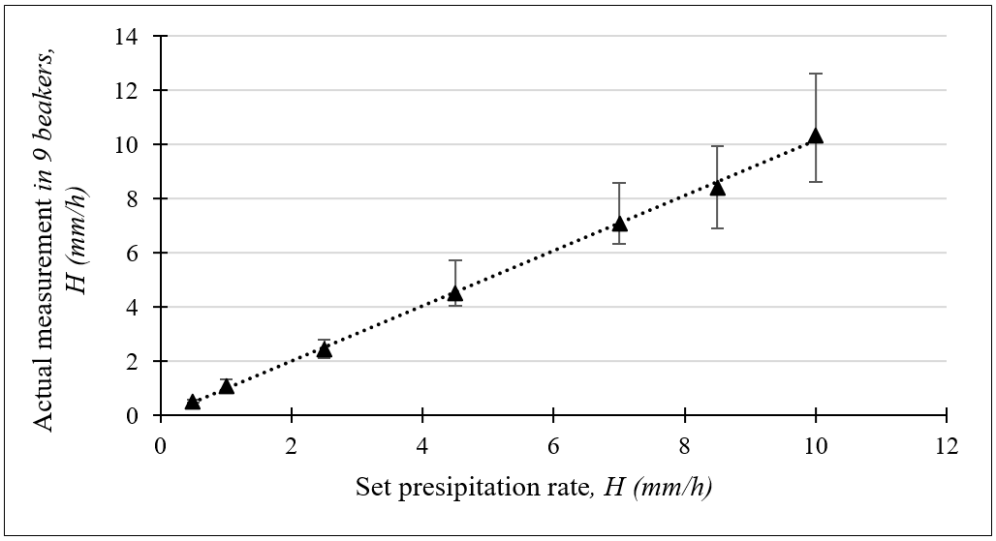

(c) Rainfall distributions in 9 beakers with different precipitation rate H (mm/h)

Fig. 9 - Measurement and adjustment of rainfall distribution [51].

2.4 Chemical Composition of Artificial Rainfall Solution

The chemical compositions of the artificial rainfall solutions were made based on the fact of the actual rain. Table 3 shows the chemical composition, pH values, and electrical conductivities of the actual rain collected at National Institute for Material Science (NIMS), Tsukuba, Japan. The chemical examination results show that several ionic species like Cl^-, SO_4^{2-}, NO_3^-, Na^+, K^+, Ca^{2+}, Mg^{2+}, and HCO_3^- were found in the rainwater. It should be noted that the concentration of Cl^- and SO_4^{2-} are

sometimes notably high. To defined the corrosivity of each ion, NaCl, KCl, Na_2SO_4, $NaNO_3$, KNO_3, $MgCl_2.6H_2O$, and $Mg(NO_3)_2.6H_2O$ were mixed with deionized water and used ask rainfall solutions with the variation of molar concentration.

Table 3- Properties of actual rainwater in Tsukuba, Japan.

Property	Date (dd-mm-yy)						
	26-11-14	**15-06-15**	**04-07-15**	**09-09-16**	**29-01-16**	**07-04-16**	**18-08-16**
pH(17 ^{0}C)	6.7	6.3	6.3	6.3	6.6	5.4	5.9
Conductivity	1.4	1	0.9	4.8	1.4	0.3	0.5
Concentration (10^{-5}mol/L)							
Cl^-	2.8	<2.8	2.8	28	2.8	2.8	<2.8
SO_4^{2-}	15	<1	<1	3.1	<1.0	<1.0	<1.0
NO_3^-	<2.1	<2.1	<2.1	<2.1	<2.1	<2.1	<2.1
Na^+	2.6	3.0	3.0	26	4.8	8.7	2.2
K^+	0.51	0.51	0.51	1.5E	1.8	0.26	0.51
Ca^{2+}	1.0	<0.25	<0.25	0.75	<0.25	<0.25	<0.25
Mg^{2+}	0.82	<0.41	<0.41	0.21	<0.41	<0.41	<0.41
HCO_3^-	<0.82	<0.82	<0.82	<0.82	<0.82	<0.82	<0.82

2.5 Experimental Setup and Measurement

In this experiment, a 1 mm thick of carbon steel sheet, with the size of 70 × 150 mm, were used as specimens. The samples were exposed to the artificial rainfall by a limited and single face (55 mm×127 mm). Thus, backside, cut edge, and fringe of the specimens were covered by polyethylene sheet in order to avoid undesired corrosion occurs (Fig. 10). Three specimens and four types of ACM sensors (Cu-Ag, Al-Ag, Zn-Ag, and Fe-Ag) were installed at the bottom of the chamber with an inclination of 45 degrees from a vertical axis (see Fig. 8). Each rainfall test was conducted about 24 hours. After the test, the corrosion products, or rust layer, were removed by immersing the samples into Hydrochloric Acid (HCl) solution based on ISO/DIS 8403.3 [52]. The weight loss of the samples was measured, then converted to the corrosion rate (CR) based on the following equation:

$$\mathrm{CR(mm/y)} = \frac{10\,W_y}{\rho A}: \quad (6)$$

W_y: Weight loss per year (g/y)

ρ: Density of carbon steel (7.86g/cm^3)

A: Exposed area; in this case study, A= 70 cm^2

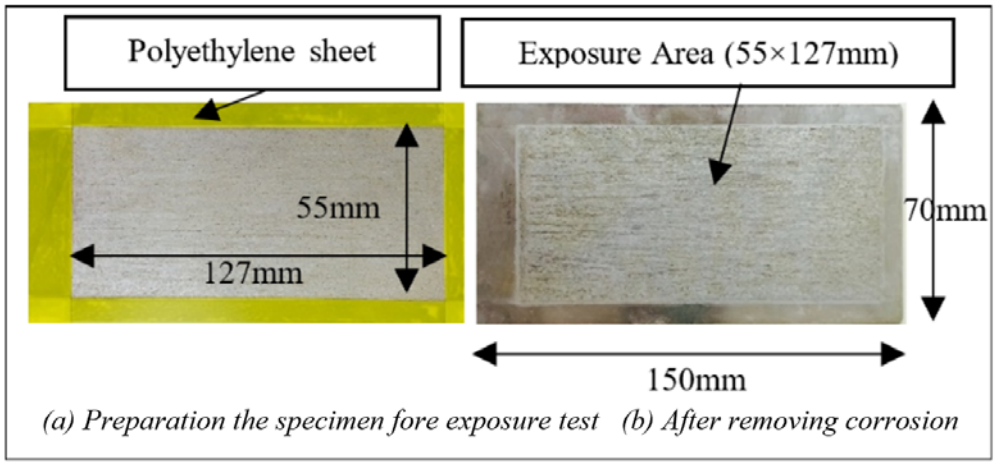

Fig. 10 - Carbon steel sheet specimens [53].

2.6 Electrical Conductivity of the Rainfall Solution

The electrical conductivity, σ (μs/cm), is sensitive to the galvanic couple sensing probe. The conductivities of all solutions are linearly increased with the increasing of concentrations. The relation between electrical conductivity and molar concentration is shown in the following form:

$$\sigma = \beta.c + D \quad (7)$$

Where σ: (μs/cm) is the electrical conductivity

β: Electrical conductivity coefficient

c: The concentration (mol/L)

D: Electrical conductivity of deionize-water at room temperature; in this experiment $D \approx 0.9$ to1.5 μs/cm.

The relations between the concentrations of the individual solutions and electrical conductivities are shown in Fig. 11. The Na_2SO_4 solution has a good electrical conductivity and follows by NaCl and $NaNO_3$ solutions respectively.

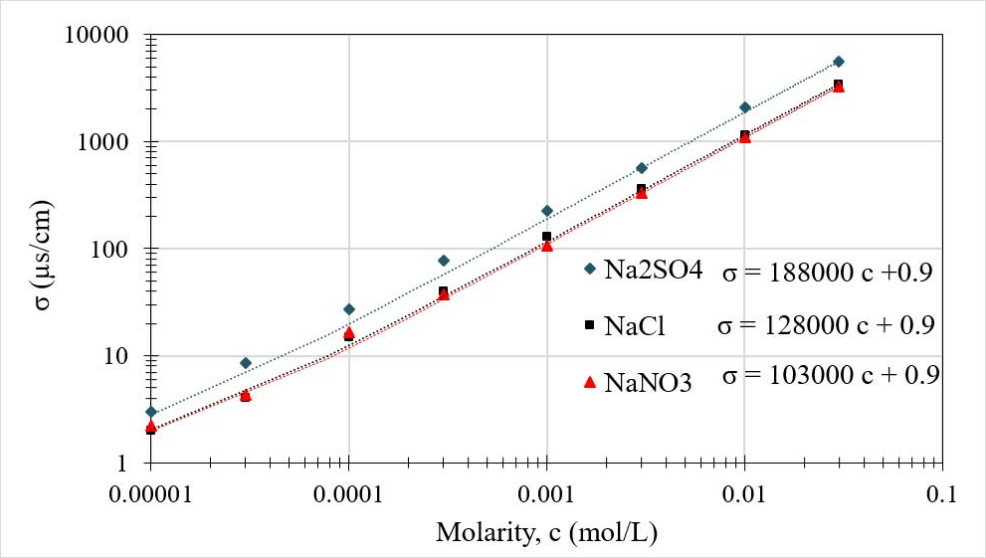

Fig. 11- The electrical conductivity of the individual solutions in function of molar concentration [53].

Fig. 12 shows the effect mixed solution, of Na_2SO_4 and NaCl, on the electrical conductivity. The figure indicated that adding up the Na_2SO_4 concentration into the NaCl solution, the trend line shifts up in a parallel manner. It means that, the electrical conductivity of the mixed solution equal to the summation of that in the individual solutions. Thus, the electrical conductivity depends mainly on the ionic species and its concentration.

2.7 Effect of Precipitation Rate to Sensor Output

In an actual environment, precipitation rate varies with time and location. In this experiments, however, precipitation rate was insensitive to CRs and ACM sensors outputs as seen in Fig. 13. It can be explained by the fact that the CR can approach maximum when the electrolyte surface film covering the metal becomes very thin, below 56 μm [17][18][55][57]. For the larger thickness of the film, especially under the rainfall with homogeneous concentration, the CRs will stabilize at a constant value [18].

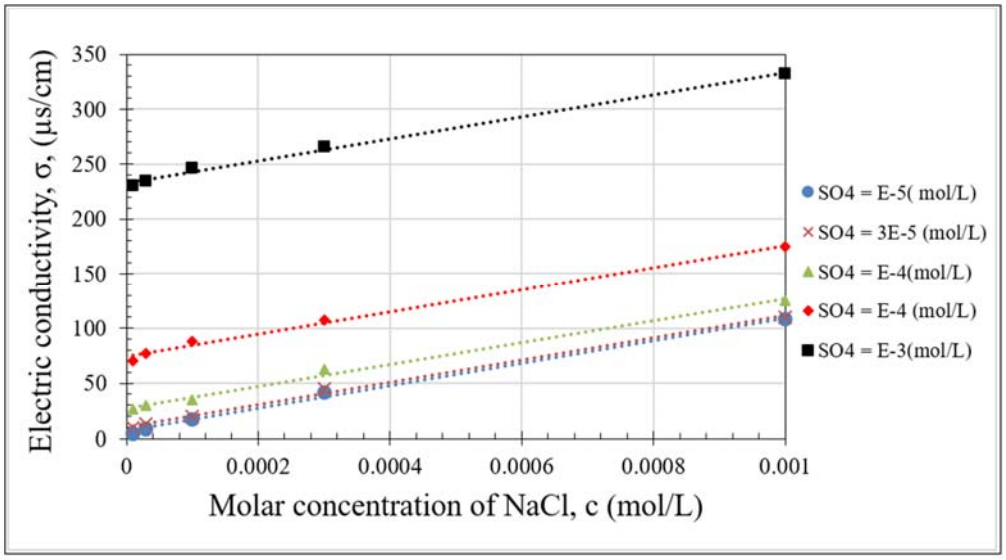

Fig. 12 - Electrical conductivity in the mix solution [54].

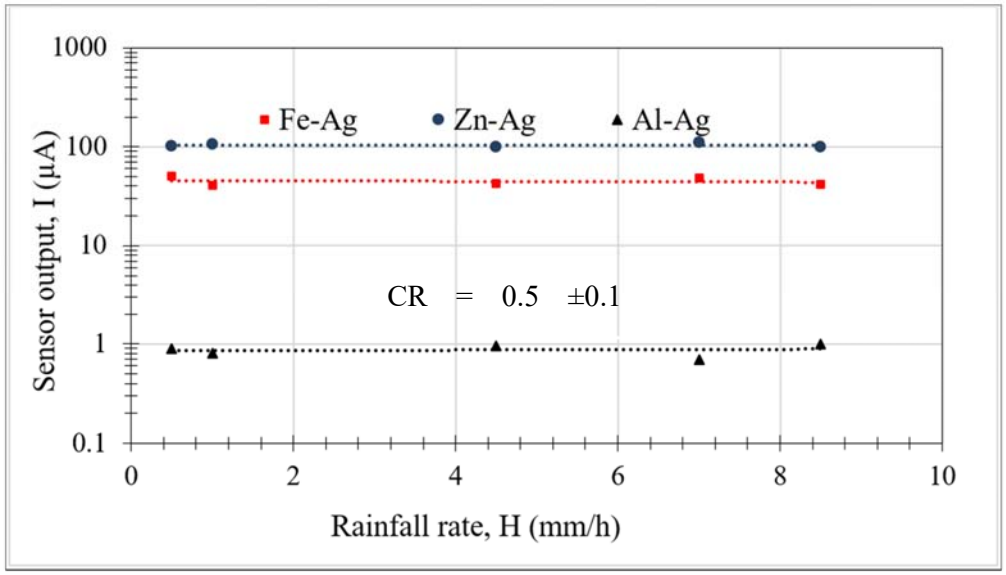

Fig. 13 - The effect of precipitation rate to the sensors outputs in Na_2SO_4 solution with the concentration of 3×10^{-4} mol/L [53].

2.8 Relation between Sensors Outputs and Chemical Concentration

Fig. 14 shows the relation between sensors outputs in function of molar concentrations. The galvanic currents of the three sensors increase with the increasing of molar concentrations, except Al-Ag galvanic current in $NaNO_3$ solution (see Fig. 14 (c)) that considerably unchangeable when $c > 10^{-4}$ mol/L. For Fe-Ag and Zn-Ag sensors, the galvanic currents in the Na_2SO_4 solutions are higher than those in NaCl and $NaNO_3$ solutions, respectively (see Fig. 8 (a) and (b)). On the contrary, the Al-Ag galvanic currents in Na_2SO_4 solutions are lower than those in $NaNO_3$ and NaCl solution (see Fig. 14 (c)). Hence, the sensibility of the ACM sensors depends on the couple sensing probe and the rainfall solution.

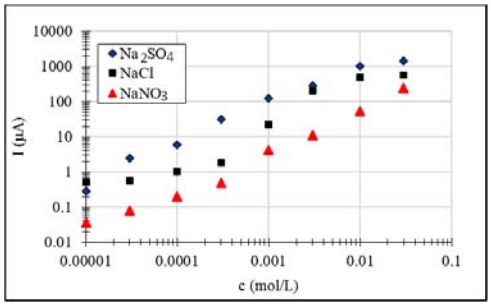

(a) Fe-Ag galvanic couple.

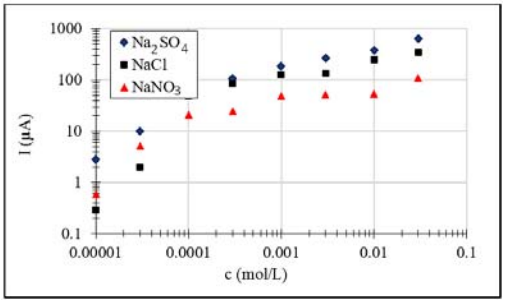

(b) Zn-Ag Galvanic couple.

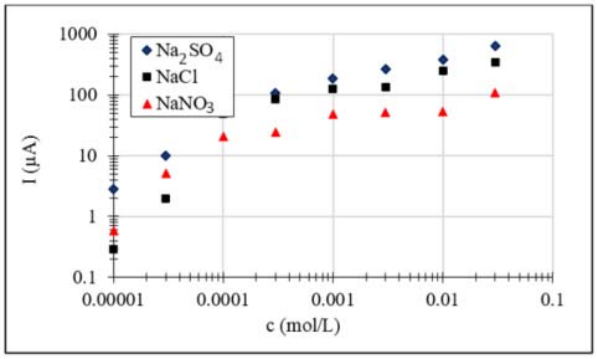

(c) Al-Ag galvanic couple.

Fig. 14 - Relation between molar concentration and sensor outputs [53].

2.9 Effect of Anion on the Corrosion under Rainfall Test

Dissolve the chemical compositions like NaCl, KCl, Na_2SO_4, $MgCl_2.6H_2O$, $NaNO_3$, KNO_3, and $Mg(NO_3)2.6(H_2O)$ into water it will decompose into a mixture of cation (Na^+, Mg^{2+}, and K^+) and anion (Cl^-, SO_4^{2-} and NO_3^-). The negative charge, called anion, is the most corrosive ion because it has much more tendency to catch electron from the metal surface. Consequently, the metal will oxidize by transferring the electron to the anion and liberating metal ion from the metal surface to form rust. Fig. 15 shows the corrosivity of anions with the variation of molar concentration. Evidently, the CRs depend mainly on Cl^- and NO_3^-, while the effect of Na^+, Mg^{2+}, and K^+ is considered negligible. This phenomenon does not mean for all cation, especially H^+ that has natural tendency to accept the electron from metallic-solution interface. In the following experiment, the effect of anion on the corrosion behaviors will be investigated and discussed in detail.

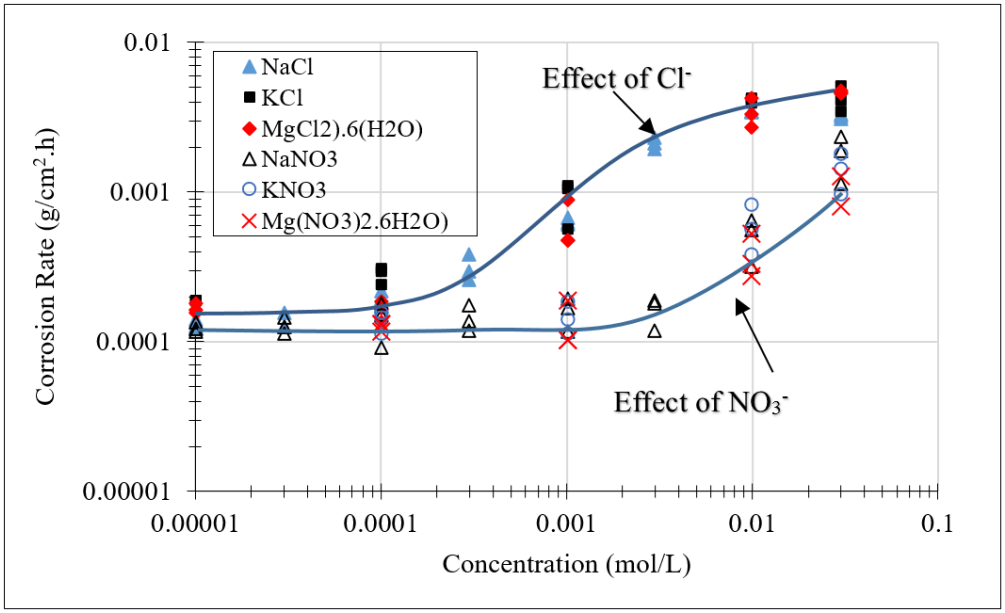

Fig. 15 - Effect of anion on CRs under rainfall solution [54].

2.10 Time-Dependent of Corrosion Stages

The atmospheric corrosion, normally, proceeds through three stages of period, induction period, transition period, and stationary period. During the induction

period the metal is covered by both the spontaneously formed oxide film (the film is usually invisible) and the aqueous layer. This oxide film provides some degree of protection, called passivation. The breakdown of the film is usually associated with time and aggressive species in the electrolyte layer. In the induction period, the corrosion attack is almost impossible since it firstly overcomes the oxide film. The authors, [56], have proved that, under the artificial rainfall with Na_2SO_4 concentration, the induction period is quite short and very short at the higher ionic concentration. The induction periods of the concentration of 10^{-2} mol/L, 10^{-3} mol/L, and 10^{-4} mol/L are about 2 hours, 15 hours, and 25 hours respectively as seen in *Fig. 16* (a) and (b). During the transition period, the corrosion reaction fully proceed, and weight loss raises up faster, then transit to the stationary period when the metal surface is fully covered by corrosion products (*Fig. 16* (b) and (c)). The corrosion kinetic in the stationary period is lower than that in a transition period since the formation of rust layer plays a role as corrosion resistance.

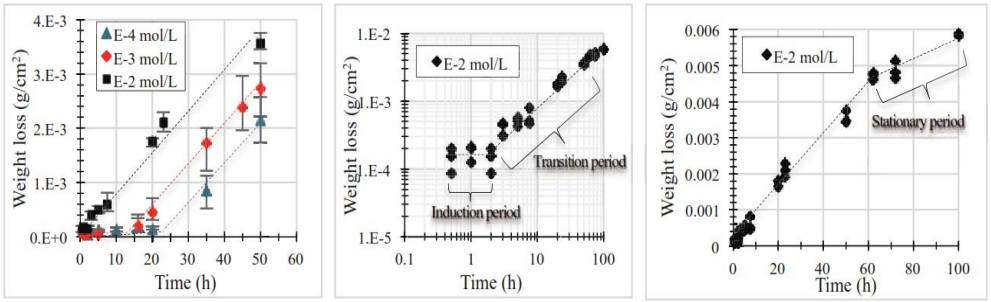

(a) Linear-scale of corrosion stage with in various concentrations.

(b) Log-scale of corrosion stage, Na_2SO_4 10^{-2} mol/L.

(c) Linear-scale of corrosion stage, Na_2SO_4 10^{-2} mol/L.

Fig. 16 - The behaviors of corrosion stages under artificial rainfall test [56].

2.11 Corrosivity of Anions in the Individual Solution

Fig. 17 shows the logarithmic scale representing the CR in function of molar concentration in the individual solution. Each data point of CR is the mean value of

two-time repeated tests with three samples during 16h rainfall test. As it can be seen in Fig. 17, the most aggressiveness anion is SO_4^{2-}, Cl^-, and NO_3^- respectively.

- ***Corrosivity of SO_4^{2-} and Cl^- anions:*** At the concentration of $c < 10^{-4}$ mol/L, the corrosion rate is very low, and the corrosion product was not visually detected. However, after performing an HCl cleaning process, a minuscule mass loss was detected. By increasing the concentrations, 10^{-4} mol/L $< c <$ 10^{-2} mol/L, the corrosion spots started to enlarge, overlap, and eventually covered the surface of the metal samples entirely. Further increase in concentrations, $c > 10^{-2}$ mol/L, the CRs did not increase. Instead, it simply reached steady state, as seen in Fig. 17.
- ***Corrosivity of NO_3^- anions:*** The corrosivity of NO_3^- anion was very low; NO_3^- concentrations did not affect to the CR at $c < 3.10^{-3}$ mol/L; it means that the oxide film still remains on the surface electrolyte. At higher concentration $c \geq 3.10^{-3}$ mol/L, the corrosion reaction starts to proceed, and corrosion kinetic starts to raise up.

A low chemical concentration is a less corrosive media that cannot overcome the oxide film. Recall that, the breakdown of the oxide film depends on the aggressivity of the media and time of wetness. For the lower ionic concentration, longer time of wetness (time of rain, in the case study) is required for corrosion to occur.

2.12 Corrosivity of Anions in the Mixed Solutions

The effects of mixed solution on the CRs are shown in *Fig. 18*. In the concentration of 10^{-5} mol/L $< c <$ 10^{-3} mol/L, CR affected by the mixed solution equal to the summation of the RC affected the by the individual solutions. Thus, corrosion kinetic depends mainly on the ionic species and its concentration. However, at high concentration, the CR will stabilize. Thus the concentration will not be sensitive to CR as seen in Fig. 17.

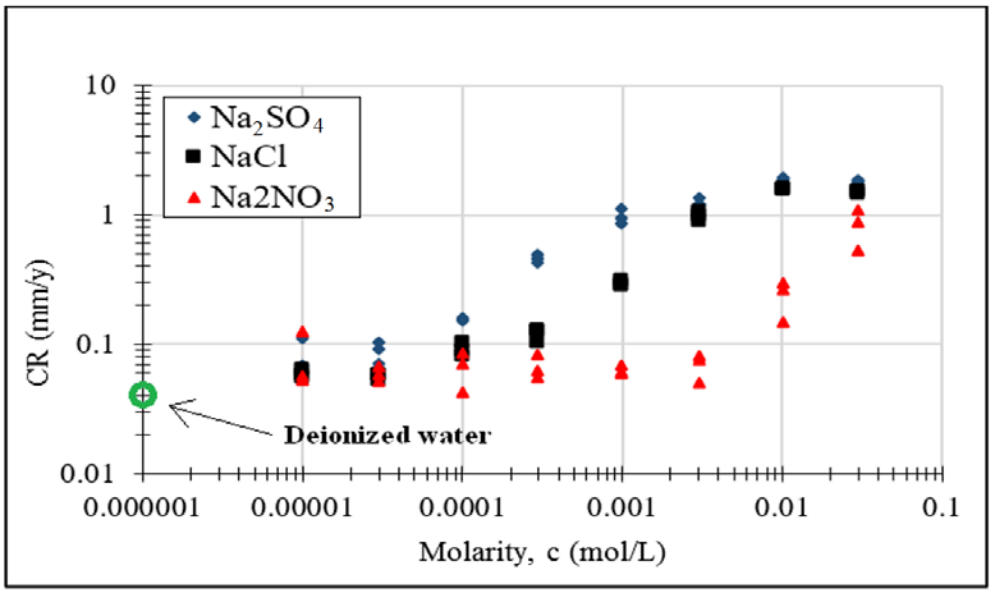

Fig. 17 - The individual effect of Cl^-, SO_4^{2-}, and NO_3^- on corrosion of carbon steel [53].

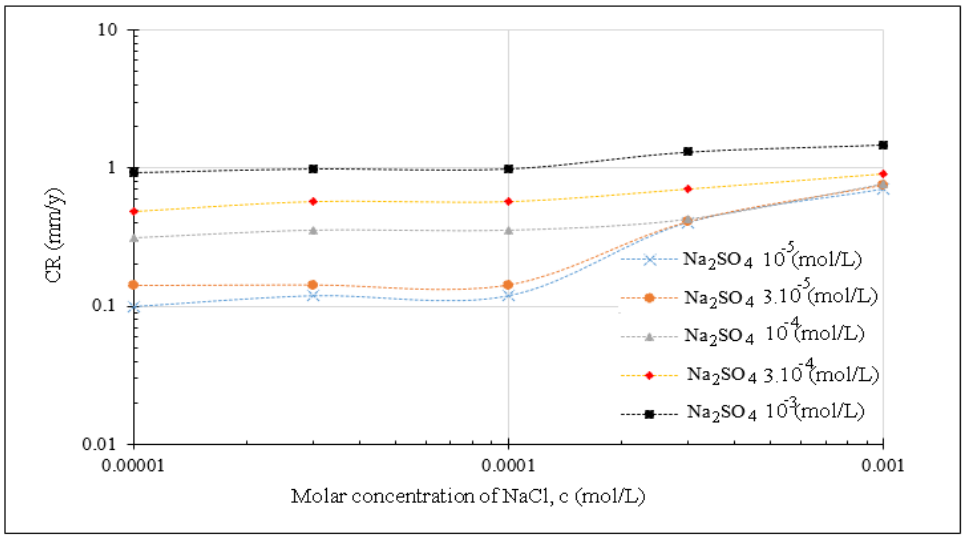

Fig. 18 - Effect of Cl^- and SO_4^{2-} on corrosion of carbon steel [54].

2.13 Relation between Sensors Outputs and Corrosion Rates

Recall that, the sensor output is a current of the galvanic couple that highly depends on ionic species of the aqueous film formed on the surface of the ACM sensors.

Fig. 19 and Fig. 20 presented the CRs in function of sensors outputs of the individual and mixed solution, respectively. The sensor outputs of Fe-Ag and Zn-Ag galvanic couples gave a good relation for estimating the CRs in both individual and mixed solution (see Fig. 19 (a) and (b) and Fig. 20 (a) and (b)); while the output of Al-Ag galvanic couple was completely differentiated by chemical species, as seen in Fig. 19 (c) and Fig. 20 (c). Obviously, the Al-Ag couple of ACM sensor was very sensitive to NaCl and $NaNO_3$ solutions, but less sensitive to the Na_2SO_4 solution. For the Cu-Ag couple, the signal output was very low (I<10 μA); it was less sensitive to any ionic species and concentration (see Fig. 19 (d) and Fig. 20 (d)).

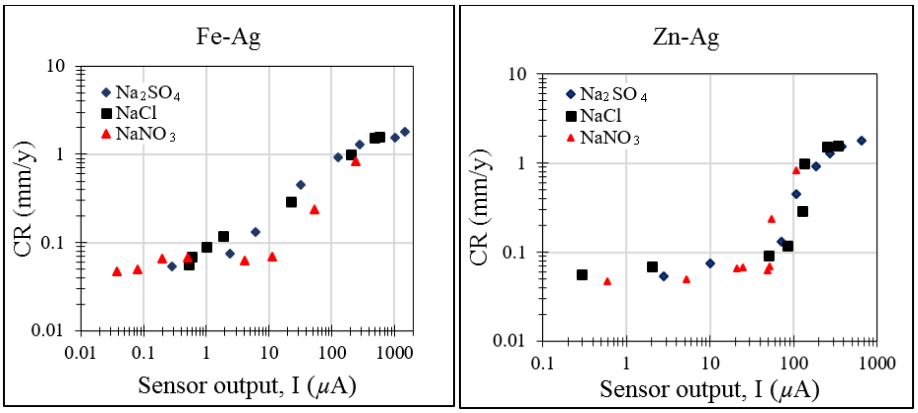

(a) Fe-Ag galvanic couple. *(b) Zn-Ag galvanic couple.*

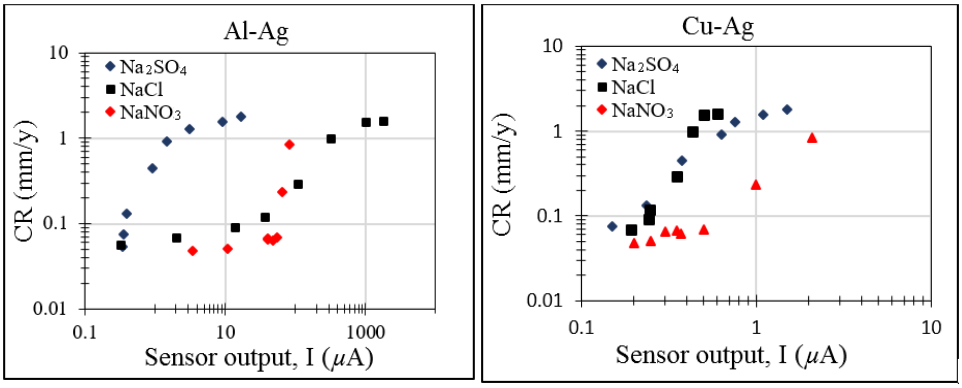

(c) Al-Ag Galvanic couple. *(d) Cu-Ag galvanic couple.*

Fig. 19 - The relationship between sensors outputs and CRs in the individual solution [54].

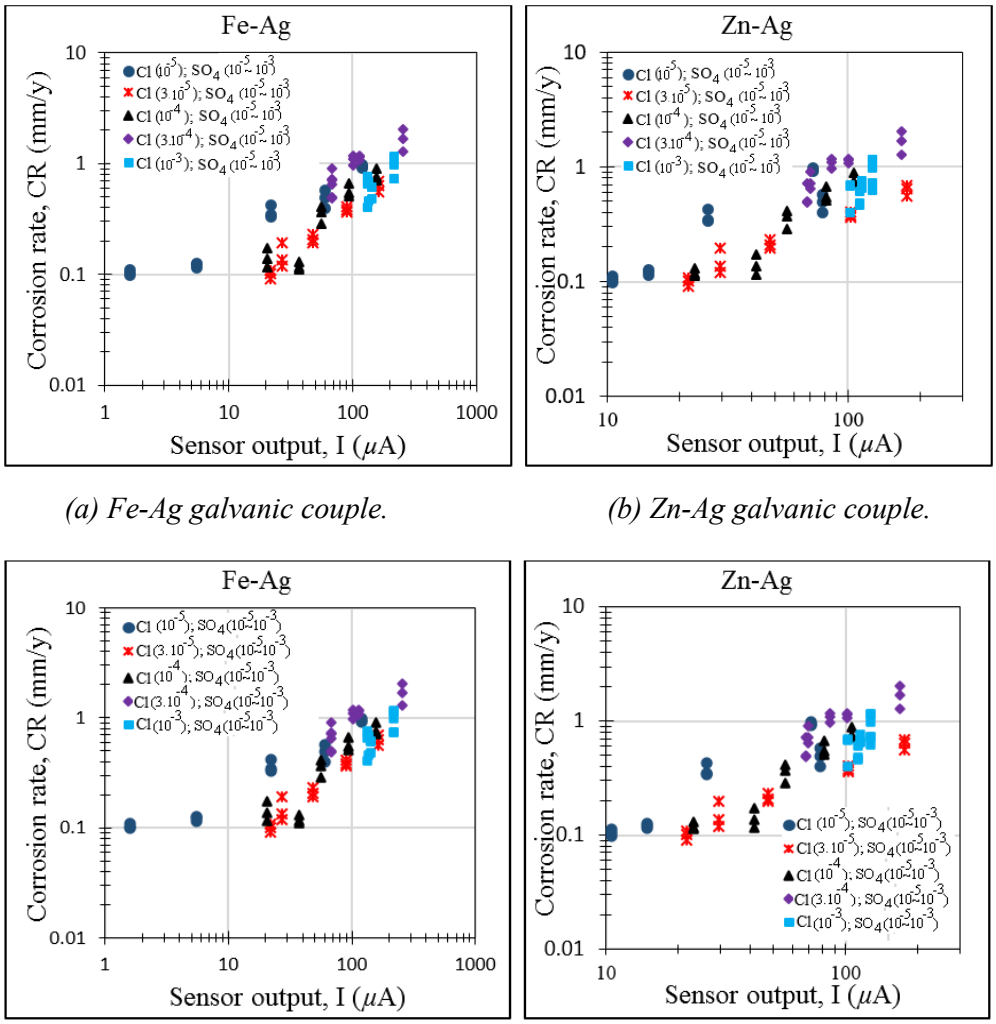

(a) Fe-Ag galvanic couple. *(b) Zn-Ag galvanic couple.*

(c) Al-Ag Galvanic couple. *(d) Cu-Ag galvanic couple.*

Fig. 20 - The relation between sensors outputs and CRs in mixed solutions [54].

2.14 Evaluation Approach to Determine Atmospheric Corrosion

2.14.1 The behaviors of ACM sensors output

ACM sensor output was not affected by precipitation rate as shown in Fig. 13. In the case of Fe-Ag galvanic couple, the output is determined by anodic reaction of *Fe* electrode, the cathodic reaction of Ag electrode, and solution resistance between Fe and Ag electrodes of the sensor:

- Anodic reaction: $Fe \rightarrow Fe^{2+} + 2e^-$ (8)

- Cathodic reaction: $(½)O_2 + H_2O + 2e^- \rightarrow 2OH^-$ (9)

The anodic reaction is affected by chemical composition, ionic species, electric conductivity, and so on; thus, it is considered to be constant for a given concentration of rainfall solution. The cathodic reaction is affected by the concentration of dissolved O_2, which is considered to be constant because the concentration of dissolved O_2 is stabilized by the renewal of the rainfall solution flows on the surface of the sensor. Moreover, most of the rainwater flows away, so the volume of the rainwater remaining on the metal surface is almost the same during raining period. It means that the thickness or electrical resistance of the water film remained on the surface of the ACM sensor is considered to be unaffected by precipitation rate. Hence, the precipitation rate did not affect the sensor output, which was explained in Fig. 13 above. Nakano and Oshikawa confirmed that SST could simulate the rain during Typhoon in Okinawa area without considering the effect precipitation rate [45].

As mentioned above, the Fe-Ag of ACM sensor output is determined by the solution resistance exists between Fe and Ag electrodes of ACM sensor; similarly for Zn-Ag, Al-Ag, and Cu-Ag of ACM sensors. Thus, the sensor output increases with increasing concentration or conductivity of the solution (see Fig. 11 and Fig. 14). However, the CR is stable under the rainwater with a high ionic concentration or high electrical conductivity, as shown in Fig. 17 and Fig. 18. It can be explained by the fact that, corrosion of carbon steel can proceed with the mechanism of microcell corrosion [58][59]. For a highly concentrated solution, the electrical conductivity is adequately high, so the solution resistance did not affect the change of CR [59]. Conversely, the corrosion reaction was sensible in the diluted solution with a small electrical conductivity or a large solution resistance, even for microcell corrosion. Thus, CR increases with increasing concentration or conductivity at low concentration ($c < 10^{-2}$ mol/L), as shown in Fig. 17.

2.14.2 Guide for Corrosion estimation

Atmospheric corrosion is an electrochemical process, which can only proceed in the presence of an electrolyte film. It is, therefore, to be considered as a discontinuous process, where the total corrosion loss, COR, in a given time or period is determined by the time of wetness, t_{wn}, and the average of corrosion rate, CR, during the each period, n, of condensation [60]:

$$\mathrm{COR} = \sum_{n} t_{wn}.\mathrm{CR}_n \tag{10}$$

The calculation the time of wetness based on meteorological data (by taking RH≥ 80% and T ≥ 0 ^{0}C) might not achieve the exact time that makes corrosion possible. Thus, the technical measurement method using ACM sensor exposure to the actual environment is more preferable. Virtually, Fe-Ag and/or Zn-Ag galvanic couples enable to estimate the time of wetness, t_{wn}, and corrosion rate, CR_n, through the empirical data as seen Fig. 19 (a-b) and Fig. 20 (a-b). Al-Ag couple, however, is unable to forecast the CR in the unknown pollution species, especially the mixed species in the atmosphere, due to the inconsistent relation of I-CR in different solutions (Fig. 19 (c) and Fig. 20 (c)). Nonetheless, the Al-Ag enables to estimate the time of wetness based on the great lifetime service. And also, it can be used to predict the chemical species in the environment. For instance, if the CR is high, and the Al-Ag sensor output is low, the SO_4^{2-} ions is assumed as the major content in the solution or the environment.

It has to be noted that the service-life of Fe-Ag galvanic sensor is much lower than those of Zn-Ag, Al-Ag, and Cu-Ag, respectively. The rust layer could be visually detected on the striped surface of the Fe-Ag sensor after about 64 hours rain (see Fig. 21), and it results in the increase of the sensor output and decreasing the sensibility of the ACM sensor. Thus, it is recommended to change the sensor frequently during the exposure test.

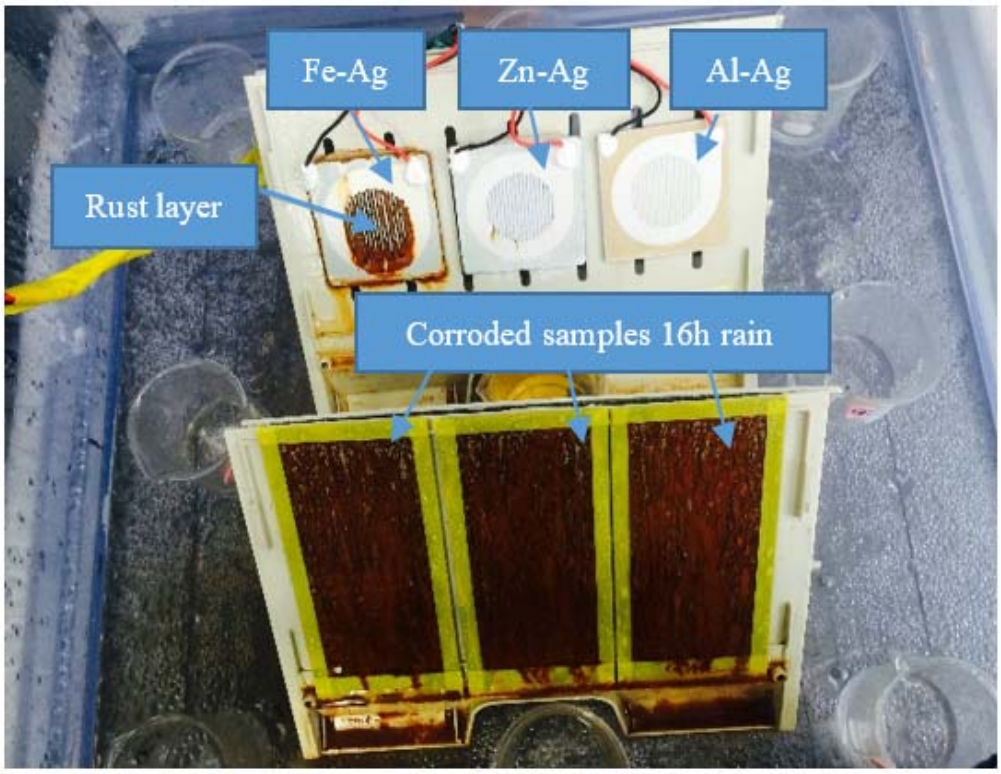

Fig. 21 - Corrosion attack on the carbon steel sample and ACM sensors.

2.15 Summary

Recall that, the atmospheric corrosion is an electrochemical process, which can only proceed in the presence of an electrolyte film. Rain is one of the main factors in initiating the time of wetness and transporting the chemical substance from the atmosphere to metal surface, guiding to accelerate the corrosion attack. Study the effect of rain and chemical species on sensors output is the primary importance aspect for atmospheric corrosion investigation. This chapter has fully demonstrated the effect of chemical species and its concentrations on the corrosion rate of carbon steel and the ACM sensors outputs by using artificial rainfall test. The following are the compiling of the effect of chemical species to the behaviors of corrosion attacks and sensors outputs:

- The development of artificial rainfall equipment is an essential and reliable tool for studying the corrosion behaviors under the effect of rain.

- The precipitation rates were insensitive to ACM sensors outputs and CRs. In contrast, the chemical species and their concentrations in the rainfall solution significantly affected the ACM outputs and the CRs.
- The corrosivity of the cations is negligible compared to the anions. For a certain of molar concentration, the most aggressiveness ions are SO_4^-, Cl^-, and NO_3^-, respectively.
- For further increasing molar concentration, the CR tends to reach a steady state at the maximum value of CR = 2mm/y.
- The corrosion kinetic affected by mixed solution equal to that in the individual solution for low ionic concentration.
- The ACM sensors are capable of estimating the time of wetness and aggressivity of atmosphere, and thus the total corrosion loss could be estimated.
- The lifetime of Fe-Ag galvanic sensor is much shorter than those of Zn-Ag, Al-Ag, and Cu-Ag respectively since the rust layer visually appears after 64 hours rain; thus the sensibility of the sensor would not perform well.
- The ACM sensors can be used for not only time of wetness meter but also atmospheric corrosivity meter based on the empirical data in Fig. 20.

CHAPTER 3

Chapter 3: Corrosion Morphology and Surface Roughness of Carbon Steel

3.1 Introduction

The atmospheric corrosion behaviors, principally mechanism of rust layer and surface roughness, are the main concern for service-life prediction of the metallic structures constructions. For steels structures exposed to the outdoor environment in long-term condition, the formation of rust layers of carbon steel, especially weathering steel, will gradually develop. These layers insulate the metal surface from its environment, leading to higher corrosion resistance, and thus slowing down the corrosion kinetic. However, the degree of surface roughness will progress with time.

This chapter will emphasize on the behaviors of atmospheric corrosion of carbon steel based on outdoor exposure test in Cambodia and laboratory corrosion test, with Salt Sprat with Constant Humidity test (SSCH) technique. The surface morphology, crystalline phase, the cross-section of rusted samples, and roughness evolution of carbon steel will be discussed. The scanning electron microscopy (SEM), X-ray diffraction (XRD), energy dispersive spectroscopy (EDS), and optical laser focus, were used as a tool for observing the corrosion product rust layers and surface roughness evaluation.

3.2 The Behavior of Atmospheric Corrosion under Outdoor Exposure Test in Cambodia

3.2.1 The behaviors of rust layer

In a corrosive environment, like marine and industrial atmospheres, the initial corrosion rate (the corrosion loss over the first year) is high. Thus corrosion reaches a stabilization period earlier. While in less severe environments like urban and rural atmospheres, the corrosion attack is small. Thus the stabilization period is prolonged as seen in Fig. 22, [19]. This behavior is caused by the properties of rust

formation on the metal surface, which involve the chemical and mechanical properties of the corrosion product resulting from wet-dry actions of the complex combinations of dew, fog, rain, and the sunshine. For steel structures like weathering steel and carbon steel, they will form a compact and well-adhering rust layer, known as patina when exposed in long-term to an environment. A patina layer will enhance corrosion resistance of the steel and help protect it from further corrosion. Surface morphological analysis, thus, plays an important role in observing the crystalline phase, chemical composition, and physical micro-aspect of the rust layers.

To study the properties of corrosion product or rust layer the investigations were made based on the outdoors exposure test in urban (Phnom Penh) and marine (Sihanoukville) atmospheres, Cambodia, for 1-year exposure test.

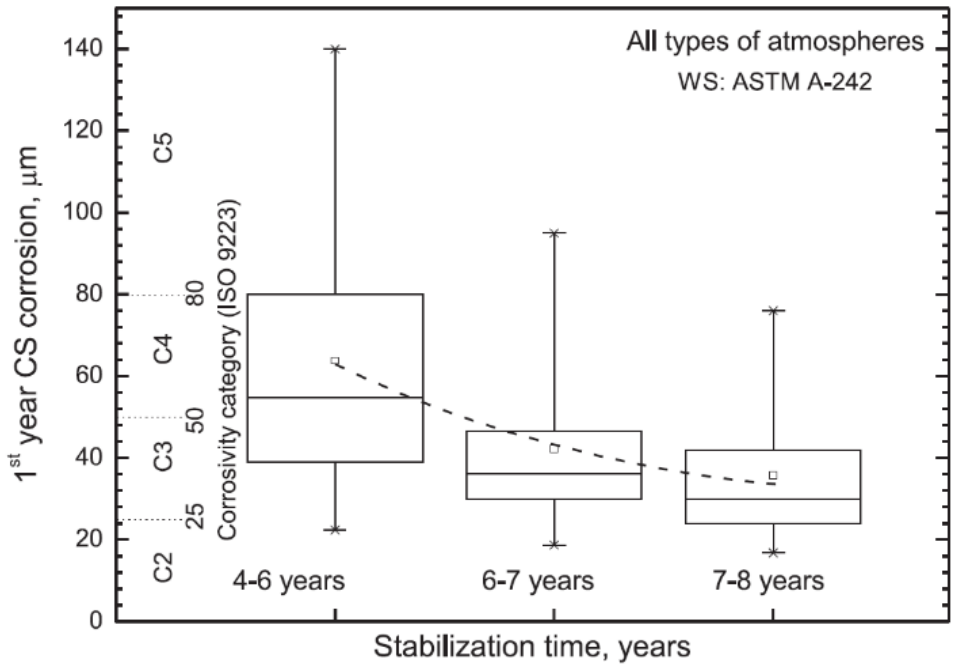

Fig. 22 - Box-whisker plots of rust layer stabilization time of weathering steel as a function of atmospheric corrosivity category (ISO 9223) [19].

3.2.2 Meteorology and outdoor exposure test sites in Cambodia

Cambodia is located in the mainland Southeast Asia and is dominated by monsoonal air flows, which is known as a tropical climate. In summer, (May to November), the Southwest monsoon flows from the Indian Ocean to inland which transports high moisture. In winter (December to April), the flow is reversed by northeast monsoon which transports dry air (*Fig. 23* [51]). The temperature is relatively uniform with a small variation from the annual mean temperature of 28^{o} C. The average annual rainfall is about 1400 mm in the central lowland regions (including Phnom Penh city) and may reach maximum 4000 mm in coastal zones or highland areas (including Sihanoukville) [61]. This natural and forecastable climate facilitates the long-term atmospheric corrosion prediction for this region. The tow exposure site, Phnom Penh and Sihanoukville, are shown in the *Fig. 23*. The one-year outdoor exposure test was conducted from January 7, 2015, to January 7, 2016.

Fig. 23 - Cambodia meteorology and exposure test sites [62].

3.2.3 The corrosion loss of carbon steel under outdoor exposure test

The corrosion loss was determined by measuring weight loss of the sample before and after the test. Fig. 24 shows the mass reduction, (g/m^2), as a function of exposure time, (day), in urban (Phnom Penh) and marine (Sihanoukville) atmosphere. Evidently, the weight loss increases gradually with exposure time. The results indicate that the initial corrosion rate for the first year in Sihanoukville is ($210 g/m^2$ or $27 \mu m$) about three times greater than those in Phnom Penh atmosphere ($70 g/m^2$ or $9 \mu m$).

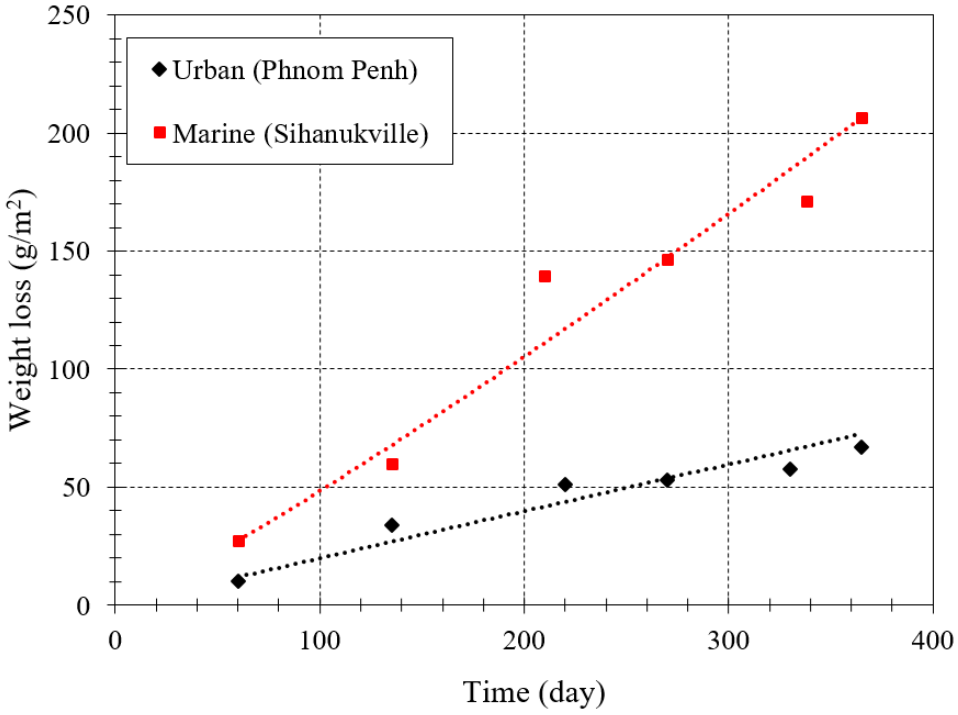

Fig. 24 - Corrosion loss of carbon steel in urban (Phnom Penh) and marine (Sihanoukville) atmosphere during one-year exposure test [62].

3.2.4 Morphology and crystal structure of rust layer

The microstructures of corrosion products can vary considerably depending on the atmospheric parameters where it is exposed. The morphologies of rust and its phases formed on the carbon steel and mild steel have been observed by a number of authors [20][41][24][62]-[64], the commonly known crystalline phases are listed

in *Table 4*. The phases most frequently found generally have structures such as Lepidocrocite, appears as small crystalline globules (sandy crystal) or as fine plate (flowery structure), Akaganeite comes out as cotton ball and rosette or cigar-shaped, Goethite appears as globular structures known as cotton balls (semi-crystalline goethite) or even as acicular structures (crystalline goethite) [20].

Table 4 - The chemical composition of rust phases frequently found in atmospheric corrosion products [20] [41] [24] [62]-[64].

Name	Phase and Composition
Oxides	
Hematite	α-Fe_2O_3
Maghemite	γ -Fe_2O_3
Magnetite	Fe_3O_4
Ferrihydrite	$Fe_5HO_8.4H_2O$
Oxyhydroxides	
Ferrous Hydroxide	$Fe(OH)_2$
Ferric Hydroxide	$Fe(OH)_3$
Goethite	α-$FeOOH$
Akaganeite	β-$FeOOH$
Lepidocrocite	γ -$FeOOH$
Feroxyhyte	δ-$FeOOH$
Others	
Ferrous chloride	$FeCl_2$
Ferric chloride	$FeCl_3$
Ferrous sulfate	$FeSO_4$
Ferric sulfate	$Fe_2(SO_4)_3$

After one-year of outdoor exposure, the samples were subjected to laboratory analysis. In this research, the SEM was used to observe the physical aspect of the rusted surface, and the crystalline phases were evaluated based on those research literature [20],[41],[24],[62]-[64]. For the corrosion morphology formed on the surface of the samples, there was no clear difference between the skyward (facing

the sky) and groundward (facing the ground) of the samples. However, there was a difference between the corrosion morphology in marine and urban atmospheres. In the marine atmosphere, Sihanoukville, the vast area of rust the layer shows numerous micro-cracking as seen in *Fig. 25* (a). The fine plate (γ-FeOOH), rosette (β-FeOOH), cigar-shaped (β-FeOOH), and globular structures (α-FeOOH) can be partially found on the rust area, as seen in *Fig. 25* (b), (c), (d), and (e) respectively. In the urban atmosphere, Phnom Penh, the morphology of rust appears as a mixture of crystal structures, as seen in the *Fig. 26* (a), and the random spot of a big flowery crystal structure of Lepidocrocite (γ-FeOOH), as seen in *Fig. 26* (b).

The X-Ray diffraction pattern indicated no significant difference between the crystal structures of corrosion products formed in Sihanoukville and Phnom Penh atmospheres as seen in *Fig. 27*. However, there is a noticeably different between the skyward and groundward of the samples. Obviously, at the diffraction angle between 26° and 28°, there are two sharp peaks of XRD pattern detected on the skyward of the samples, but there is only one peak for the groundward of the samples of both atmospheres. The peaks indicate the presence of dust (SiO_2) deposition on the skyward of the samples, which are tiny grains of sand. A general view of the XRD results, the majority of the crystal structures in both Sihanoukville and Phnom Penh atmospheres were Lepidocrocite, Goethite, and Maghemite. However, Lepidocrocite and Magnetite appear more in the corrosion product of carbon steel exposed to Sihanoukville, and less so in Phnom Penh atmosphere. Akaganeite may be present in the rust formed in both atmospheres, but it is not clear because the intensities of the Akaganeite peaks are slightly small.

3.2.5 Cross section observation of rust layer

- Physical micro-aspect: To observe the cross section of rust layer, the rusted samples were covered by epoxy resin, cut by refine-cut machine, washed with deionized water, dried by air pressure cleaner, and examined by SEM. The SEM images indicate that the rust layers are curly and uneven with thick and thin parts. Thus, it may result in high degree of roughness, especially the surface of metal exposed to the marine atmosphere (*Fig. 28* (b)). The rust layer formed on the

samples exposed to the urban atmosphere (Phnom Penh) is more compact and dense than that of the marine atmosphere. For both atmospheres, the rust on the skyward side of the samples is more compact and well-adhering than the groundward side. This phenomenon is the result of drying effect of solar radiation and washing effect of raining action [20]. The corrosion products formed in marine atmosphere indicate the formation of multiple strata, or layer, at the outermost rust layers for both skyward and groundward side of the samples (*Fig. 28* (b)). The strata seem to indicate a fast development of rust periodically at a corrosive atmosphere.

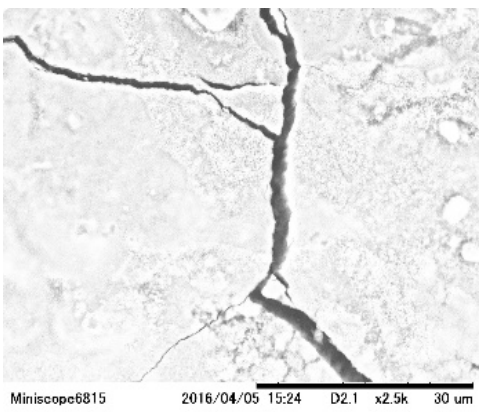

(a) Rust with micro-cracks.

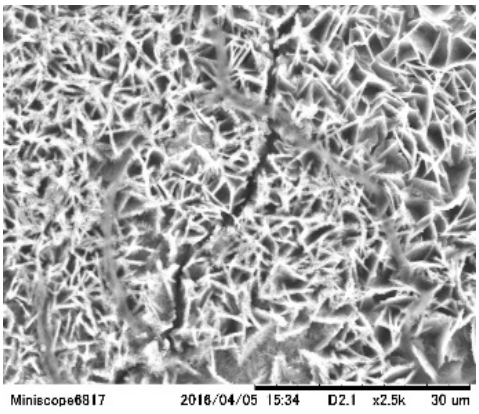

(b) Flowery structure of Lepidocrocite.

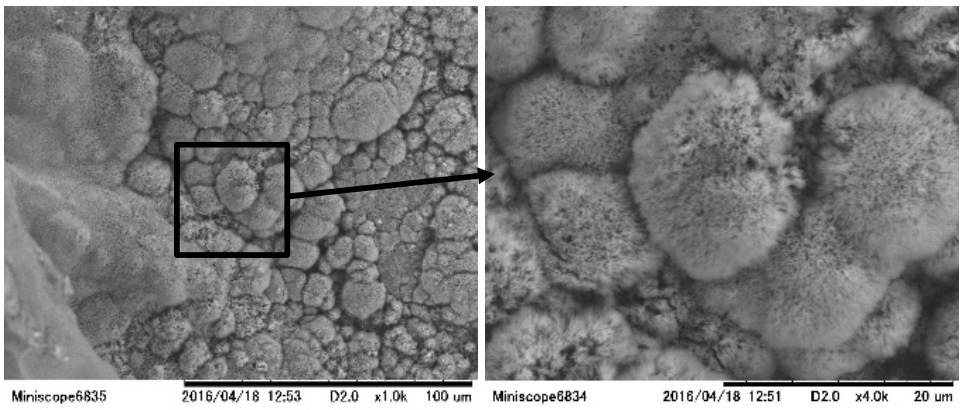

(c) Rosette structure of Akaganeite.

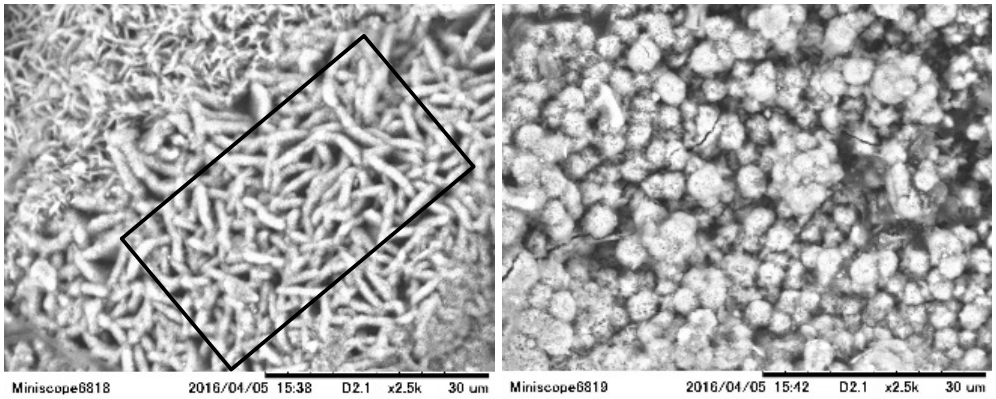

(d) Cigar-shape of Akaganeite. *(e) Cotton balls of Goethite.*

Fig. 25 - Morphology of rust at the marine atmosphere (Sihanoukville) [62].

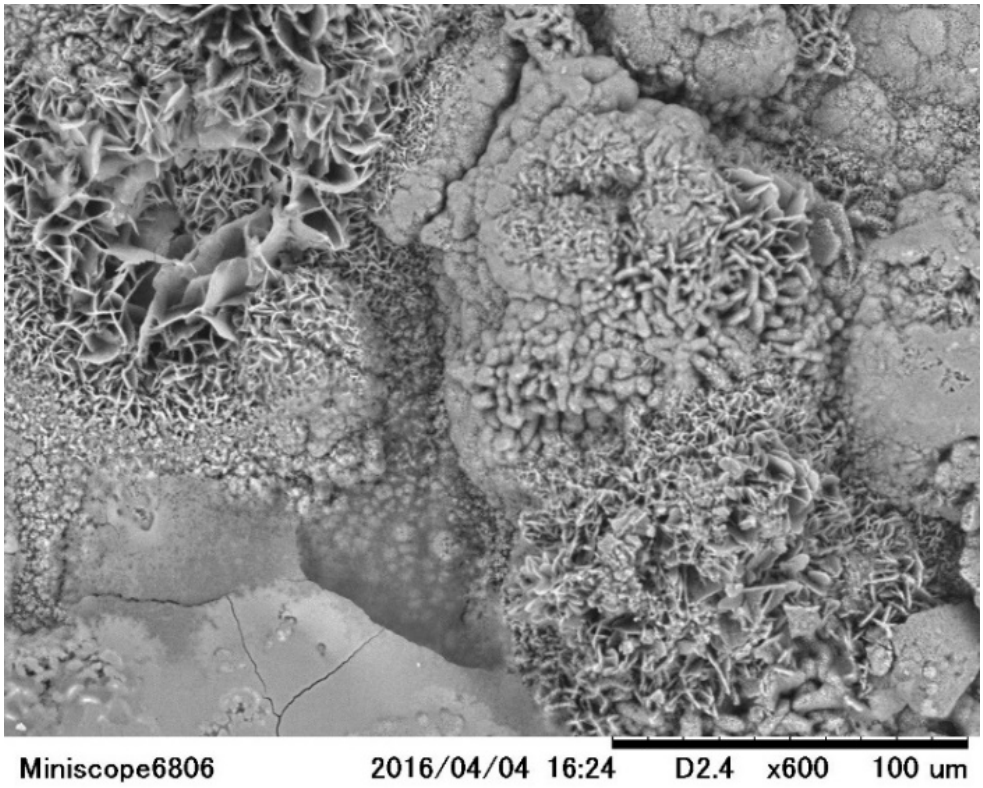

(a) Mixed crystal structure.

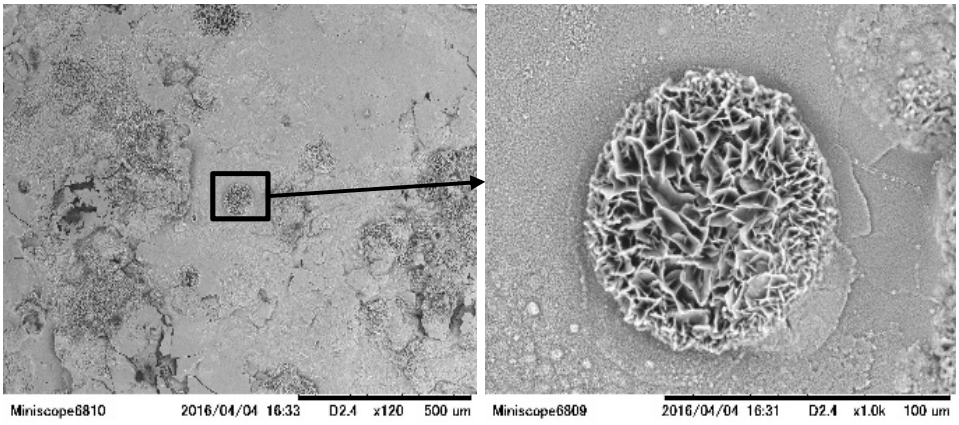

(b)A random spot of the big flowery crystal structure of Lepidocrocite.

Fig. 26 - Morphology of rust at the urban atmosphere (Phnom Penh).

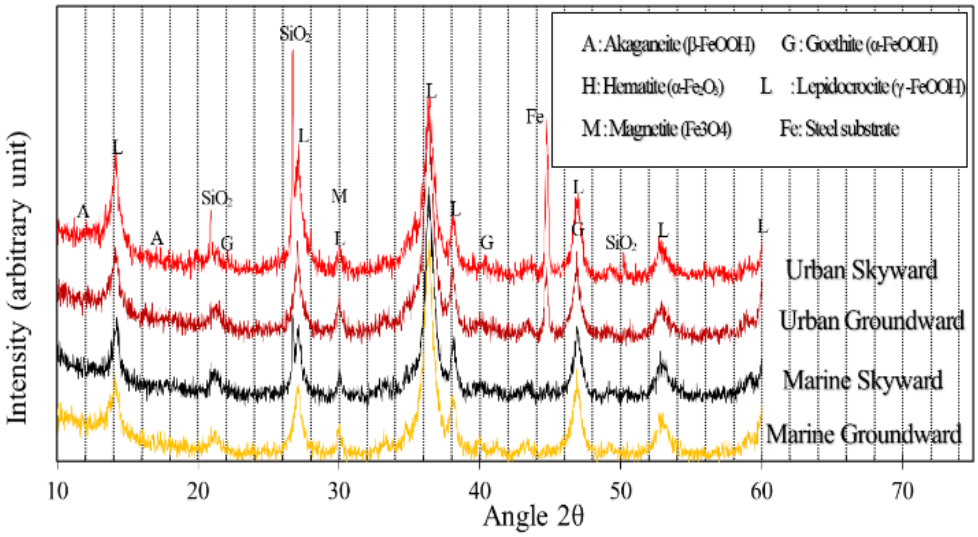

Fig. 27 - X-Ray Diffraction patterns of corrosion products exposed to marine (Sihanoukville) and urban (Phnom Penh) atmospheres [62].

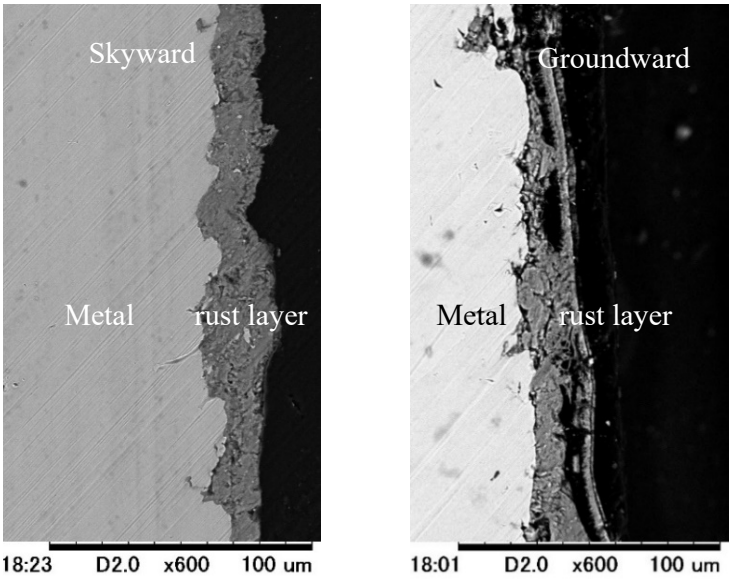

(a) skyward and groundward of the urban atmosphere (Phnom Penh).

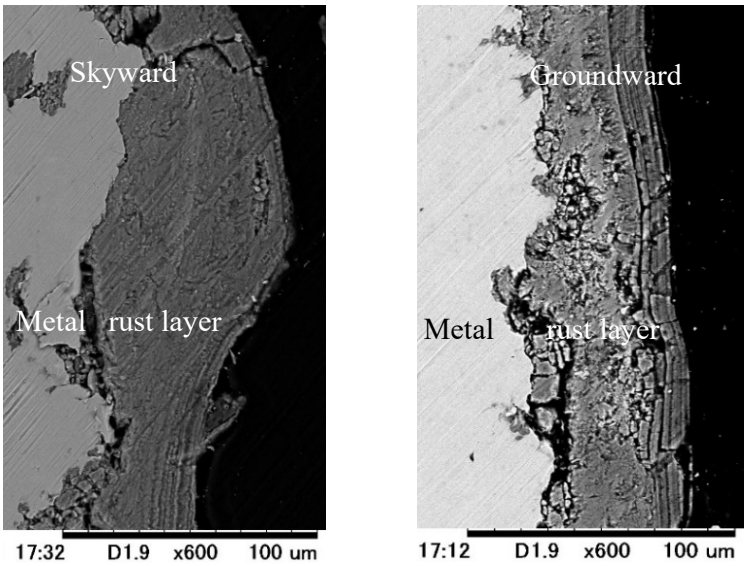

(b) skyward and groundward of the marine atmosphere (Sihanoukville)

Fig. 28 - SEM images show the cross-section observation on the particular area of the rusted sample after one-year exposure test [62].

- Chemical properties: The chemical compositions of the corrosion products were observed by SEM/EDS. The semi-quantitative with line-scanning approach was used to inspect the corrosion products through the cross section of the rusted

samples, from metal/rust interface to the outermost rust layer, in both marine and urban atmosphere, as seen in Fig. 29. The line scanning increment used was 0.1 μm within the detected 30 μm segment, this generated 300 data points. The relevant results from the EDS test are shown in Fig. 30 (a)-(d), where quantities of atoms (At %) of Fe, O, S, and Cl were detected and observed. The results revealed that oxygen and iron are the major substances of the corrosion products, while sulfur and chlorine are the minorities as shown in Table 5. The quantity oxygen substances are twice of iron substances. Thus, the *FOOH* is considered as the main compound of corrosion products. Partially, the ratio of the peaks Fe/O ≈ 2/3 indicated the presence of Fe_2O_3 as seen in Fig. 30 (a) and (b). The trend lines in the figures also indicated that as we move from the outermost layer towards the innermost layer the iron concentration increases, while oxygen concentration decreases. So, the innermost rust layer is considerably more dense and compact with Fe atom.

Fig. 30 (c) and (d) show that the sulfur and chlorine contained in the rusted sample exposed to the Sihanoukville are slightly higher than that of the Phnom Penh atmosphere. And the values of these elements strongly fluctuate between 0 and 1 percent of the total atoms.

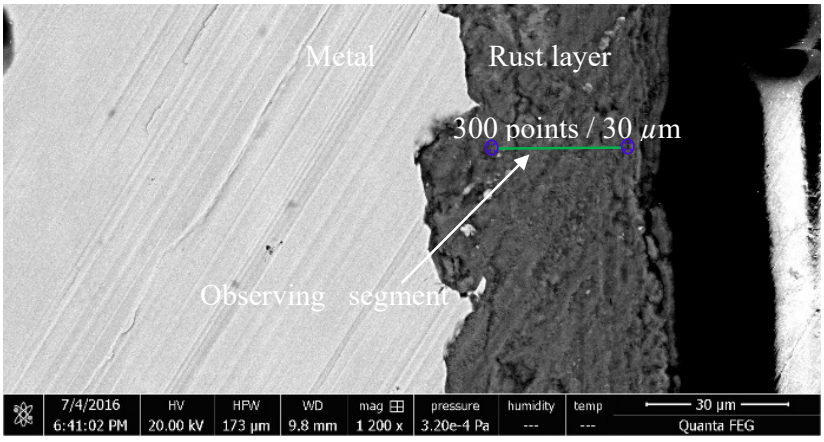

Fig. 29 - EDS pattern of semi-quantitative analysis with the line-scanning approach.

Table 5 - The mean value of Atomic percent observed through the cross section of the rusted samples in both urban and marine atmosphere in skyward faces [62].

Atmosphere	*Province/City*	*Fe (%)*	*O (%)*	*S (%)*	*Cl (%)*
Marine	*Sihanoukville*	*32.05*	*67.18*	*0.45*	*0.33*
Urban	*Phnom Penh*	*31.22*	*68.22*	*0.36*	*0.20*

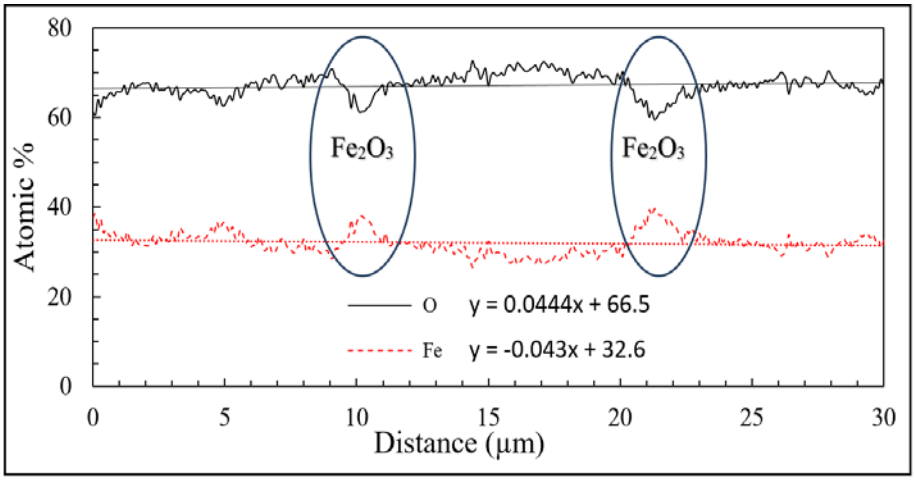

(a) EDS-pattern of O and Fe in the marine atmosphere.

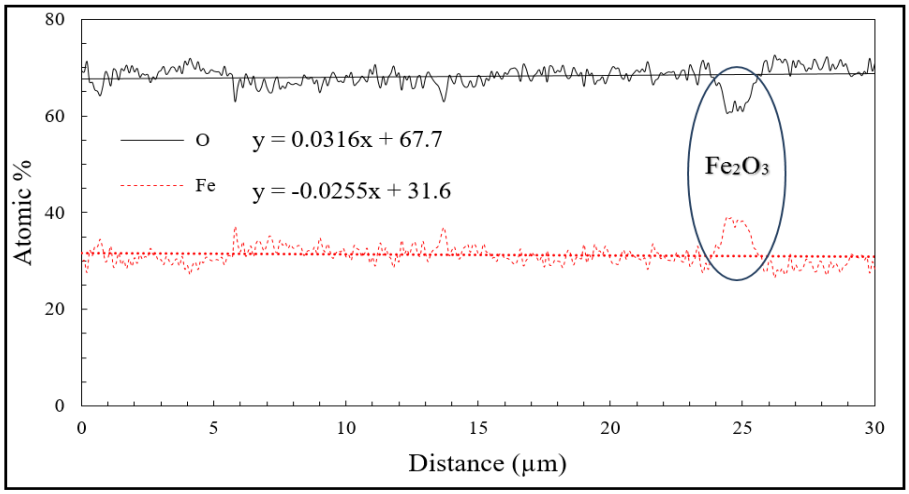

(b) EDS-pattern of O and Fe in the urban atmosphere.

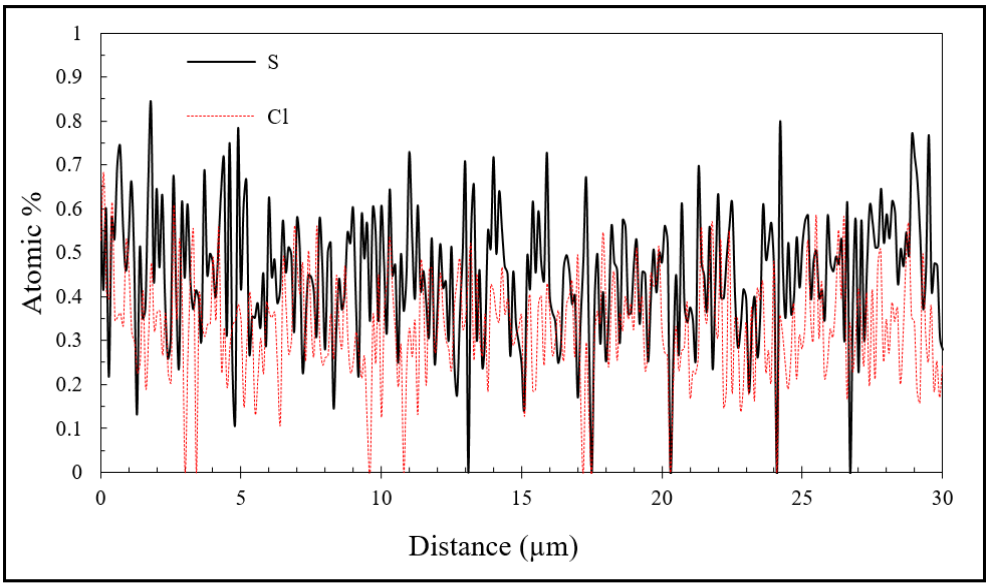

(c) EDS-pattern of S and Cl in the marine atmosphere.

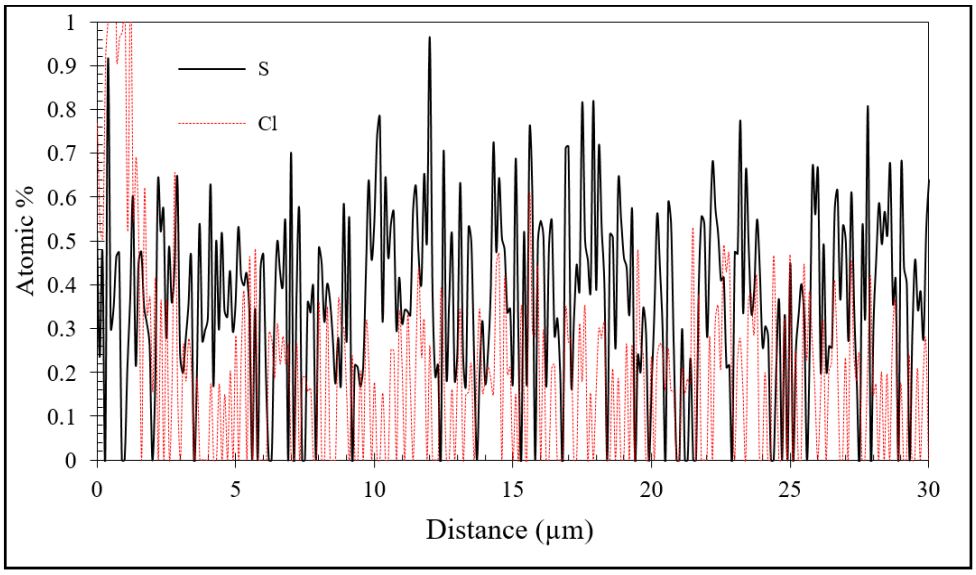

(d) EDS-pattern of S and Cl in the urban atmosphere.

Fig. 30 - Cross-section observation of rusted samples after one-year exposure test [62].

3.2.6 Discussion

- Corrosion kinetic: In Sihanoukville, the CR is notably greater than that in Phnom Penh atmosphere, because of the Cl and SO_2 deposition rates in Sihanoukville are higher than those in Phnom Penh atmosphere, which was confirmed by EDS-pattern

as seen in Table 5. The large amount Cl disposition rate in Sihanoukville is the consequence of monsoon airflow, which transports airborne salinity containing corrosive, Cl, species inland. On the other hand, the SO_2 deposition rate in the Sihanoukville atmosphere is also higher than that in Phnom Penh atmosphere due to the gas emission from the industrial zone located nearby the Sihanoukville test station. Furthermore, Phnom Penh is located relatively far from the coast (about 150 Km, straight-line), so the Cl deposition rate is notably low. Also, the pollutant gas emission, SO_2, in Phnom Penh atmosphere is also low [65]. The other main important parameters, which enhance corrosion kinetic is the time of wetness. Time of rain is essential for atmospheric corrosion. The annual precipitation rate in Sihanoukville (Pr = 4000 mm/y) is significantly higher than the rain in Phnom Penh (Pr = 1400 mm/y), [61], which leads to higher corrosion kinetic. However, both Sihanoukville and Phnom Penh atmospheres are not considered to be the severe atmospheres for corrosions. According to ISO 9223, Sihanoukville and Phnom Penh atmospheres are classified as medium and low corrosivity respectively.

- Characteristic of corrosion product layer: Sulfur and chlorine are the minority elements presented in the corrosion products. However, these substances most likely perform as the catalyst for corrosion acceleration since it effectively breakdown the oxide film in the initial stage of corrosion. Further reaction of S^{2-} and Cl^- with Fe^+ and oxygen formed rust such as $FeCl_2$, $FeCl_3$, $FeSO_4$, and $Fe_2(SO)_3$. However, these chemical compounds are very limited and rarely observed. The most predominant substance, which frequently found in atmospheric corrosion products is the Oxyhydroxides (*FOOH)* that presents in deference crystal phases. The rust layer of the samples exposed to the marine atmosphere, Sihanoukville, is loose, porous, and contains many cracks; while that exposed to urban, Phnom Penh, atmosphere is dense and compact. The porousness rust layer allows water, oxygen, and others corrosive species to penetrate to reach the metal surface; it has a poor capability for atmospheric corrosion protection. In contrast, the dense and compact rust layer acts as an insulation to effectively inhibit the diffusion of oxygen and other species to reach the metal surface, leading to a lower CR.

3.3 Surface Roughness Evolution of Carbon Steel Subjected to Corrosion

One of a crucial problem of atmospheric corrosion is the sudden collapse of the metallic structure without consciousness. Mechanical properties of the structure are significantly affected by corrosion pit or notch. These courses by the revolution from pitting corrosion or localize corrosion to microcrack initiation and grow due to the tensile stress and fatigue loading…etc. Roughness evaluation is often a good predictor of the performance of a mechanical structure and component, since irregularities in the surface may form nucleation sites for cracks. For metal structures like carbon steel, the atmospheric corrosion attack is generally known as uniform corrosion; depth pitting is very rare in observing. However, at the corrosive atmosphere with high Cl concentration, the pitting and/or localize corrosion could be detected. This section will emphasize on the surface evolutions of carbon steel subject to 1-year atmospheric corrosion test in Cambodia, and salt spray constant humidity test.

3.3.1 Salt spray with constant humidity (SSCH) test

With a high concentration of Cl^- in the electrolyte layer, the corrosion reactions proceed faster than it behaves in an actual environment. The corrosion test in artificial atmosphere, called salt spray with constant humidity test, was used to accelerate corrosion in order to observe metal surface evolution in the most severe environment, especially the coastal zones. The 3% of NaCl solutions were sprayed uniformly on the surface of the samples with the mass distribution of $0.4 g/cm^2$. And the samples were kept in the humidity chamber with a constant relative humidity of RH=85%. The samples were continuously retrieved (2 days to 300 days) from the chamber. Then, the metal surface evolutions were observed by using a 3D scanner (Fig. 31).

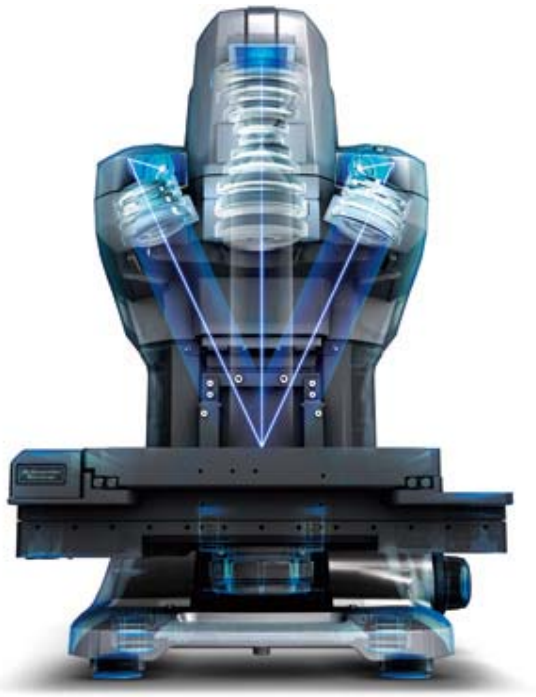

Fig. 31 - 3D scanner KEYENCE

3.3.2 Roughness parameters and method for analysis

Surface roughness commonly refers to the random deviations in the height of the surface from the mean line, *m*, or reference plane. It is measured along the single line profile (2D profile analysis) or a set of parallel profiles (3D surface profile).

- ***Two-dimensional (2D) analysis***

The parameters descript the roughness behaviors are Maximum height (R_z), arithmetic average (R_a), standard deviation or variance (σ), Skewness, and Kurtosis. R_a is the arithmetic mean of absolute values of vertical deviation from the mean line (*m*) through the profile *Z(x)*. It is physically defined as the absolute area bounded by the profile, *Z(x)*, and the mean line, *m*, (see *Fig. 32*). The standard deviation is the square root of the arithmetic mean of the square of vertical deviation from the mean. The mathematical expression of R_a and σ are:

$$Rz = max\ Z(x) - min\ Z(x) \tag{11}$$

$$Ra = \frac{1}{L}\int_0^L |Z - m| dx \tag{12}$$

$$m = \frac{1}{L}\int_0^L Z dx \tag{13}$$

$$\sigma^2 = \frac{1}{L}\int_0^L (Z - m)^2 dx \tag{14}$$

Where L is the sampling length of the profile of metal surface.

Other parameters, which are rarely used in most of the statistical analysis, are Skewness, *Sk*, and Kurtosis, *Ku*. Skewness is a measure of the degree of asymmetry of the probability distribution of the random variable (Fig. 33 (a)). If the left tail is longer than that of the right, the function is said to have negative Skewness. If it reverse is true, it has a positive skewness. But then, if the two tails are equal, it has zero skewness. The Skewness is an essential method for estimating the behavior corrosion pit or localizes corrosion in function of exposure time. Kurtosis is a measure of whether the data are peak or flat relative to the random distribution (Fig. 33 (b)).

$$Sk = \frac{1}{\sigma^3 L}\int_0^L (Z - m)^3 dx \tag{15}$$

$$Ku = \frac{1}{\sigma^4 L}\int_0^L (Z - m)^4 dx \tag{16}$$

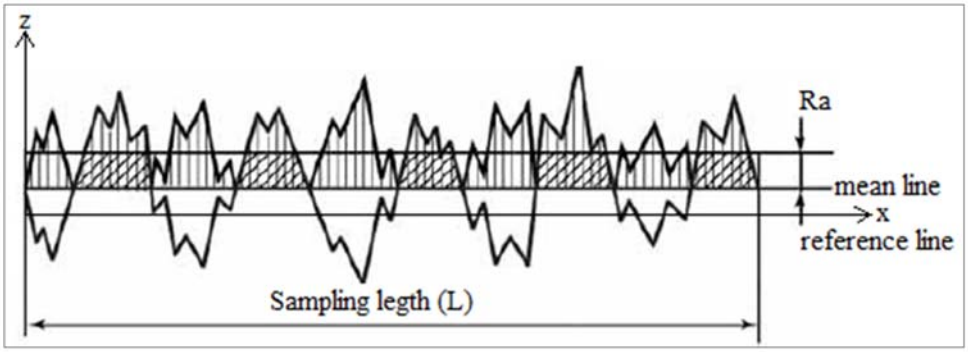

Fig. 32 - Arithmetical mean height (single profile of roughness).

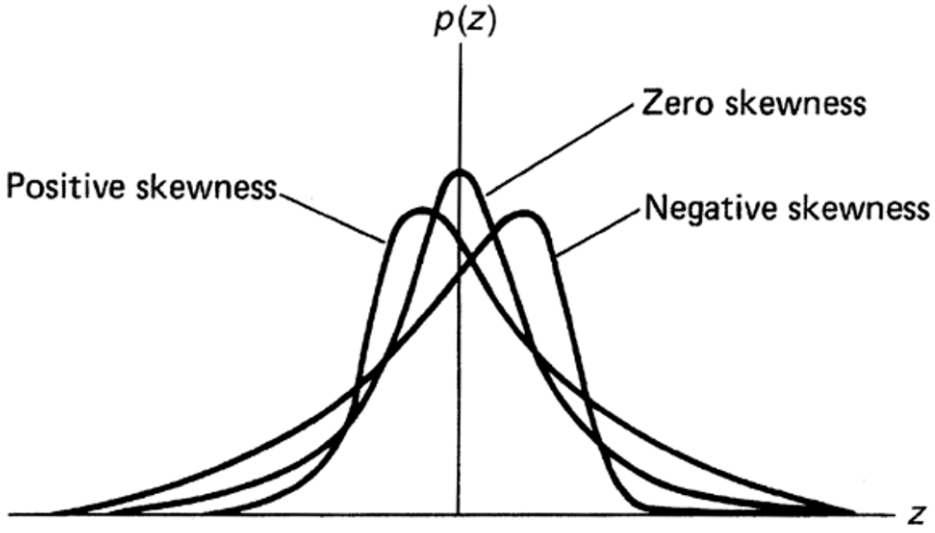

(a) Skewness

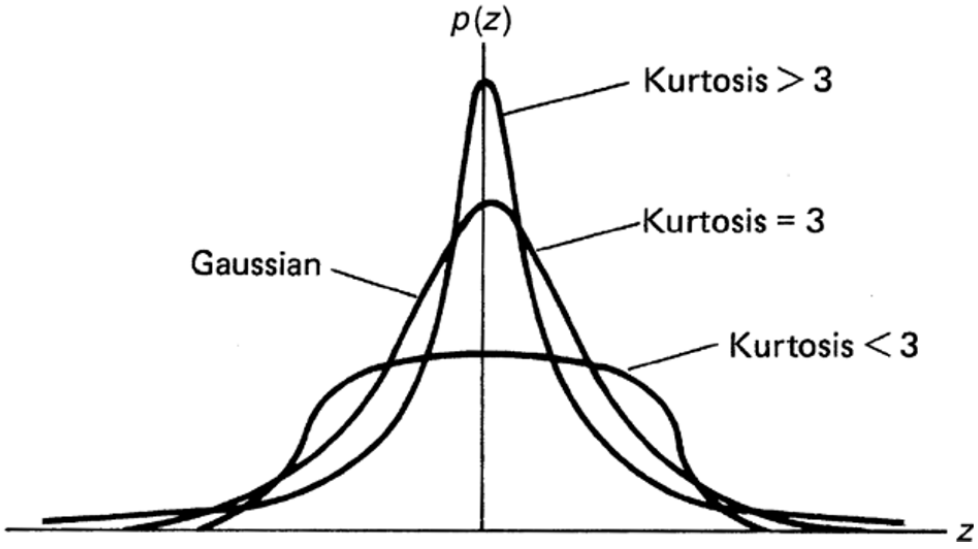

(b) Kurtosis

Fig. 33 - Probability density function representation of (a) Skewness and (b) Kurtosis.

- ***Three-dimensional (3D) analysis***

The 3D parameters analysis provide more accurate results, which were used in this case study. It expresses the arithmetic average (Sa), Skewness (Ssk), kurtosis, (Sku), within the measuring area of Z(x,y). To simplify in the calculation, the mean

plan is considered to be coincident with reference plan. And thus the mathematical expression of the 3D roughness parameters are shown as below:

$$\mathrm{Sz} = \mathrm{Max\ Z(x,y)} - \mathrm{min\ Z(x,y)} \tag{17}$$

$$Sa = \frac{1}{A}\iint_A |Z(x,y)|dxdy \tag{18}$$

$$\sigma^2 = \frac{1}{A}\iint_A Z^2(x,y)dxdy \tag{19}$$

$$Ssk = \frac{1}{\sigma^3 A}\iint_A Z^3(x,y)dxdy \tag{20}$$

$$Sku = \frac{1}{\sigma^4 A}\iint_A Z^4(x,y)dxdy \tag{21}$$

In this case study, the 3D scanner KEYENCE VR-300 was used to observe the 3D data of corroded surfaces of carbon steel sheet samples. Thereafter, the roughness parameters and graphs were computed and plotted by numerical analysis software, MATLAB.

3.3.3 Corrosion pit evolution

- The samples exposed to the outdoor environment: The surface characteristics of corroded samples exposed to the urban and marine atmospheres in Cambodia were observed and shown in the Fig. 34 and Fig. 35 respectively. Initially, the corrosion attacks locally to form pits or notches on the surface of carbon steel samples. For the samples exposed to the urban atmosphere (Phnom Penh), the corrosion continues to attack at the bottom of the pits. Thus the pits go deeper and deeper throughout 1-year of exposure test, as seen in Fig. 34 (a-c). In contrast, the samples exposed to the marine atmosphere (Sihanoukville), where the corrosion was more severe, the corrosion pits evolved in deep direction for the first 6-months. After that, the corrosion attacked both deep and wide directions. After 1-year exposure test, the pits evolved as open-mouth mode (see Fig. 35 (c)) and formed overlapping pits.

It is expected that extending longer-term exposure test, the pits or notches will be diminished and formed as valleys.

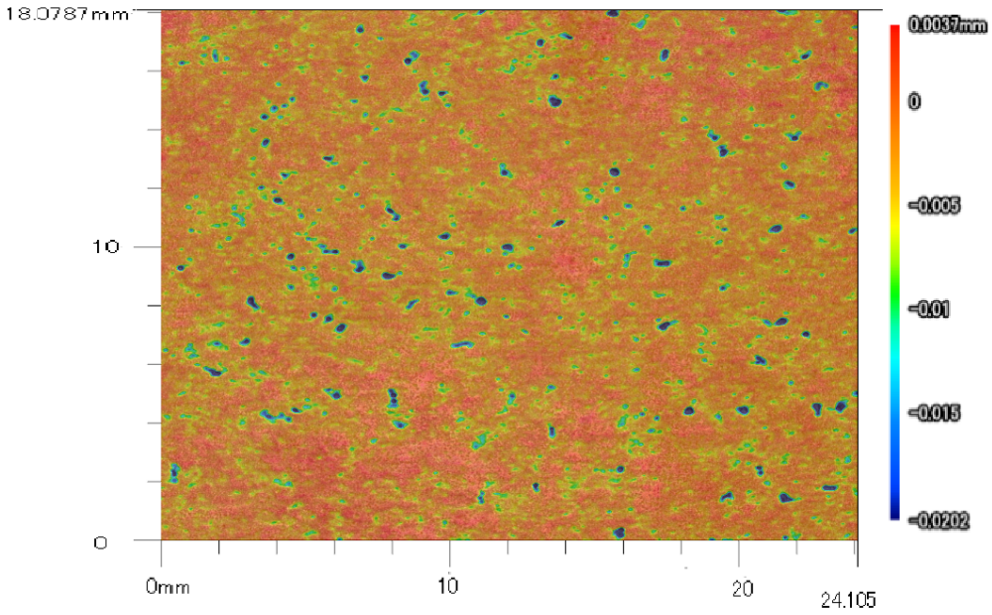

(a) 1-month

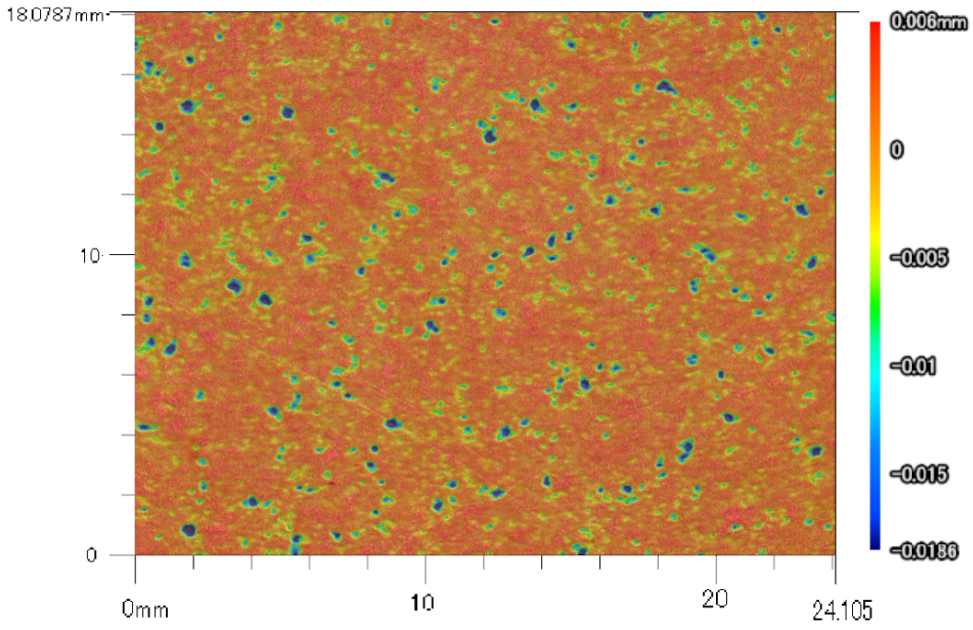

(b) 6-months

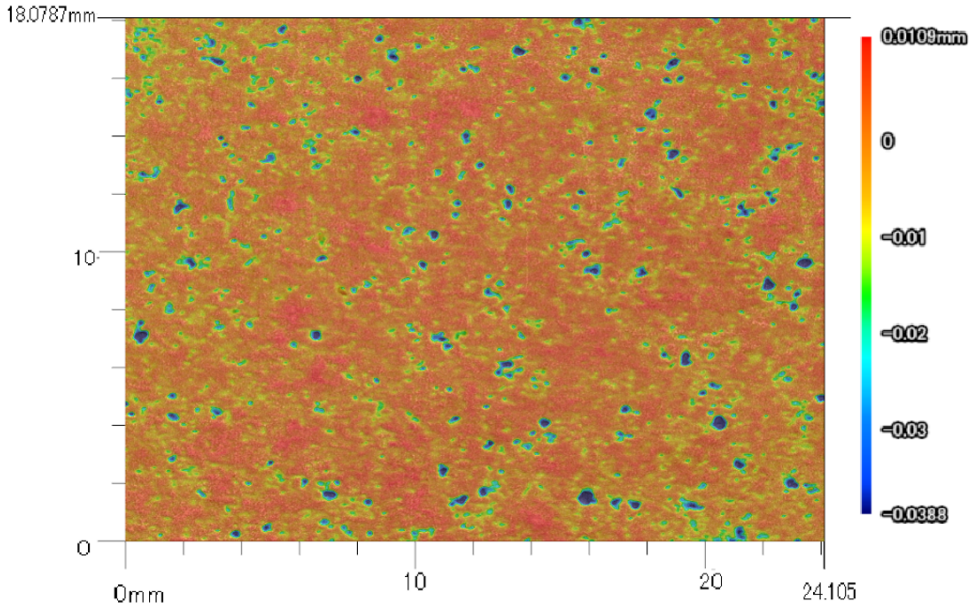

(c) 1-year

Fig. 34 - Surface evolution of carbon steel exposed to urban atmosphere (Phnom Penh).

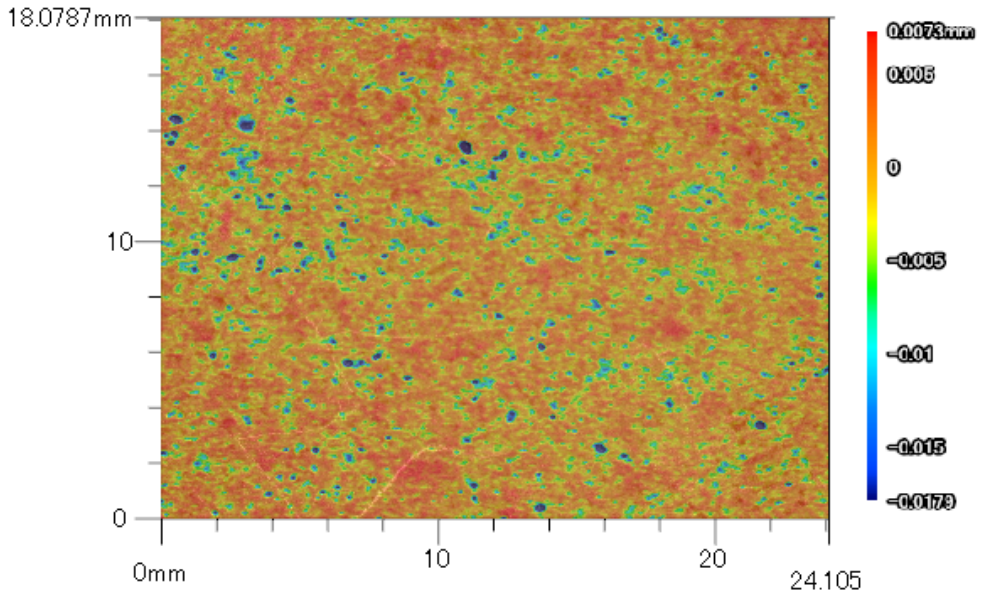

(a) 1-month

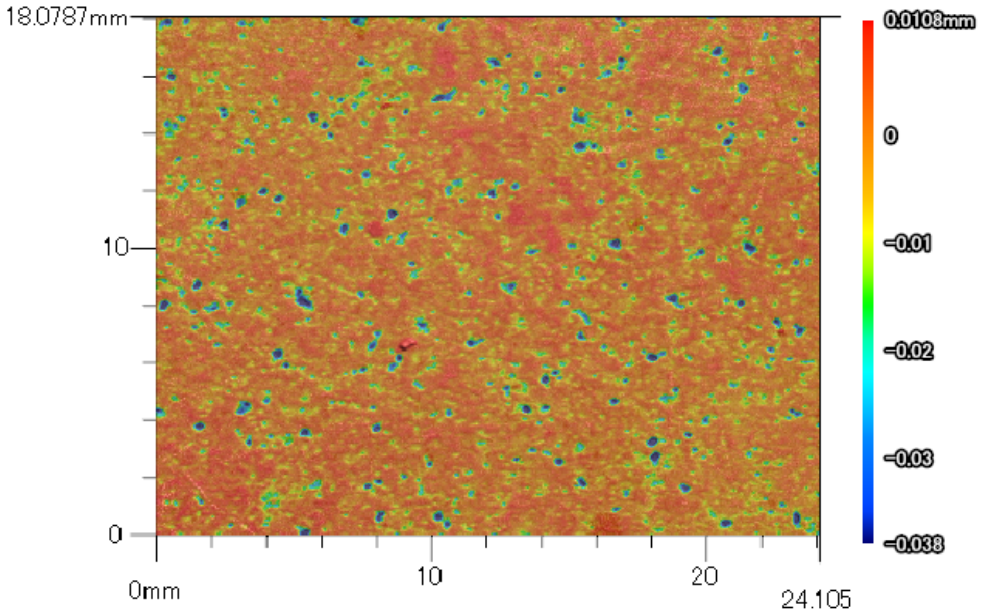

(b) 6-months

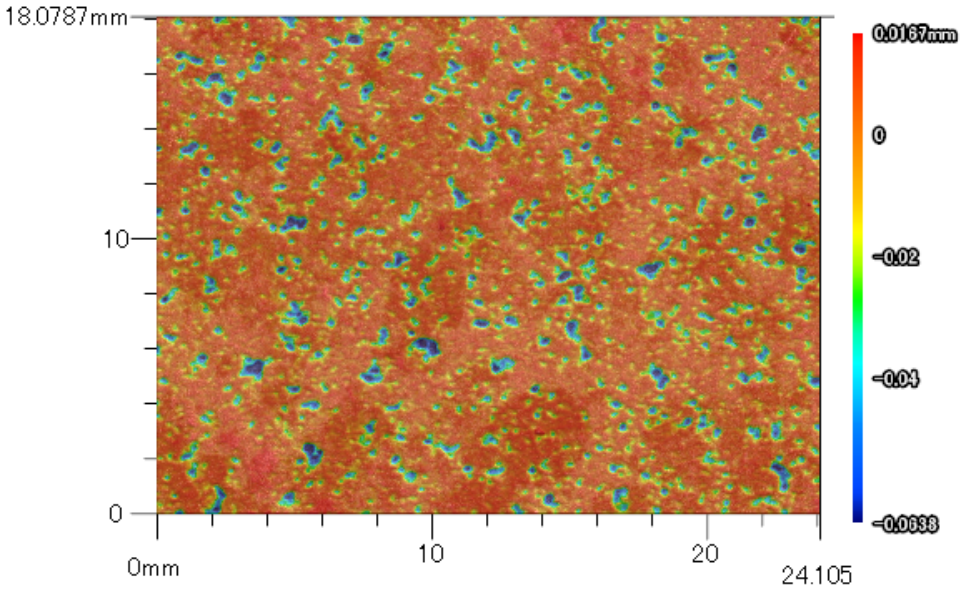

(c)1-year

Fig. 35 - Surface evolution of carbon steel exposed to marine atmospheres (Sihanoukville).

- Salt spray with constant humidity (SSCH) test: To find the characteristic of a corroded surface under long-term atmospheric condition accelerated corrosion test SSCH was used. The surface evolutions resulted by SSCH during 10-months are shown in the Fig. 36 and Fig. 37 below. In general view, the corroded surface of carbon steel normally formed as shallow pits, since the ratios of *a* over *b* were found to be greater than one, *(a/b>1)*, as seen in Fig. 36 (a). In the early stage of corrosion, the shallow pits sparely formed (Fig. 37 (a)), and then the pits distributed densely to form overlapping shallow pits (Fig. 36 (b)). Finally, after 5-month of SSCH, the corrosion entirely attacked on the surface of the metal and formed as valleys, which result in uniform corrosion as seen in Fig. 36 (c). The Fig. 37 shows the overview of the corrosion pits evolution during 10-months of SSCH, including shallow pits (Fig. 37 (a)), overlapping pits (Fig. 37 (b)), and valley pits know as uniform corrosion (Fig. 37 (c) and (d)).

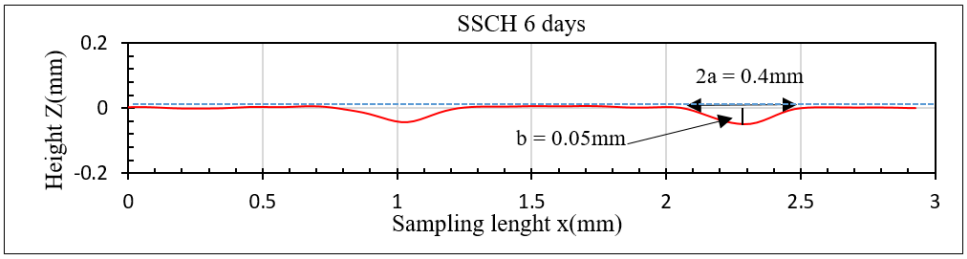

(a) Shallow pits.

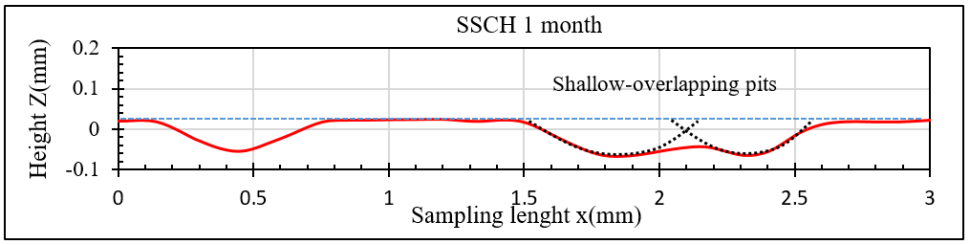

(b) Overlapping shallow pits.

(c) Valley pits formed after 5-months: Uniform corrosion.

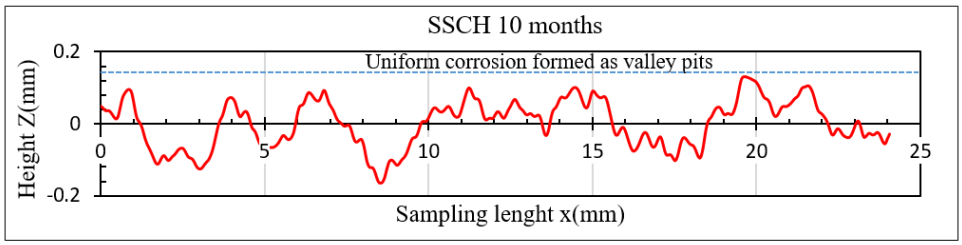

(c) Valley pits formed after 5-months: Uniform corrosion.

Fig. 36 - 2D profile represented the corrosion pits evolution.

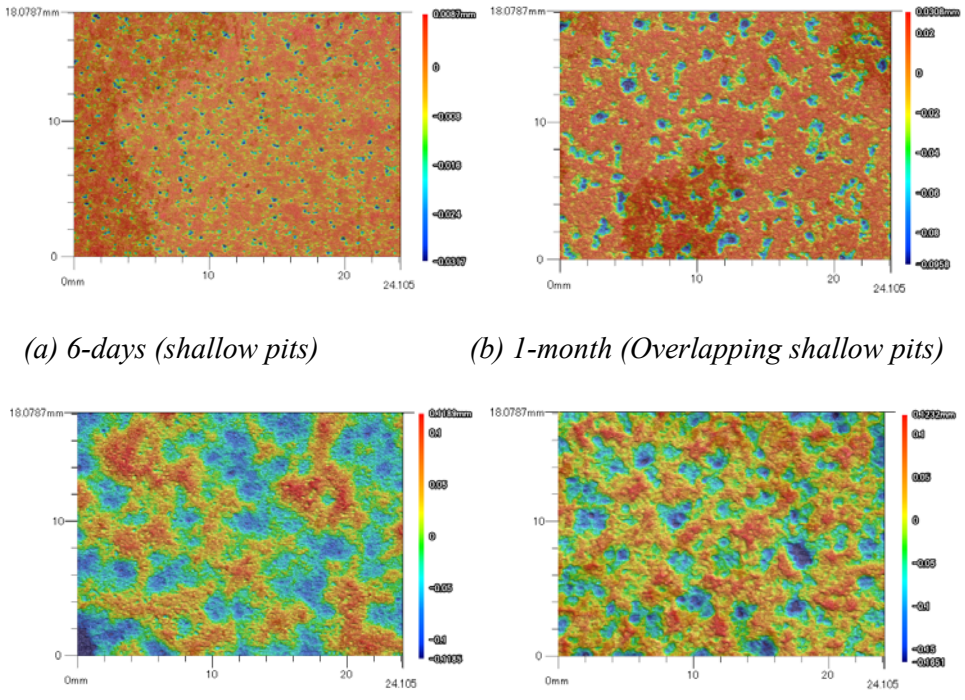

(a) 6-days (shallow pits) *(b) 1-month (Overlapping shallow pits)*

(c) 5-months (uniform corrosion) *(d) 10-months (uniform corrosion)*

Fig. 37 - Surface evolution of carbon steel under SSCH.

3.3.4 Result of roughness parameter analysis

The maximum height (Sz), arithmetic average (Sa), standard deviation (σ), Skewness (Sk), and Kurtosis (K) of the atmospheric corrosion test and SSCH test were shown in Table 6. The degree of Sz, Sa, and σ of carbon steel corrosion increased with exposure time.

Table 6 - Roughness parameters

Atmospheres	Time	Maximum height	Arithmetic average	Standard deviation	Skewness	Kurtosis
	Day	Sz	Sa	σ	Sk	K
Urban (Phnom Penh)	30	0.055	0.0023	0.004	-3.3228	16.13
	180	0.056	0.0032	0.0044	-1.8437	8.1551
	365	0.115	0.0057	0.0081	-2.445	11.1639
Marine (Sihanoukville)	30	0.0532	0.0029	0.0041	-2.1402	11.09
	180	0.1266	0.0064	0.0089	-2.03396	9.6438
	365	0.152	0.0124	0.0168	-1.7712	6.036
SSCH	2	0.0458	0.0026	0.0035	-1.4622	6.4474
	4	0.0488	0.0025	0.0035	-2.0708	10.154
	6	0.0708	0.0046	0.0066	-2.299	10.9785
	8	0.1134	0.0083	0.0113	-1.827	7.0704
	30	0.1864	0.0204	0.0267	-1.5354	5.0555
	150	0.3527	0.0352	0.04	0.0835	2.6944
	300	0.3839	0.0463	0.0579	-0.3226	3.0113

Skewness explains the degree of asymmetry from the mean value. On the corroded surface, it was normally found that the probability density function (PDF) of random variable Z(x,y) have negative Skewness because of the left tail longer than the right. This negative Skewness indicated the non-uniformly distribution of random variable Z(x,y) due to the existing of pits on the corroded surface as seen in Fig. 38. The Fig. 39 and Fig. 40 show the density distribution of corroded samples exposed to marine and urban atmospheres during 1-year in Cambodia. In the early stage of corrosion, the variable Z(x,y) of the corroded face was highly concentrated around the mean of zero (which show the sharp peak of PDF), and skewed with a long tail to the left; it means that the pits were sparsely initiated. Prolonged the exposure time, till 1-year, the number of pits increased and distributed densely; thus, the density distribution of corroded surface widely distributed around the mean plan which shown the blunt peak of PDF. Under 1-year of exposure test, the data distributions are peaked, since the values of Kurtosis were higher than 3 (see Table 6). However, the results of SSCH show that, when the carbon steel samples strongly corroded into some level (after 5-months of the SSCH test, for example) the data distributions of PDF fit to normal distribution which has the degrees of Skewness about zero (Sk=0) and Kurtosis about three (K≈3), as seen in the Fig. 41. When the data set of corroded surface reaches to a normal

distribution, the form of corrosion is considered as uniform corrosion, as seen in the Fig. 37 (c) and (d).

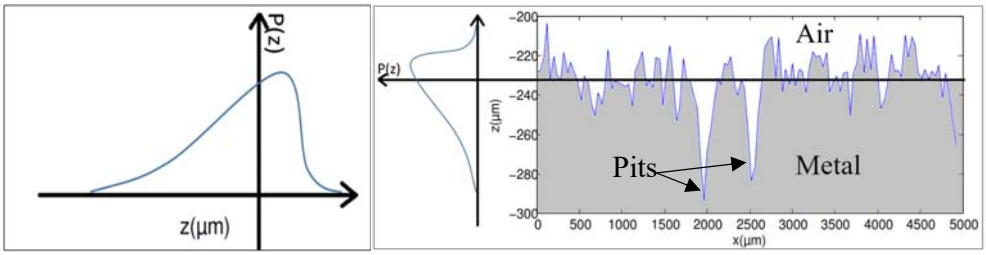

Fig. 38 - Single profile represented the probability density function of roughness.

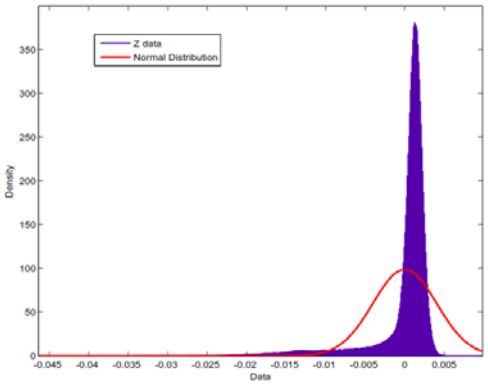

(a) Exposed 1-month in Phnom Penh

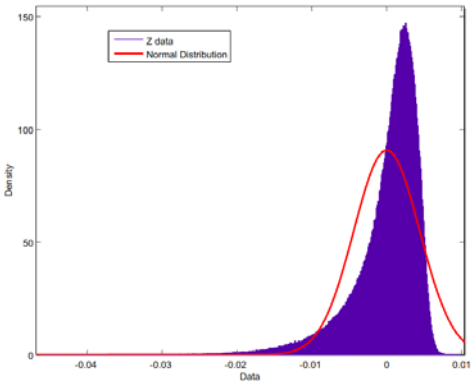

(b) Exposed 6-months in Phnom Penh

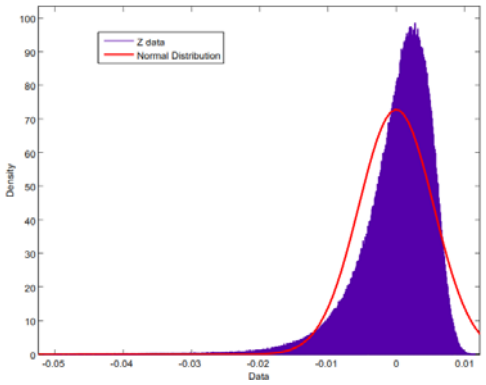

(c) Exposed 12-month in Phnom Penh

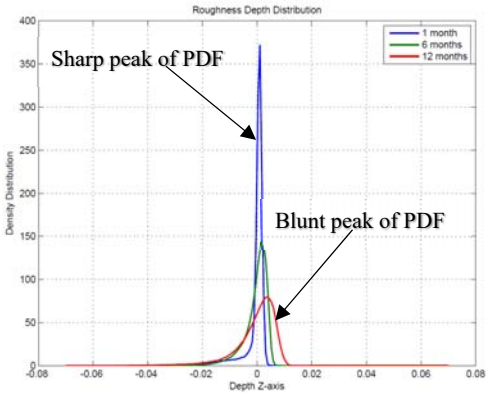

(d) Combine results of PDF

Fig. 39 - The data distribution and normal distributions of the corroded surface of carbon steel exposed to urban (Phnom Penh) atmosphere in Cambodia.

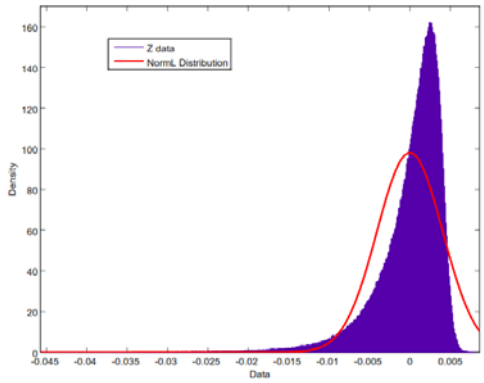

(a) Exposed 1-month in Sihanoukville

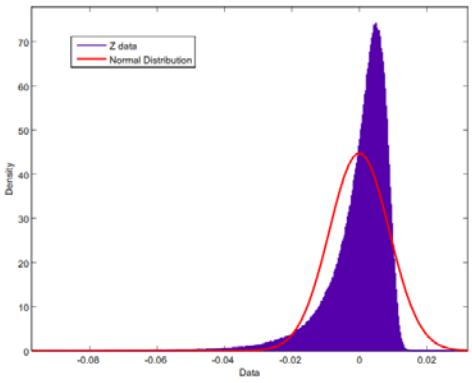

(b) Exposed 6-months in Sihanoukville

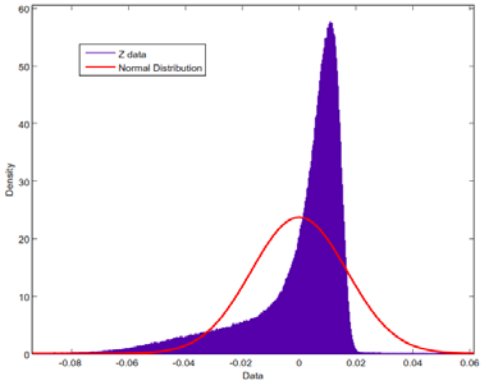

(b) Exposed 12-months in Sihanoukville

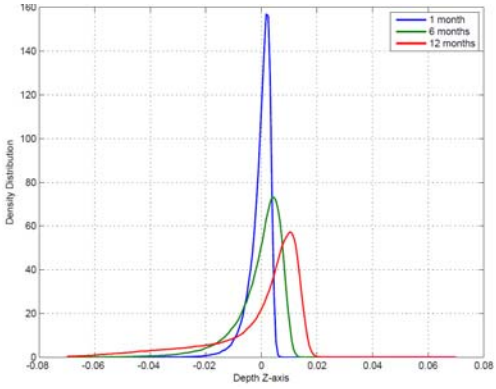

(c) Combine results of PDF

Fig. 40 - The data distributions and normal distributions of the corroded surface of carbon steel exposed to marine (Sihanoukville) atmosphere in Cambodia.

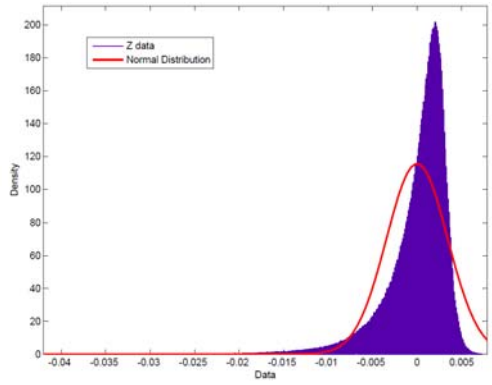

(a) 2-days: Negative Skewness

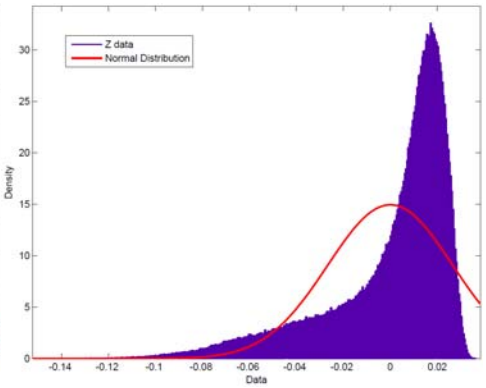

(b)1-month: Negative Skewness

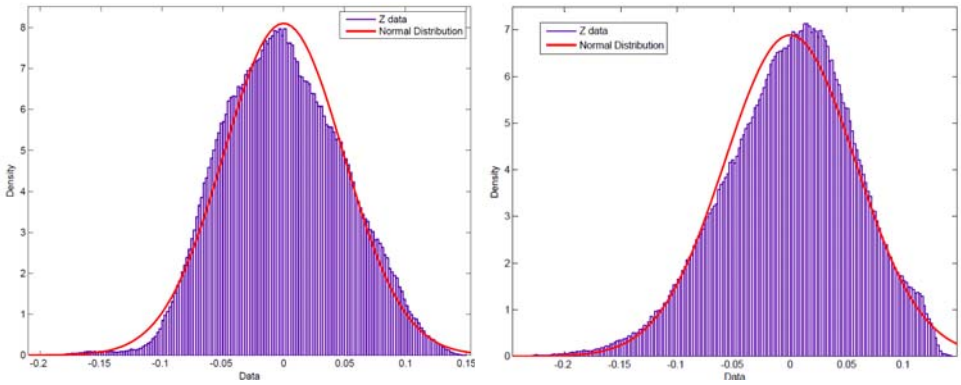

(c) 5-months: Normal distribution *(d) 10-months: Normal distribution*

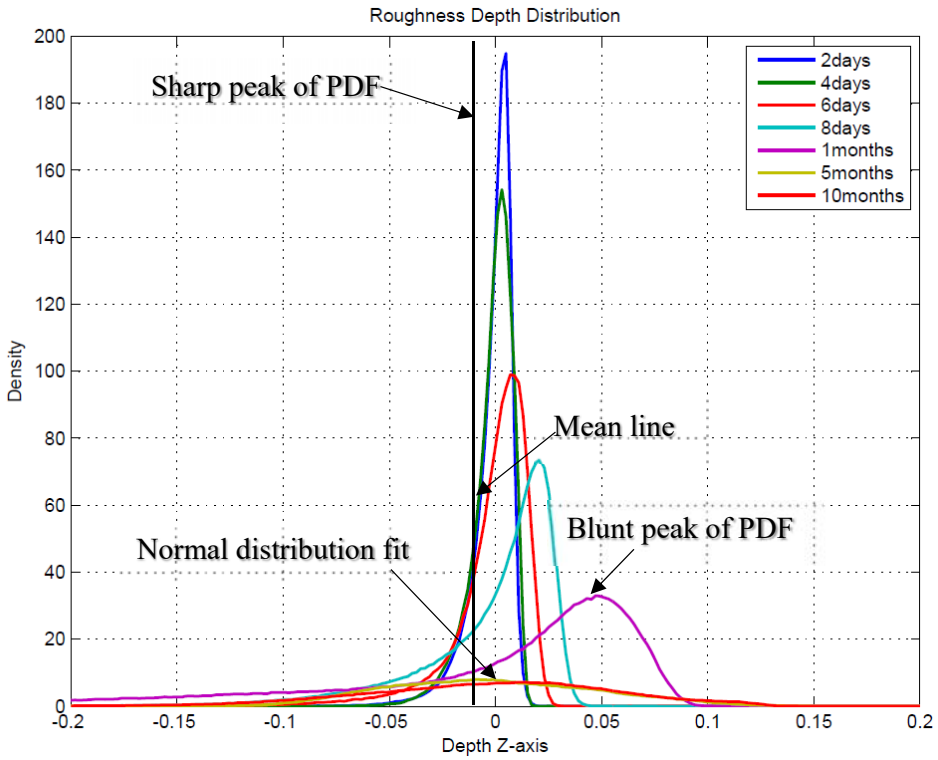

(e) Probability density function (PDF) evolution.

Fig. 41 - Probability density distribution of variable Z(x,y) on the corroded surface of carbon steel samples, subjected to SSCH during 10-months

3.4 Summary

The atmospheric corrosion behaviors including the physical aspect of rust layers, crystal structures and chemical composition of corrosion products, and the

evolution of surface roughness of carbon steel have been investigated by outdoor corrosion test and salt spray test with constant humidity.

- Characteristics of atmospheric corrosion under outdoor exposure test: The atmospheric corrosion behaviors of carbon steel exposed to urban and marine atmospheres in Cambodia are listed as below:

1. The regular and uniform monsoon airflow in Cambodia transports airborne salinity, which contains high chloride concentration, from ocean to landward. However, the high drying effect of the sun in this region enhances the corrosion resistance of metal exposed to the atmospheres.
2. The initial corrosion rate in the Phnom Penh and Sihanoukville was about 9 μm/y and 27 μm/y respectively. According to the category of corrosivity classification, ISO 9223, Phnom Penh is classified as a low corrosive atmosphere, C2 category, while Sihanoukville is classified as medium corrosive atmosphere, C3 category.
3. The corrosion could proceed after the breakdown of the oxide film that concerns with the time of wetness and corrosivity of aqueous media. In term of molar concentration, the sulfur ion is more corrosive than the chlorine ion. Thus the breakdown of the oxide film caused by the sulfur ion is faster than that by chlorine ion.
4. The rust layer of the samples in skyward direction is more dense and well-adhering than that of the groundward for both marine (Sihanoukville) and urban (Phnom Penh) atmospheres. In addition, the corrosion product of the sample exposed to marine was dominated by numerous micro-cracking and porousness that can absorb water to enhance the penetration of oxygen and other chemical species to reach the metal surface, therefore lead to high corrosion kinetic.
5. There was no clear difference between the crystal structure of corrosion products formed in marine (Sihanoukville) and urban (Phnom Penh) atmospheres. γ –FeOOH, α-FeOOH, and β-FeOOH are the majority of crystal structure contained in the rust layer of both marine and urban atmospheres.

- Corroded surface evolution: The surface roughness of carbon steel subject to corrosion varies with time and types atmospheres. The maximum height (Sz), arithmetic average (Sa), and Standard deviation (σ) increased with exposure time. In the early stage of corrosion, pits or notches started to form and resulted in negative Skewness and high degree of kurtosis (K>3). Extending exposure test time, a number of overlapping pits existed and formed as shallow pits. When the surfaces of the material were completely corroded the random variable in height, Z(x,y), of the corroded surface fits the normal distribution, with the value of $Sk \approx 0$ and $K \approx 3$ (see Fig. 41 (c) and (d)). The completely corroded surface is called uniform corrosion. According to the 3D images, the uniform corrosion contained shallow pits which are not so harmful to cause fracture mechanics. Thus, the lifetime prediction of metals structures, subject to atmospheric corrosion, is normally made based on the thickness reduction.

CHAPTER 4

Chapter 4: Atmospheric Corrosion Mapping in Asia Region

4.1 Introduction

The atmospheric corrosion investigations have been widely made in Europe countries to develop ISO standards for corrosion measurement, estimation, corrosivity classifications, and recommendations. However, those standards were created based on those local climates, where the atmospheric corrosion behaviors may be different from Asia region. To rectify such unfortunate situation, corrosion mapping of structural materials in Asia area with understanding effects of environmental factors was investigated under E-Asia research project, by conducting exposure tests in several countries such as Japan, Vietnam, and Thailand. The author has also been studying the atmospheric corrosion in three test stations Cambodia. The exposure test procedures and results will be elaborated in the following sections.

4.2 Exposure Test Stations in Asia Countries

The investigations of atmospheric corrosion mapping in Asia region were made based on the outdoors exposure test in Japan (16-sites), Vietnam (14-sites), and Thailand (7-sites) as shown in the Fig. 42. The metallic samples, ACM sensors, Relative Humidity and temperature sensors, and equipment for measuring Cl^- (dry gauze) and SO_2 (wet candle of the PbO_2 cylinder) were installed at the exposure test stations.

4.2.1 Metallic samples and procedure for exposure test

The structural materials like carbon steels, weathering steels, galvanized steels, and 55% Al-Zn coated steels were used as samples for the expose tests. The carbon steel and weathering steel sheets with the thick of 3mm were cut into 70 mm×150 mm and polished to #600 for exposure tests. While the 1 mm thick of the galvanized

steel and 55% Al-Zn coated steel sheets were cut into 70mm×150mm, then covered by insulation tape and keeping 50mm×120mm for exposure area.

All the metallic samples and ACM sensors were attached to exposure racks with an inclination of 45 degrees angle of horizontal axis and face to the sea or the north as seen in the Fig. 43.

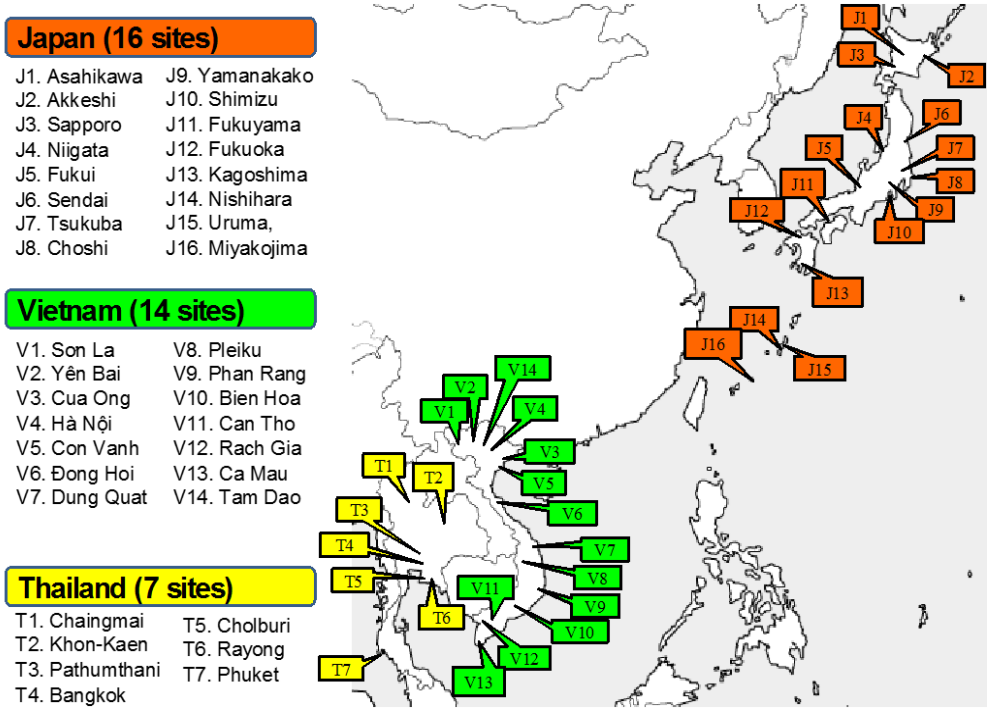

Fig. 42 - The 37-exposure test sites in the E-Asia project.

4.2.2 Atmospheric corrosion parameters collection

Chloride and SO_2 deposition rates were measured by using dry gauze and PbO_2 cylinder in accordance with JIS Z 2381 and ISO 9225, respectively. The dry gauze and PbO_2 cylinder were installed in an instrument shelter or a rainproof location with opened airflow, and they were renewed monthly. ACM sensors and RH-Temperature sensors were exposed at all the exposure stations in Japan and Thailand, but only four exposure sites in Vietnam. The signal outputs of all sensors were recorded every 10 minutes and stored in data loggers that supported by solar energy. The detail of the exposure test samples and equipment are shown in the Fig. 43.

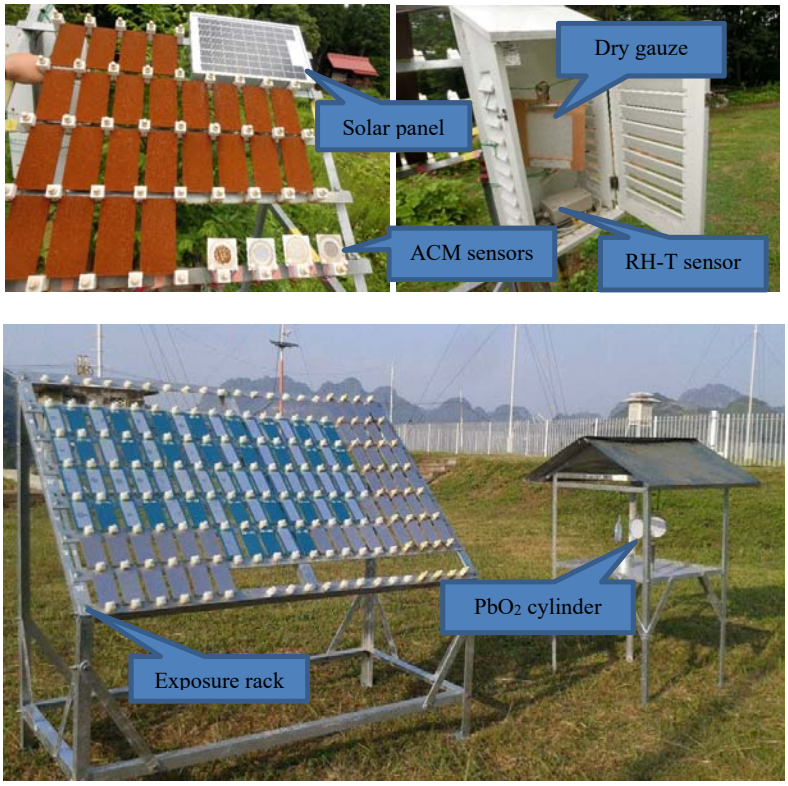

Fig. 43 - Samples and equipment for exposure test.

4.2.3 Corrosion rate calculation

It is the most important step for atmospheric corrosivity evaluation; the proper procedures must be used. Mass reduction of the specimen, caused by corrosion attack, is used for corrosion rate calculation. Accordingly, complete or incomplete removal corrosion product is strongly affected to corrosion rate measurement. In this research, the procedure for removal corrosion product was done in accordance with ISO/DIS 8403.3. And the corrosion rates were calculated based on the Eq. (6), as shown in chapter 2.

4.3 Results

Atmospheric corrosion tests were conducted at a number of exposure test stations where the climates were typical in Asia. A systematic analysis was performed to create a corrosion database including environmental data, ACM sensors outputs, and actual corrosion rates in various types of atmospheres, extending from the

temperate/frigid zone (Japan) through to the tropical zone (Vietnam, Thailand, and Cambodia). Based on the analyzed results, a database of corrosivity classification and environmental parameters were established. The chapter will, however, discuss on only the initial stage of atmospheric corrosion, which emphasizes on the corrosion of carbon steel and weathering steel affected by environmental parameters. The behaviors of ACM sensors outputs and corrosion rate of other metallic material like galvanized steels and 55% Al-Zn coated steels, are taken in to account for future research.

4.3.1 Corrosivity classification

The atmospheric corrosivity classifications were made based on the ISO 9223 as seen in Appendix III. The results are shown in Table 7 and mapped in Fig. 44. It was found that the corrosivities in most of the atmospheres were below or equal to C3 category, except Miyakojima-Japan and Phuket-Thailand that reach C4 category. The high corrosion attacks in these two regions are the consequent of high airborne salinity in the marine atmospheres. In Phuket, the exposure test site faced to the Indian Ocean and, thus, dominated by wet-monsoon airflow, which transports high Cl^- deposition rate from the Ocean to landward. The Miyakojima is a small Island located remotely from the mainland; it is frequently facing to the storm, especially typhoons, which transport high salinity into the land, causing high corrosivity.

It should be noted that all of the atmospheres, except coastal zone, the corrosion rates are relatively small (C2 category), especially those in Thailand, Cambodia, and South of Vietnam. The north of Vietnam is covered by the mountainous area where the RH is notably high, leading to higher corrosion rate than that of the south part. In Japan, the corrosivity categories range from C2 to C4. It seems that the corrosivity decreases with decreasing temperature from the south to the north part of Japan.

Table 7 - Corrosivity category classifications

Country	**Japan**		**Vietnam**	
No	Test sites	Category	Test sites	Category
1	Asahikawa	C2	Son La	C2
2	Akkeshi	C2	Yen Bai	C3
3	Sapporo	C2	Cua Ong	C3
4	Niigata	C2	Hanoi	C3
5	Fukui	C2	Con Vanh	C3
6	Sendai	C2	Dong Hoi	C3
7	Tsukuba	C2	Dung Quat	C3
8	Choshi	C3	Pleiku	C2
9	Yamanakako	C2	Phan Rang	C2
10	Shimizu	C2	Bien Hoa	C2
11	Fukuyama	C3	Can Tho	C2
12	Fukuoka	C3	Rach Gia	C2
13	Kagoshima	C3	Ca Mau	C2
14	Nishihara	C3	Tam Dao	C3
15	Uruma	C3		
16	Miyakojima	C4		
Countries	**Thailand**		**Cambodia**	
No	Test sites	Category	Test sites	Category
1	Chiangmai	C2	Phnom Penh	C2
2	Khon-Kaen	C2	Kampong Cham	C2
3	Pathumthani	C2	Sihanoukville	C3
4	Bangkok	C2		
5	Cholburi	C2		
6	Rayon	C2		
7	Phuket	C4		

4.3.2 Effect of environmental parameters on atmospheric corrosion

The main factors affected to atmospheric corrosion are RH, TOW, Temperature, and chemical species. The environmental characteristics of the Asia region are reputed to be high temperature and humidity, with the strong effect of airborne salinity.

- ***Effect of temperature on corrosion rate:*** The ISO 9223 stated that the maximum of corrosion peak is at the temperature of 10 ^{o}C as seen in the Fig. 45. That means the corrosion rate increases with the increasing of temperature up to 10 ^{o}C and then decreases elsewhere higher temperature. Nonetheless, the results of atmospheric

corrosion investigations in the Asia atmospheres show that the corrosion rates have a peak at the temperature of 20 °C (see Fig. 46), except Miyakojima (J16) and Phang Nga (T7) where the amount of airborne sea salt is particularly high (in excess of 36 mg/m^2 day). This phenomenon can be interpreted by the fact that, at high humidity atmospheres, especially the tropical and subtropical zones, the electrolyte layer (very thin water film) can exist on the surface of the metal at the higher temperature, up to 20 °C. When the temperature is higher than 20 °C, drying effect eliminates the water film; and thus, the electrochemical reaction is going to be impossible. Another reason for the corrosion rate decreases with higher temperature is that the formation of rust layer is compact and well-adhering. This layer acts as corrosion resistance that can insulate the metal surface from its environment, as seen in Fig. 28 (a). However, the results of the MICAT research program, [66], show that in South America the temperature did not affect the corrosion rate as seen in the Fig. 47.

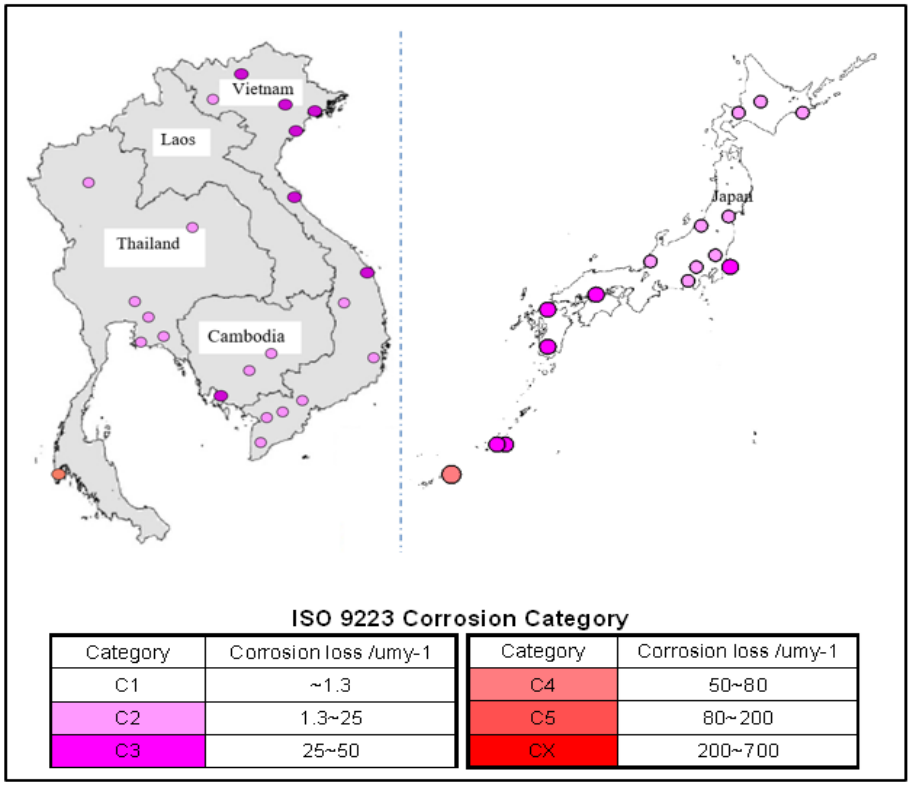

ISO 9223 Corrosion Category

Category	Corrosion loss /umy-1
C1	~1.3
C2	1.3~25
C3	25~50

Category	Corrosion loss /umy-1
C4	50~80
C5	80~200
CX	200~700

Fig. 44 - Atmospheric corrosivity classification based on the corrosion rate of carbon steel.

- Comparison with ISO method: The ISO 9223, [26], stated that the corrosivity of the atmosphere could be classified either by one-year exposure test results or by estimating based on environmental parameters with an advocated formula, called *Dose-responses functions*. The corrosion rate calculated based on these two methods were plotted and shown in Fig. 48. The values of corrosion rates measured from the actual exposure test stations (vertical axis) in Asia region were higher than those estimated by advocated formula (ISO: horizontal axis), and some values were about 4-times greater, as seen in the Fig. 48 (a). However, in South America and Europe atmospheres, the corrosion thickness losses seem to fit with the *Dose-responses functions* (see Fig. 48 (b)). Thus the *Dose-responses functions* suggested by ISO standard was applicable for western countries, and may not be applicable for Asia atmospheres. Hence, developing a damage function for corrosion prediction in Asian atmospheres is needed.

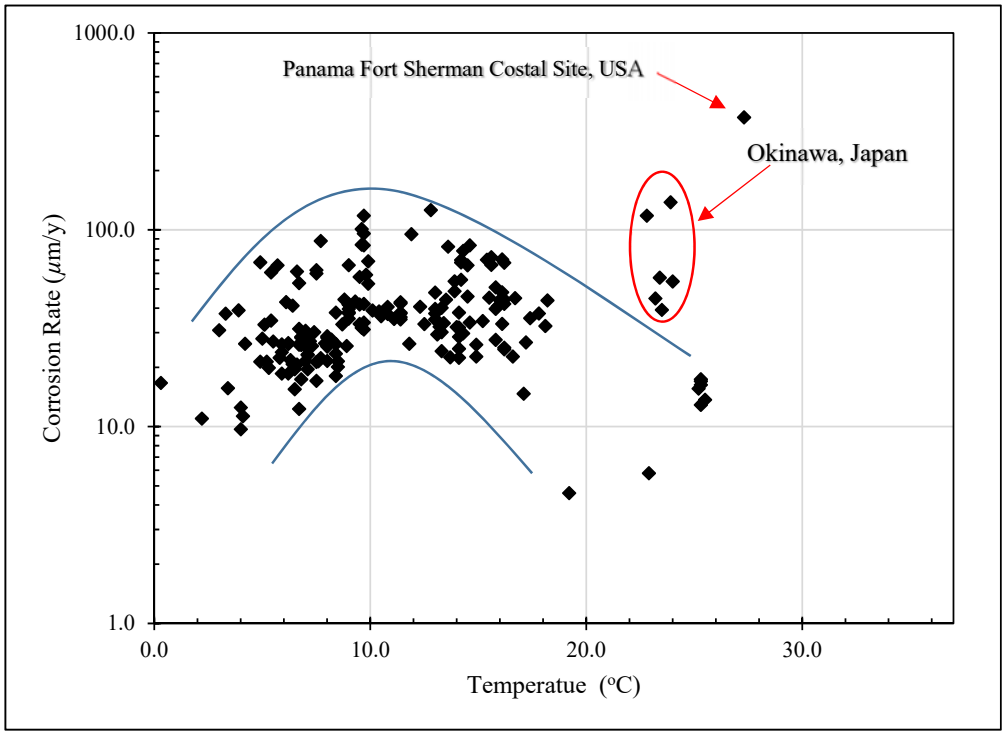

Fig. 45 - Effect of temperature on corrosion rate (ISO CORRAG program [67]).

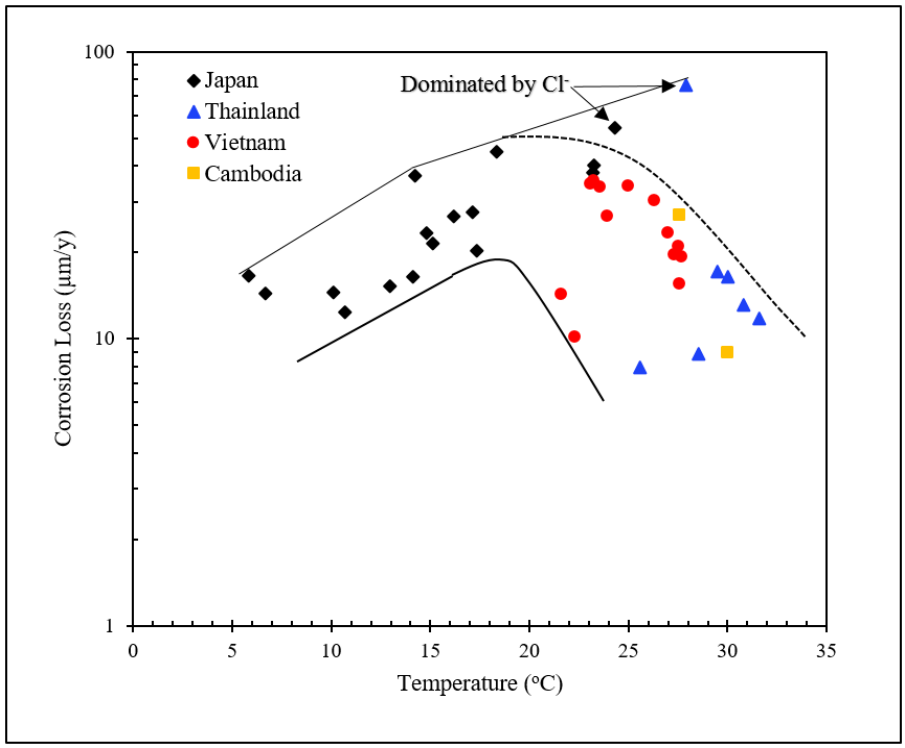

Fig. 46 - Effect of temperature on the corrosion rate of carbon steel.

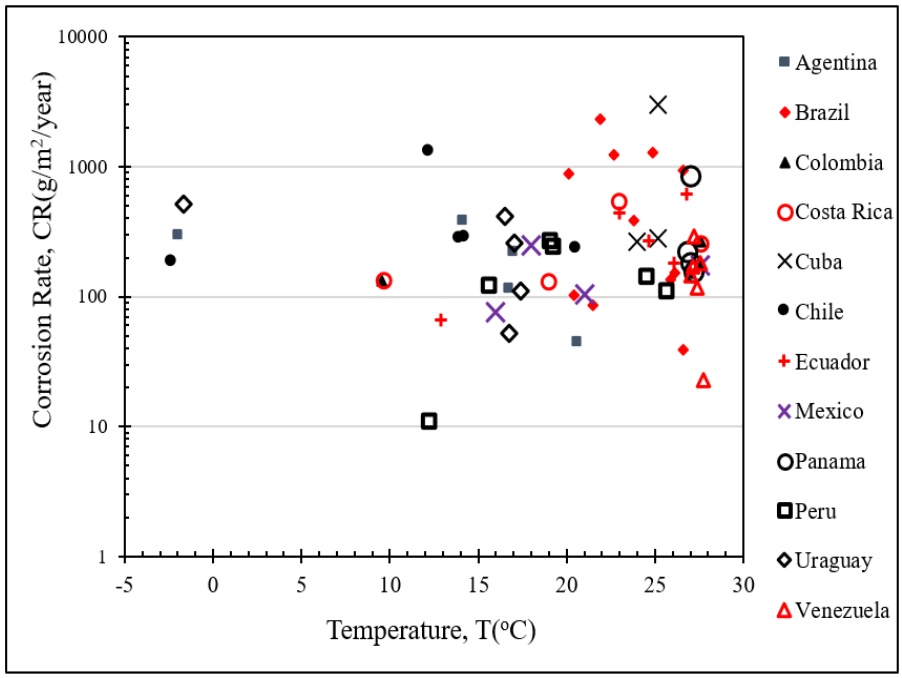

Fig. 47 - Effect of temperature on the corrosion rate in South America atmospheres (MICAT program).

- Factor predominate corrosion: Fig. 49 shows the effect of temperature and RH to the corrosion rate of Carbon Steel (CS) and Weathering Steel (WS) in Japan region. The Figure reveals that the corrosion rates were most likely predominated by temperature (except Chosi and Fukui, where predominated by Cl), while the effect of RH was negligible. This effect is related to the fact that the temperatures in Japan atmospheres were great differences. The temperature difference from the north (Asahikawa, T ≈ 4 ^{o}C) to the south (Miyakojima T ≈ 24 ^{o}C) of Japan was about 20 ^{o}C. In Vietnam, the temperatures are uniformly distributed; the temperature differences were relatively small as seen in Fig. 50. Thus, the corrosion rates were insensitive to temperature but predominated by RH. And these phenomena are the same to Cambodia and Thailand.

In most of the exposure test results, the corrosion rates of WS were slightly lower than those of CS; the comparisons of corrosion rate of the both materials are shown in the Fig. 51. In general, the corrosion resistance of WS is much better than CS for long-term expose to an atmosphere, because the formation corrosion product of WS, known as patina, enhance corrosion resistance; thus, slowing down corrosion kinetic. For the initial atmospheric corrosion attack, the patina was not fully formed, hence the corrosion rate of WS and CS in the initial corrosion tests were similar as seen in the Fig. 49 to Fig. 51.

4.3.3 Damage function for atmospheric corrosion prediction in Asia atmospheres

Atmospheric corrosion is a complicated process that caused by the complex environmental parameters including climatic condition and pollutants substances. To predict the corrosion attack, many types research were conducted to develop the mathematical formula, called damage function. The formula was made in function of environmental parameters like temperature, relative humidity, time of wetness, chloride deposition rate, and sulfate deposition rate.

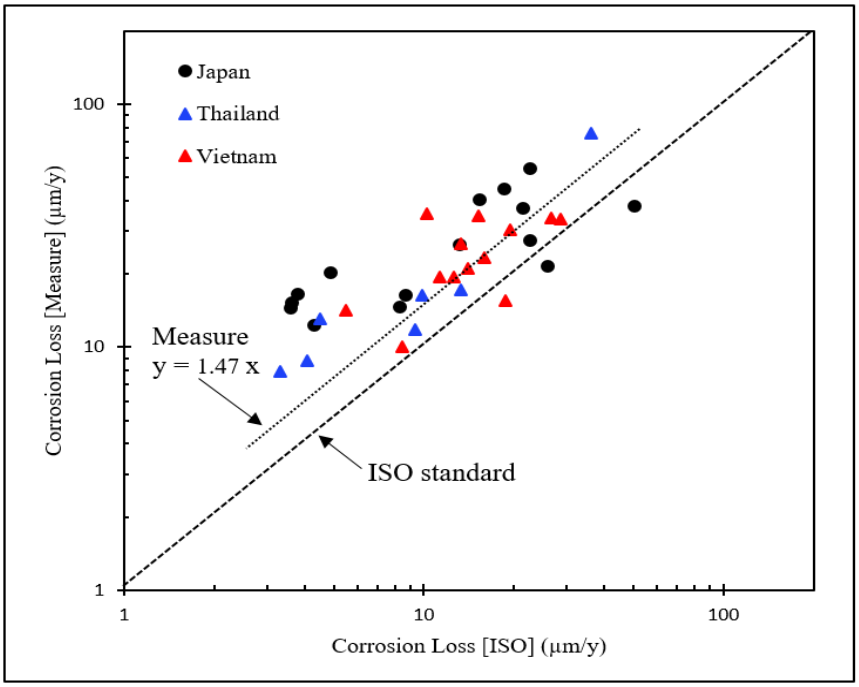

(a) Atmospheric corrosion in Asia countries

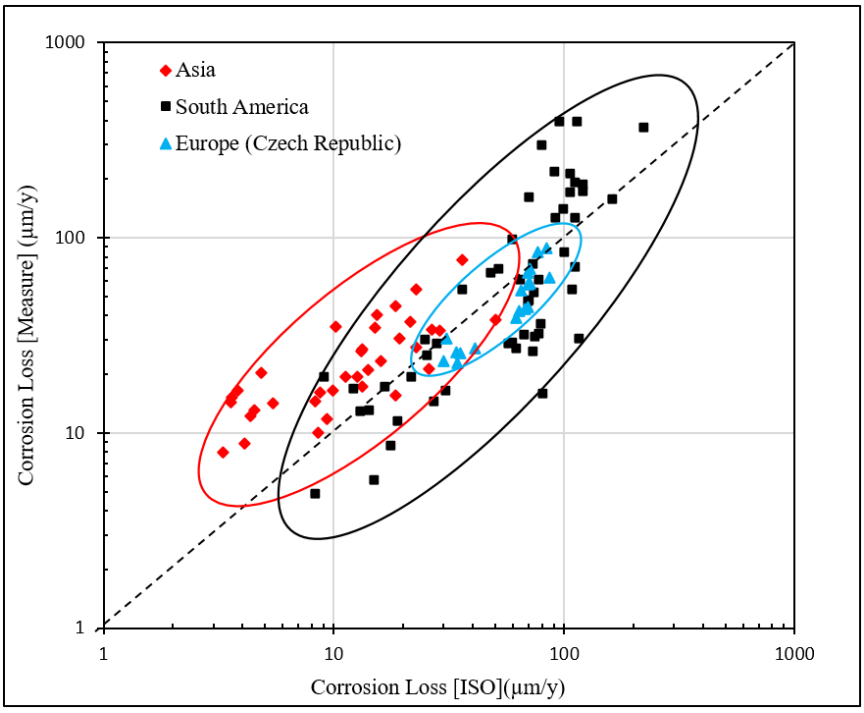

(b) Comparison the Atmospheric corrosion in Asia, Europe, and South America

Fig. 48 - Comparison of corrosion loss of carbon steel between the actual measurement (vertical axis) and the estimated based on Dose-response functions, ISO 9223.

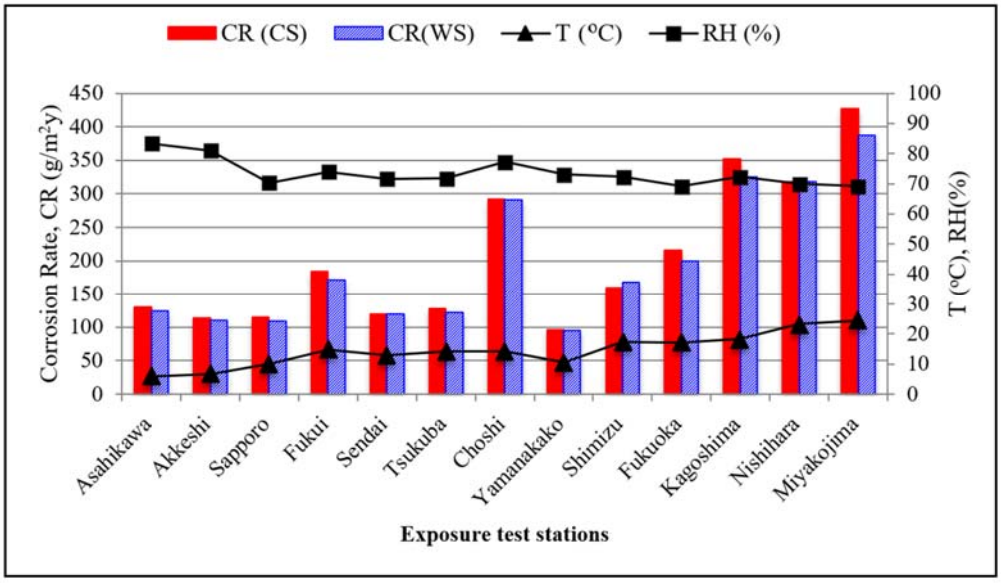

Fig. 49 - One-year corrosion test of CS and WS in Japan: effect of temperature and RH.

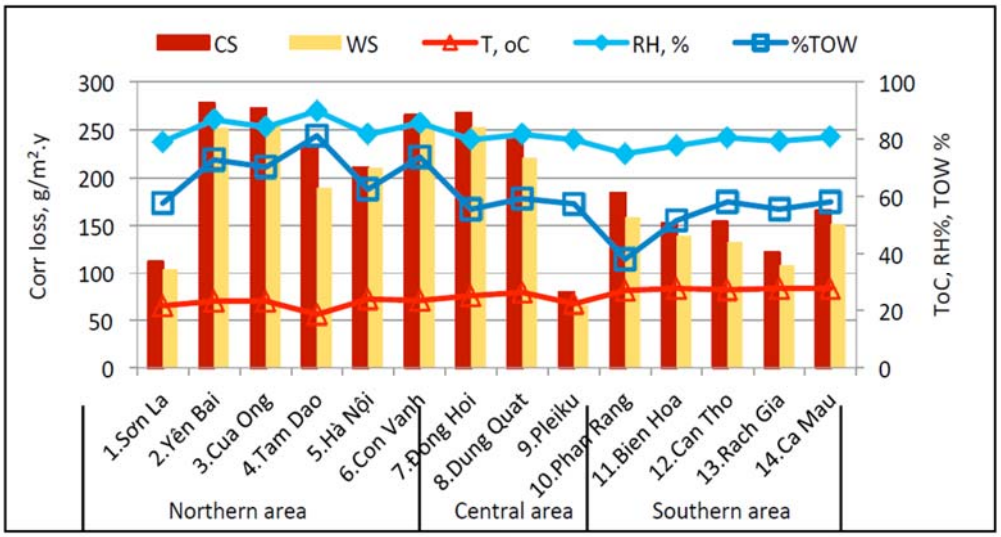

Fig. 50 - One-year corrosion test of CS and WS in Vietnam: effect of temperature RH and TOW [68].

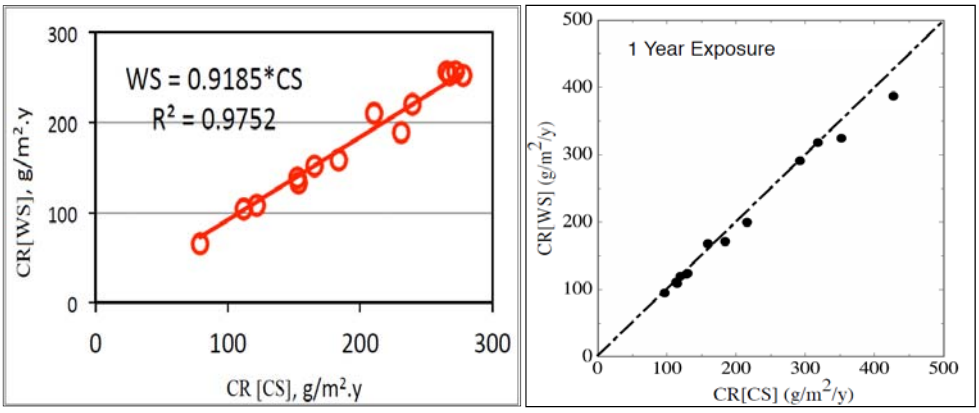

(a) Exposure test in Vietnam *(b) Exposure test in Japan*

Fig. 51 - Comparison of CR (CS) and CR (SW) [68],[69].

- *Linear function:* Hong Lien, [68], proposed a linear equation to predict the corrosion rate in Asia atmospheres based on the results of E-Asia research project. The equation is shown as below:

$$r_{corr} = a_1T+a_2RH+a_3Cl+a_4SO_2+a_5TOS+a_6 \quad (22)$$

Where:

r_{corr} – First-year corrosion loss

T – Annual air temperature, ^oC

RH – Annual air relative humidity, %

Cl – Chloride deposition rate, mg Cl/m^2day

SO_2 – Sulfur dioxide deposition rate, mg SO_2/m^2day

TOS – Time of sunshine, h/y

a_{1-6} – constants

According to the first-year exposure test in Asia atmospheres, with the 37 exposure test sites, the corrosion rates and environmental parameters were collected. Substitute those into the Eq (22), the first-year corrosion rates of carbon steel (CS) and Weathering Steel (WS) can be estimated by the following mathematical equations:

$$r_{corr}(CS) = 11.18\,T + 2.88\,RH + 2.64\,Cl + 1.86\,SO_2 - 0.064\,TOS - 225.86 \quad (23)$$

$$r_{corr}(WS) = 10.6T + 2.62\,RH + 0.99\,Cl + 11.56\,SO_2 - 0.067\,TOS - 202.05 \quad (24)$$

The formulas show the maximum errors of about ± 20%. The accuracies of these formulas are much more improved compared to the *Dose-response functions*, which previously discussed in section 3.2.1. Taking time-of-sunshine (TOS) into account for corrosion rate prediction is one of the reasons for improving the accuracies compare to the formulation suggested by ISO 2293.

The Eq (23) and Eq (24) show that, the constants coefficients, a_1 to a_6, of CS similar to those of WS, except a_3 and a_4. Certainly, CS was strongly affected by Cl deposition rate (a_3 (CS) = 2.88, a_3 (WS) = 0.99), while WS was strongly affected by SO_2 deposition rate (a_4 (CS) = 1.86, a_4 (WS) = 11.56).

- Modify the coefficients of Dose-response function to fit the Asia atmospheres:
As it was explained in the ISO 9223, the utilization of linear equations to predict corrosion attack may not achieve the most accurate results. In this case study, the *Dose-response function*, Eq(25), was modified, Eq(26), to fit the actual atmospheric corrosion test of the E-Asia research results as seen in the Fig. 52. However, more atmospheric corrosion tests in the Asia countries should be conducted to verify and rectify the Eq(26).

- Dose-response function ISO 9223:

$$r_{corr} = 1.77 P_d^{0.52} \exp(0.02RH + f_{St}) + 0.102 S_d^{0.62} \exp(0.033RH + 0.040T) \quad (25)$$

$$f_{St} = 0.150(T-10) \text{ where } T \leq 10\ ^oC; \text{ otherwise } -0.054(T-10)$$

- Modified Dose-response function:

$$r_{corr} = 1{,}77 . P_d^{0.52} . \exp(0{,}02 . RH + f_{St}) + 0{,}4 . S_d^{0.3} . \exp(0{,}033 . RH + 0{,}040 . T) \quad (26)$$

$$f_{St} = 0{,}1 . (T-20) \text{ where } T \leq 20\ ^oC; \text{ otherwise } -0{,}15 . (T-20)$$

Where:

S_d: Chloride deposition rate, mg/mm^{2}day

P_d: Sulfur dioxide deposition rate, mg/mm^{2}day

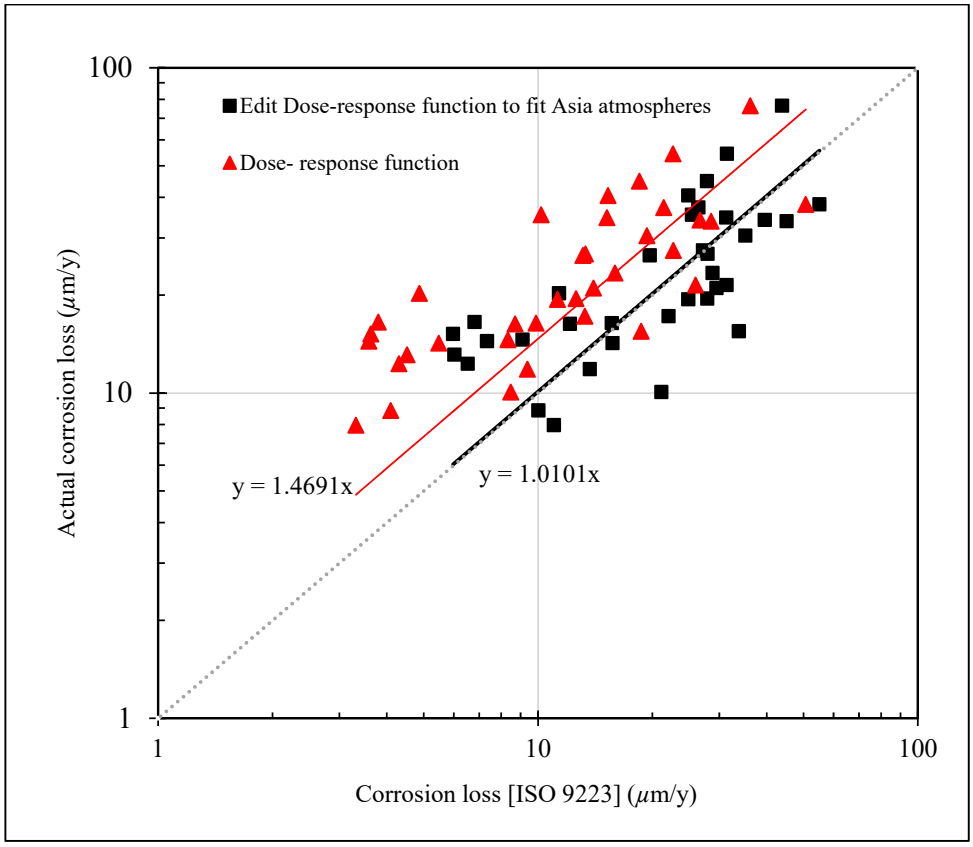

Fig. 52 - Modification of coefficients of Dose-response function, (ISO 9223), to fit the E-Asia research results.

4.4 Discussion

As it was previously described, the corrosion rates in Asia atmospheres were highly affected by temperature and Cl^- deposition rate; while those in the Europe atmospheres, (Czech Republic [67]), the corrosion rates were predominated by SO_2 depositions rates as seen in the Fig. 53. These atmospheric corrosion phenomena were due to the predominated environmental factors, where the materials were exposed. As it was reported by the MICAT research program [66], where the atmospheric corrosion surveys were conducted in the South-America, the temperatures, relative humidity, and time of wetness were insensitive to corrosion rates, as seen in the Fig. 54; while the SO_2 and Cl^- deposition rates notably affected to the atmospheric corrosion, as seen in Fig. 55. The different factors of corrosion predomination provoke the corrosion prediction much more complicated. The damage functions, called *"Dose-response functions"*, suggested by ISO 9223 are

not applicable to predict the atmospheric corrosion rate of metals structures exposes in Asia atmospheres.

4.5 Summary

The atmospheric corrosion is the worldwide problems. In western countries, many research on atmospheric corrosions of metals structures were extensively made, and results can be found in the research literature. The common knows of two massive atmospheric corrosion research projects are ISO CORRAG program and MICAT Program. And those two research programs were conducted based on outdoor exposure test in South America and Europe atmospheres, respectively. Unfortunately, there is very limited information about the atmospheric corrosion in Asia atmospheres. This chapter, the atmospheric corrosion behaviors in Asia atmospheres were discussed based on the results of E-Asia research program, which was conducted in Japan, Vietnam, and Thailand. The author has also been conducting the atmospheric corrosion tests in Cambodia. The results of the research are listed below:

- The corrosivity in Cambodia, Thailand, Vietnam, and Japan was classified into the range of C2 – C4 category.
- In the tropical zone like Cambodia, Thailand, and Vietnam, the atmospheric corrosions were predominated by Cl^- deposition rate that resulted from the airborne salinity of monsoons airflow. The temperature was insensitive to the corrosion rate since it behaved relatively uniform in this tropical zone.
- In Japan, temperate/frigid zone, the corrosions were predominated mainly by temperature and relatively by Cl^- deposition rate. The corrosion rate decreased from the South to the North along with the decreasing annual average temperature.
- Based on the results of atmospheric corrosion tests in the E-Asia research project, the corrosion rate reached a maximum at the critical temperature of 20 ^oC, while that in Europe atmospheres (ISO CORRAG program) was found at 10 ^oC.

- The corrosion rates calculated by using the *Dose-response functions* (ISO 9223) were much lower than those measured from the actual exposure tests. Thus the ISO 9223 may not be applicable in the Asia atmospheres.
- The modification of Dose-response function (ISO 9223) for atmospheric corrosion prediction in Asia atmospheres was made, and this new function is suitable to predict the corrosion rate in Asia atmospheres.

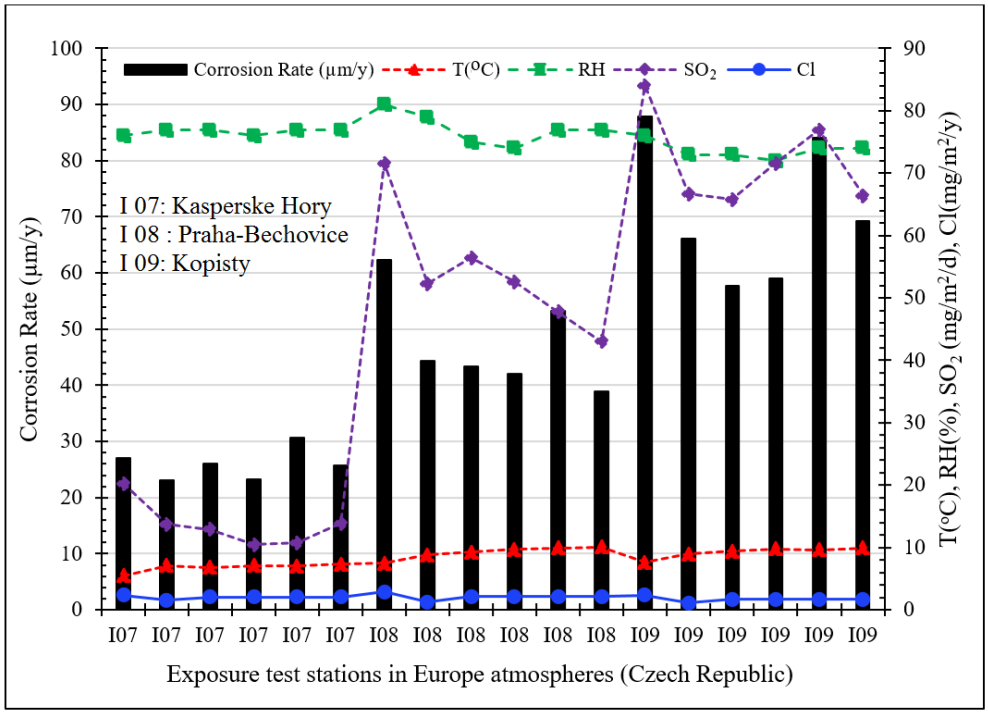

Fig. 53 - Effect f SO_2 on the corrosion rate of carbon steel in Europe atmospheres (Czech Republic [67]).

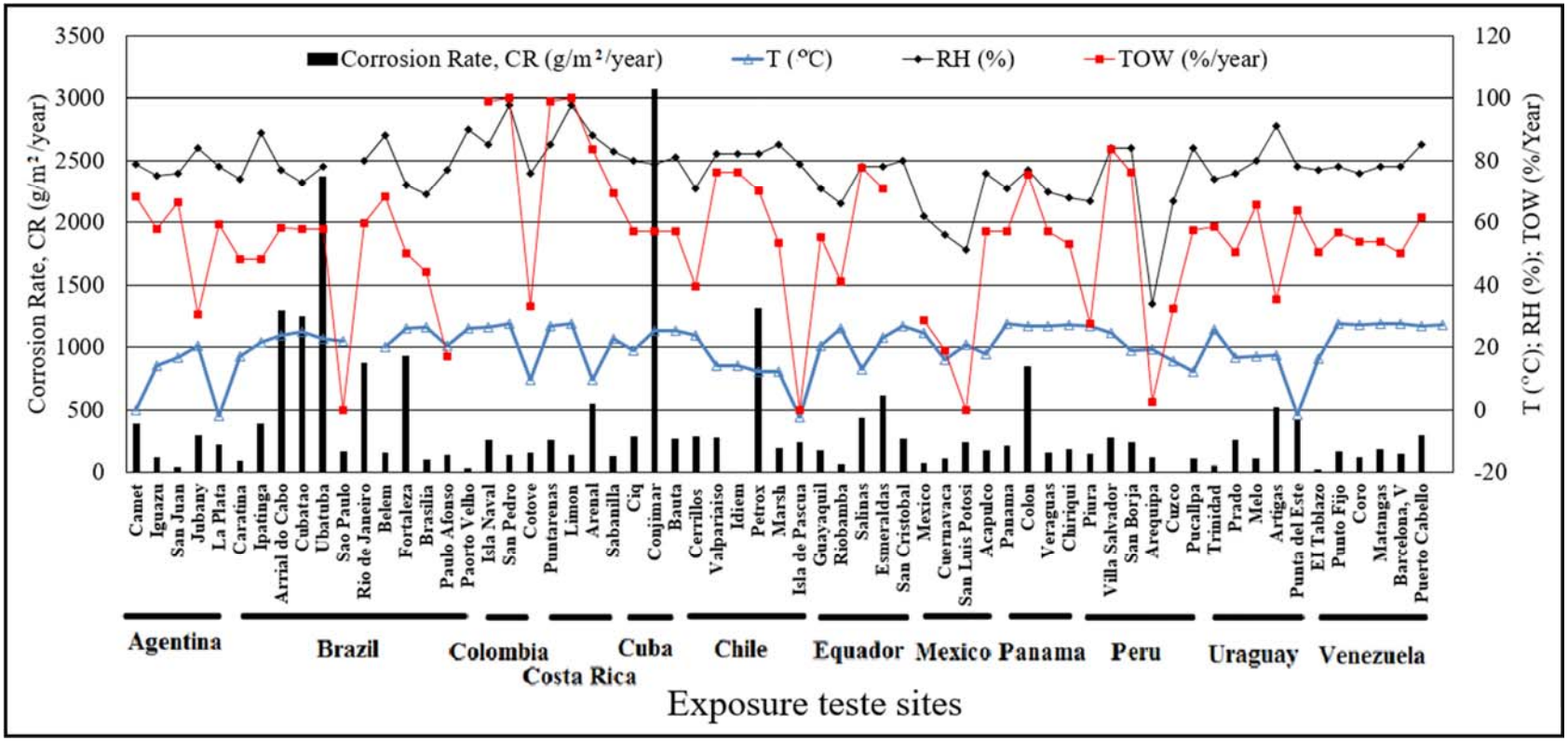

Fig. 54 - Effect of temperature, T (°C), relative humidity, RH (%), and time of wetness, TOW (% /year), on corrosion rate, CR (g/m²/year): (MICAT Program).

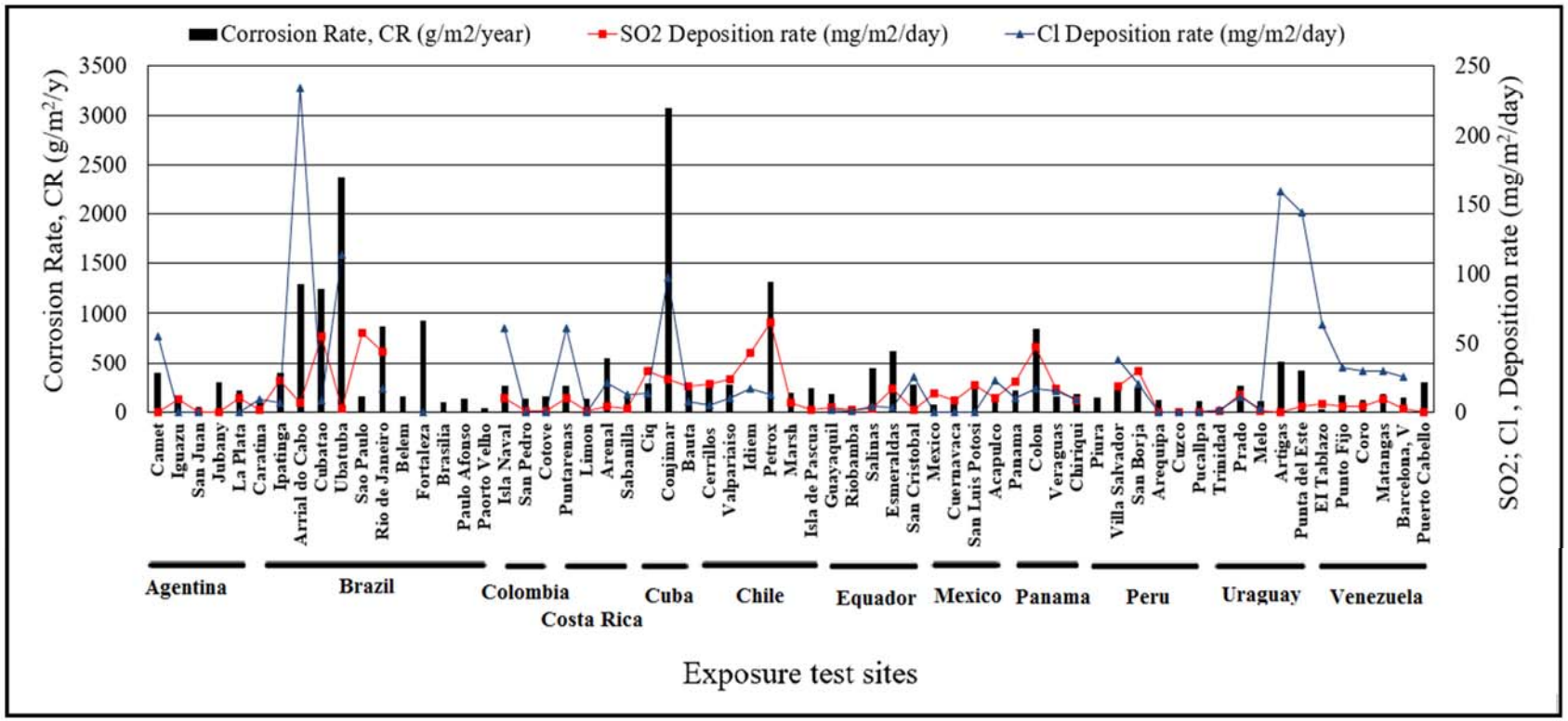

Fig. 55 - Effect of SO_2 and Cl deposition rates on Corrosion Rate, CR (g/m^2/year): MICAT Program.

CHAPTER 5

Chapter 5: Discussions and Conclusions

5.1 Discussion

5.1.1 Chemical species predominated atmospheric corrosion in Asia and Europe atmospheres

The thesis has demonstrated the behaviors of atmospheric corrosion and the procedure to develop corrosion mapping in Asia atmospheres based on laboratory study and outdoor exposure tests. The results show uncertainties between atmospheric corrosion behaviors in Asia, Europe, and South America atmospheres. Under the artificial rainfall test, it was found that in term of molarity, the corrosivity of SO_2 ions was higher than that of Cl^- ions. The *Dose-response functions* stated in the ISO 9223, which was developed based on the Europe atmospheres, also indicated that the corrosion attack caused by SO_2 giving higher risk than that caused by Cl^-. In contrast, the results of outdoor exposure tests in Asia Countries, including Japan, Vietnam, and Thailand, reveal that the corrosion attacks in these regions were dominated by Cl^- because SO_2 deposition rates were relatively lower than Cl^- deposition rates. The high Cl^- deposition rates in Asia atmospheres resulted from airborne salinity, especially the regular monsoon airflow (Southeast Asia) and occasional typhoon storm (Japan). The presence of Cl^- will not only accelerate corrosion reaction but also prolong the time of wetness.

T. Shinohara, [18] [70], investigated the effect of temperature and Cl^- concentrations on the thickness of electrolyte layer formed on the surface of the metal, with a variation of relative humidity. He suggested that airborne sea salt, which contains Cl^- particle, has a further effect on corrosion rate. The existing of Cl^- on the surface of metal absorbs moisture to form an electrolyte layer. The layer is less sensitive to temperature, which is not dry easily and thus provokes long time of wetness for corrosion to occur. Evidently, the *Dose-response functions* given by ISO 9223 is not applicable for the Asia atmospheres since it was made based on the European Atmospheres, where were dominated mainly by SO_2. And thus, the

mathematical models for corrosion prediction which have been made in this research are the most applicable results suited to Asia atmospheres.

5.1.2 Long-term Corrosion Prediction

It was known that the corrosion rate of metallic material exposed to the natural outdoor atmospheres is not constant; it decreases with exposure time, because of the accumulation of rust layer acts as corrosion resistance. For most of the metallic engineering structures, the total corrosion thickness loss follows the power function as seen in Eq (5). In this case, the constant r_{corro} and exponent b must be defined to predict total thickness loss. Based on the results of 1-year exposure test in this research project, the values of r_{corro} were observed. And the values of exponent b can be selected from the table of ISO 9224. According to the mismatch of factors predominated corrosion between Asia and Europe atmospheres, the exponent b suggested by ISO standard is not recommended to be used in Asia atmospheres. Long-term exposure test, up to 20 years, for calculating exponent b is preferable.

5.2 Conclusion

The case study and the E-Asia research project collaboration are the good initiatives to develop atmospheric corrosion database with a reliable used for Asia environment. The corrosivity categories classifications mapping in Asia atmospheres were made, and the environmental parameters were collected and kept in the corrosion database for long-term corrosion investigation. The results of the research are the great references, which provides necessary information for material selection and protective method against atmospheric corrosion in the stage of design and construction; and particularly, leading to service life prediction of metal structures.

5.3 Recommendation

The compatibility of metal to its environment is a prime requirement for its reliable performance. The material should be considered during design stage; the best material with the wrong environment will not achieve the desired optimum

performance. The corrosion rates and environmental parameters, which have been established in this research, are the primary information for material selection and service life prediction of metal structures exposed to the natural environment. The evaluation of this research results, however, were made based on the 37 exposure tests sites, where the climates were typical in Asia. It is expected that expanding exposure test sites to others countries in Asia region allow clarifying this uncertainty.

5.4 Thesis Review

- Artificial rainfall test: The artificial rainfall equipment is an essential and reliable tool for studying the effect of chemical species on the ACM sensors outputs and corrosion rates, under the effect of rain. The corrosivity of chemical species was also observed. It was found that, in the atmospheric condition, the anion like SO_2^{2-} and Cl^- are the most corrosive ion; and it must be taken into account for atmospheric corrosion estimation. Despite several other chemical species were found in the atmosphere, those species show a negligible effect on the corrosion kinetic, notably the cation like Na^+, Mg^{2+}, and K^+.

- ACM sensors: All types of ACM sensors can be employed to predict the time of wetness, especially Al-Ag and Cu-Ag sensors that show long service life. The Fe-Ag galvanic couple of ACM sensors is capable of estimating not only time of wetness but also aggressivity of atmosphere. However, the service life of Fe-Ag sensor is relatively short; thus it is required to renew frequently during exposure test. For the Al-Ag sensor, the service life is notably long, but the signal output is inconsistent; it is strongly affected by the type of chemical species. Thus it gives the advantage to predict the majority of a chemical constituent of rainwater.

- Corrosion morphology of rust layers: The corrosion product rust layer formed on the metals exposed to a corrosive atmosphere show high porousness of rust layer with many cracks giving rise to paths for water, oxygen, and others corrosive species to penetrate to reach metal surface. This type of rust layer has a poor capability for atmospheric corrosion resistance. In contrast, the dense and compact rust layer, which normally forms on the metal exposed to the low corrosive

atmosphere, acts as an insulation to effectively inhibit the diffusion of oxygen and other species to reach the metal surface, therefore lead to high corrosion resistance. The solar radiation and washing effect of rain also can enhance corrosion resistance since it was found that the rust layer formed on the skyward samples were more compact than those formed on the groundward samples.

- *Surface roughness evolution:* The metal structure like carbon steel undergoes uniform corrosion when it exposed naturally to an atmosphere for long-term. In the initial stage of corrosion, shallow pits or notches were formed. Extending exposure time the number of pits increased to form overlapping-shallow pits. When the entire surface of metal was corroded, there were no pits appeared, and the whole surface covered by shallow-valleys shape, known as uniform corrosion. To observe the corroded surface evolution, the Skewness and Kurtosis were used. Based on the statistical analysis, the negative Skewness indicates the appearance of pits. When the surface of the metal is entirely corroded to reach the uniform corrosion, the Skewness is about zero, and the Kurtosis is about three. And it was found that the random variable in height, z(x, y), fits the normal distribution for uniform corrosion.

- *Atmospheric corrosion mapping in the Asia region:* The corrosivity classifications were categorized and mapped into several countries in Asia. The results of the research indicate some mismatch between the behaviors of atmospheric corrosion in Asia region and those stated in the ISO standards; especially the critical temperature for maximum atmospheric corrosion attack and the corrosion rate estimated based on *Dose-response functions (ISO 2293)*. The validations use of the ISO standard were limited to the range of temperature between -17.1 to 28.7 ^{o}C (see Appendix III, Table III-3), while the annual averages temperatures in some Asia countries located in a tropical climate are over the upper limit [71]. In some Asia regions, the maximum temperatures are over 35 ^{o}C and occasionally reach 40 ^{o}C. Thus, establishing atmospheric corrosion data in Asia, especially the tropical zone, is needed.

5.5 Future Research

The evaluation of this research results, however, were made based on the 37 exposure tests sites, where the climates were typical in Asia. It is expected that expanding exposure test sites to others countries in Asia region allow clarifying this uncertainty.

To develop the most accurate and reliable results of atmospheric corrosion mapping in Asia area, the group of research commits to continue the atmospheric corrosion investigation for long-term exposure test in order to define the exponent *b* of the power function (ISO 9224 [23]) for long-term corrosion estimation. The researchers in others countries (Philippine, Indonesia, Taiwan…etc.) are also interesting in this joint research project program. Thus, the corrosion mapping is expected to be expanded.

The author has been conducting and continues to conduct the atmospheric corrosion tests in Cambodia; future research collaboration is needed.

REFERENCES

[1]. J. Kruger, "Cost of Metallic Corrosion", Uhlig's Corrosion Handbook, Second Edition, pp.3-10, John Wiley & Sons, Inc., (2000).

[2]. Pierre R. Roberge, Handbook of Corrosion Engineering, 1999.

[3]. *Survey of Corrosion Cost in Japan*, Japan Society of Corrosion Engineering, Japan Association of Corrosion Control, 1997.

[4]. Corrosion failure: Fukushima Nuclear Plant Tank Leak < https://www.nace.org/CORROSION-FAILURES-Fukushima-Nuclear-Plant-Tank-Leak.aspx> [January 10, 2017].

[5]. Silver Bridge Collapse <http://corrosion-doctors.org/Bridges/Silver-Bridge.htm> [January 12, 2017].

[6]. The Point Pleasant Bridge Disaster <https://www.youtube.com/watch?v= TDc2x obl4lw> [January 12, 2017].

[7]. April 22, 1992: sewers explosion in Guadalajara <http://www.history. com/this-day-in-history/sewers-explode-in-guadalajara/print> [January 13, 2017].

[8]. Aloha airline incident record <https://www.thisdayinaviation.com/28-april-1988/> [07-2-17].

[9]. Miller, D., Corrosion Control on Aging Aircraft: What Is Being Done? *Materials Performance,* **29**, p.10–11 (1990).

[10]. Hoffman, C., 20,000-Hour Tuneup, *Air & Space,* **12,** p. 39–45 (1997).

[11]. 1992 Guadalajara Explosions Disaster <http://www.history.com/this-day-in-history/sewers-explode-in-guadalajara/print> [January 16, 2017].

[12]. Fontana, M. G., *Corrosion Engineering,* New York, McGraw Hill, (1986).

[13]. Pierre R. Roberge., Handbook of Corrosion Engineering, New York, McGraw Hill, (1999).

[14]. Corrosion<https://saylordotorg.github.io/text_general-chemistry principles-patterns-and-applications-v1.0/s23-06-corrosion.html>[March 22, 2017].

[15]. F. Mansfeld and S. TSAI, Corr. Sci. **28**, p. 939 (1988).

[16]. Electrochemical and Optical Techniques for the Study and Monitoring of Metallic Corrosion, *Series E: Applied Sciences – Vol.203, p. 571-584.*

[17]. M. Stratmann, H. Strecke, K.T. Kim, S. Crockett, Corros. Sci. **30**, p. 715–734 (1990).

[18]. T. Shinohara, ISSN 0892-4228, Corrosion Engineering, **63**, No.4, p.86-92 (2014).

[19]. M. Morcillo, B. Chico, Atmospheric corrosion data of weathering steels. A review, Corrosion Science 77, p. 6–24 (2013).

[20]. D. de la Fuente, I. Díaz, Long-term atmospheric corrosion of mild steel, Corrosion Science 53, p. 604–617 (2011).

[21]. Le Thi Hong Lien and Pham Thy San, Results of studying atmospheric corrosion in Vietnam 1995–2005, Science and Technology of Advanced Materials **8**, p. 552–558 (2007).

[22]. I. Diaz, H. Cano, D. de la Fuente, Atmospheric corrosion of Ni-advanced weathering steel in the marine atmosphere of moderate salinity, Corrosion Science **76**, p. 348–360 (2013).

[23]. ISO 9224, Corrosion of metals and alloys, Corrosivity of atmospheres, Guiding values for the corrosivity categories (2012).

[24]. Wei Han, Chen Pan, Zhenyao Wang, A study on the initial corrosion of carbon steel exposed to outdoor wet-dry cyclic condition, corrosion science **88**, p. 89-100 (2014).

[25]. Robert E. Melchers, Bi-modal trend in the long-term corrosion of Aluminum alloys, Corrosion Science 82, p. 239–247 (2014).

[26]. ISO 9223, Corrosion of metals and alloys — Corrosivity of atmospheres — Classification, determination and estimation. (2012)

[27]. DEAN, S.W. and REISER, D.B., "Analysis of Long Term Atmospheric Results From ISO CORRAG Program", *Outdoor Atmospheric Corrosion*. ASTM STP 1421, TOWNSEND, H.E. Ed., ASTM International, West Conshohocken, PA, USA, 2002, pp. 3-18

[28]. D.M. Buck, Copper in steel – the influence on corrosion, J. Ind. Eng. Chem. **5**, p 447–452 (1913).

[29]. D.M. Buck, Recent progress in corrosion resistance, Iron Age, p 1231–1239 (1915).

[30]. COR-TEN – Weathering & corrosion resistant steel <http://www.webcitation.org/5mkm6z6UZ> [March 9, 2017]

[31].] C.P. Larrabee, S.K. Coburn, The Atmospheric Corrosion of Steels as Influenced by Changes in Chemical Composition, First International Congress on Metallic Corrosion, London, 1961. pp. 279–285.

[32]. ISO 2924, Corrosion of metals and alloys — Corrosivity of atmospheres — Guiding value for the corrosivity categories. (2012)

[33]. ISO 2925, Corrosion of metals and alloys — Corrosivity of atmospheres —Measurement of environmental parameters affecting corrosivity of atmospheres. (2012)

[34]. ISO 9226, Corrosion of metals and alloys — Corrosivity of atmospheres — Determination of corrosion rate of standard specimens for the evaluation of corrosivity. (2012)

[35]. J. Morales, S. Martin-Krijer, F. Diaz, J. Hernandez-Borges, S. Gonzalez, Atmospheric corrosion in subtropical areas: influences of time of wetness and deficiency of the ISO 9223 norm Corrosion Science **47,** p. 2005–2019 (2005).

[36]. ISO 9223, Corrosion of metals and allows-Corrosivity of atmospheres-Classification, determination and estimation (2012)

[37]. Zhenhua Dan, Izumi Muto, Nobuyoshi Hara, Corrosion Science **57,** p. 22 (2012).

[38]. A. Dehoux, F. Bouchelaghem, Y. Berthaud, Corrosion Science **97, p.** 49 (2015).

[39]. M. Esmaily, M. Shahabi-Navid, J.-E. Svensson, M. Halvarsson, L. Nyborg, Y. Cao, L.-G. Johansson, Corrosion Science **90**, p. 420 (2015).

[40]. Naixin Xu, Lingyuan Zhao, Cuihong Ding, Corrosion Science, **44**, p. 163 (2002).

[41]. J. Alcántara, B. Chico, I. Díaz, D. de la Fuente, M. Morcillo, Corrosion Science, **97**, p. 74 (2015).

[42]. Yu.M. Panchenko and A.I. Marshakov, Long-term forecast of corrosion mass losses of technically important metals in various world regions using a power function, Corrosion Science **88**, p. 306–316 (2014).

[43]. Tadashi Shinohara, Shin-ichi Motoda and Wataru Oshikawa, Material Forum, ISSN: 1662-9752, Vols. 475-479, pp 61-64, Switzerland, (2005)

[44]. W. Oshikawa, Y.Sasaki, T. Shinohara, Proc. 52nd Jpn. Conf. Materials and Environments, p.53, JSCE (2005).

[45]. A.Nakano and W. Oshikawa, Zairyo-to-Kankyo, **60**, 135 (2011).

[46]. T. Shinohara, Proc. JSCE Materials and Environments, p.122, JSCE (2014).

[47]. P.J. Sereda: ASTM Bulletin, No. 228, (1958) pp. 53: ibid., No.238. (1958) pp. 61; ibid., No. 246, p. 47 (1960)

[48]. P.R. Grossman: "*Atmospheric Factors Affecting Corrosion of Metals*," Ed. By S.K Conburn, p. 5, ASTM STP 66 (1978).

[49]. P.J. Sereda, S.G. Croll and H.F. Slade: "*Atmospheric Corrosion of Metal*," Ed. By S.W. Dean, Jr. and E.C Rhea, p. 267, ASTM STP 767 (1982).

[50]. S.i. Motoda, Y. Suzuki, T. Shinohara: Corrosion Engineering. **43**, p. 583-594 (1994).

[51]. To Dara, Tadashi Shinohara, Osamu Umezawa, JSCE Material and Environment, **66**, No. 2, p. 58-61 (2017).

[52]. ISO/DIS 8403.3, Metals and alloys. Procedures for removal of corrosion products from corrosion test specimens, 1985.

[53]. Dara To, Tadashi Shinohara, Osamu Umezawa, IJRET, **05**, p. 382-387 (2016).

[54]. Dara To, T. Shinohara, and O. Umezawa, The Electrochemical Society (ECS) Transactions, 75 (29), (2017).

[55]. F. Mansfeld: Applied Sciences, **203** (Electrochemical and Optical Techniques for the Study and Monitoring of Metallic Corrosion), p. 571-584 (1991).

[56]. To Dara, Tadashi Shinohara, Osamu Umezawa, Proc. JSCE Materials and Environments 2016, p.298-302 (2016).

[57]. T. Tsuru, A. Nishikata: Mater. Sci. Technol. A198 (1995) 161–168.

[58]. P. Rodriguez, E. Ramirez, S. Feliu, J.A. Gonzalez, W. López, Corrosion, **55**, p. 319 (1999).

[59]. M. Miyasaka, Proc. 68th JSCE Symposium, p.11, JSCE (1986).

[60]. F. Mansfeld: Applied Sciences, **203** (Electrochemical and Optical Techniques for the Study and Monitoring of Metallic Corrosion), p. 571-584. (1991).

[61]. Heng Chan Thoeun, Weather and Climate Extremes, **7**, p. 61–71 (2015).

[62]. Dara To, Tadashi Shinohara, Osamu Umezawa, Zairyo-to-Kankyo, **66**, No.4, p. 131-135 (2017)

[63]. D. de la Fuente, J. Alcántara, B. Chico, I. Díaz, J.A. Jiménez, M. Morcillo, Corrosion Science **110**, p. 253–264 (2016).

[64]. A.Raman, S. Nasrazadani, L. Sharma, Morphology of rust phases formed on weathering steels in various laboratory corrosion test, metallography, **22**, p. 79-96 (1989)

[65]. Ambient air quality standards in Asia survey report, <https://www.scribd.com/document/ 215141641/AQ-Standards-Report-Draft-2-Dec-FINAL> [July 28, 2016]

[66]. M. Morcillo," Atmospheric corrosion in Ibero-America: the MICAT project", Atmospheric corrosion ASTM International, p. 257-271(1995)

[67]. Belén Chico, Daniel de la Fuente, Iván Díaz, Joaquín Simancas and Manuel Morcillo, Annual Atmospheric Corrosion of Carbon steel Worldwide. An Integration of ISO CORRAG, ICP/UNECE, and MICAT Databases, Madrid, Spain (2017)

[68]. Le Thi Hong Lien, et al., Proc. JSCE Material and Environment 2016, p.280-284 (2016)

[69]. Tadashi Shinohara, Akira Tahara and To Dara, Proc. JSCE Material and Environment 2016, p.285-288 (2016)

[70]. Tadashi Shinohara, Yoji Hosoya, Wataru Oshikawa, ECS Transactions, Vol. 2004-14, pp. 121-132 (2004)

[71]. Annual Average Temperature Map, < https://commons.wikimedia.org/wiki/File:Annual_Average_Temperature_Map.jpg> [April 26, 2017].

[72]. 外川靖人、「大気の腐食性の分類システムに関する国際共同暴露試験（ISO CORRAG）について」、防錆管理、No.2、55-66（1993）

[73]. （財）日本ウェザリングテストセンター、「開発成果標準フォローアップ等標準化調査研究事業新発電関連要素機器の長期耐久性及び寿命予測の標準化に関する調査研究」、平成 17 年度（独）新エネルギー・産業技術総合開発機構委託成果報告書（2006）

[74]. L. T. H. Lien, P. T. San, "The effect of environmental factors on carbon steel atmospheric corrosion: The prediction of corrosion "Outdoor Atmospheric Corrosion, ASTM STP 1421, ed.H. E. Townsend ASTM International（2002, pp.103-108）

[75]. L. T. H. Lien, P. T. San, H. L. Hong, "Atmospheric corrosion of carbon steel in Vietnam, The relationship between corrosion rate and environmental parameters, The classification of atmospheric corrosivity of carbon steel", Zairyou-to-Kankyo 2009, A-305（2009）

Appendix I: Exponent *b* for Corrosion Thickness Loss Prediction (ISO 9224[23])

Table II-1 Time exponent values for predicting and estimating corrosion attack

Metal	B1	B2
Carbon steel	0,523	0,575
Zinc	0,813	0,873
Copper	0,667	0,726
Aluminium	0,728	0,807

Table II-2 Metal-environment-specific time exponents for standard metals (t^b)

	Steel		Zinc		Copper		Aluminium	
	B1	B2	B1	B2	B1	B2	B1	B2
b values	0,523	0,575	0,813	0,873	0,667	0,726	0,728	0,807
t (years)								
1	1,000	1,000	1,000	1,000	1,000	1,000	1,000	1,000
2	1,437	1,490	1,757	1,831	1,588	1,654	1,656	1,750
3	1,776	1,881	2,443	2,609	2,081	2,220	2,225	2,427
4	2,065	2,219	3,087	3,354	2,521	2,736	2,743	3,061
5	2,320	2,523	3,701	4,076	2,926	3,217	3,227	3,665
6	2,553	2,802	4,292	4,779	3,304	3,672	3,685	4,246
7	2,767	3,061	4,865	5,467	3,662	4,107	4,123	4,808
8	2,967	3,306	5,423	6,143	4,003	4,525	4,544	5,355
9	3,156	3,537	5,968	6,809	4,330	4,929	4,951	5,889
10	3,334	3,758	6,501	7,464	4,645	5,321	5,346	6,412
11	3,505	3,970	7,025	8,112	4,950	5,702	5,730	6,925
12	3,668	4,174	7,540	8,752	5,246	6,074	6,104	7,428
13	3,825	4,370	8,047	9,386	5,534	6,438	6,471	7,924
14	3,976	4,561	8,547	10,013	5,814	6,793	6,829	8,413
15	4,122	4,745	9,040	10,635	6,088	7,142	7,181	8,894
16	4,263	4,925	9,527	11,251	6,355	7,485	7,527	9,370
17	4,401	5,099	10,008	11,863	6,618	7,822	7,866	9,839
18	4,534	5,270	10,484	12,470	6,875	8,153	8,200	10,304
19	4,664	5,436	10,955	13,072	7,127	8,480	8,530	10,764
20	4,791	5,599	11,422	13,671	7,375	8,801	8,854	11,218
30	5,923	7,069	15,882	19,477	9,666	11,814	11,814	15,561
35	6,420	7,724	18,002	22,283	10,713	13,213	13,307	17,622
40	6,885	8,340	20,067	25,038	11,710	14,558	14,666	19,627
45	7,322	8,925	22,083	27,749	12,668	15,857	15,979	21,585
50	7,737	9,482	24,058	30,423	13,590	17,118	17,252	23,500
60	8,511	10,530	27,902	35,672	15,347	19,541	19,701	27,225
70	9,225	11,506	31,627	40,810	17,009	21,855	22,041	30,831
80	9,893	12,424	35,254	45,856	18,593	24,079	24,291	34,339
90	10,521	13,295	38,797	50,822	20,113	26,229	26,466	37,764
100	11,117	14,125	42,267	55,719	21,577	28,314	28,576	41,115

Appendix II: The E –Asia Joint Research Program

1. Project title: Corrosion Mapping of Structural Materials in Asian Area with Understanding Effects of Environmental Factors

2. Joint Research period: October 1, 2012 ～ March 31, 2016

3. Research Team:

- Japan team (up to 6 people including the Principal Investigator)

Funding period: October 1, 2012 ～March 31, 2016

Total Funded Amount (in Local Currency):17,992,000JPY

	Name	Position	Affiliation	Role in the project
PI	Tadashi Shinohara	Special Researcher	National Institute for Materials Science (NIMS)	General manager
Collaborator	Akira Tahara	Senior Researcher	NIMS	Analysis of exposure test results of carbon steel
Collaborator	Daisuke Mizuno	Senior Researcher	JFE Steel Co.	Analysis of exposure test results of galvanized steel
Collaborator	Sakae Fujita	Senior Fellow	JFE Techno-Research Co.	Summarizing exposure test results, collection of past exposure tests
Collaborator	Toshiyasu Nishimura	Chief Researcher	NIMS	Analysis of exposure test results of weathering steel
Collaborator	To Dara	Trainee	NIMS	Analysis of ACM sensors
Total number of participants including students: 7				

- Vietnam team（up to 6 people including the Principal Investigator）

Funding period: February 18, 2013 – June 30, 2016

Total Funded Amount (in Local Currency): 3,700,000,000VND

	Name	Position	Affiliation	Role in the project
PI	Le Thi Hong Lien	Senior Researcher	Institute of Materials Science (IMS)	General manager
Collaborator	Pham Thy San	Senior Researcher	IMS	Analysis of data and mapping corrosion
Collaborator	Hoang Lam Hong	Senior Researcher	IMS	Measurement of corrosion loss of samples, and analysis of ACM sensor
Collaborator	Nguyen Thi Thanh Nga	Researcher	IMS	Measurement of environmental factors
Collaborator	Nguyen Trung Hieu	Researcher	IMS	Measurement of environmental factors
Collaborator	Dao Chi Tue	Researcher	IMS	Perform the exposure tests
Total number of participants including students: 11				

- Thailand team (up to 6 people including the Principal Investigator)

Funding period: January 16, 2013 – January 16, 2016

Total Funded Amount (in Local Currency): 4,490,000 THB

	Name	Position	Affiliation	Role in the project
PI	Amnuaysak Chianpairot	Researcher	National Metal and Materials Technology Center (MTEC)	General manager
Collaborator	Ekkarut Viyanit	Senior Researcher	MTEC	Project advisor, troubleshooting, site survey
Collaborator	Wanida Pongsaksawad	Researcher	MTEC	Analysis of ACM and environmental data, linear regression model
Collaborator	Namurata Sathirachinda	Researcher	MTEC	Characterization of corrosion products, analysis of corrosion data
Collaborator	Siam Kaewkumsai	Principal Engineer	MTEC	Supervising student interns
Collaborator	Piya Khamsuk	Senior Engineer	MTEC	Measurement of environmental factors
Total number of participants including students: 9				

Appendix III: Corrosivity Classification of the Atmosphere (ISO 9223[26])

Table III-1 Category of corrosivity of atmospheres.

Category	Corrosivity
C1	Very low
C2	Low
C3	Medium
C4	High
C5	Very high
CX	Extreme

Table III-2: Corrosion rate, r_{corr}, for the first year of exposure for the different corrosivity categories.

Corrosivity category	Corrosion rates of metals r_{corr}				
	Unit	Carbon steel	Zinc	Copper	Aluminium
C1	g/(m^2·a)	$r_{corr} \leq 10$	$r_{corr} \leq 0{,}7$	$r_{corr} \leq 0{,}9$	negligible
	µm/a	$r_{corr} \leq 1{,}3$	$r_{corr} \leq 0{,}1$	$r_{corr} \leq 0{,}1$	—
C2	g/(m^2·a)	$10 < r_{corr} \leq 200$	$0{,}7 < r_{corr} \leq 5$	$0{,}9 < r_{corr} \leq 5$	$r_{corr} \leq 0{,}6$
	µm/a	$1{,}3 < r_{corr} \leq 25$	$0{,}1 < r_{corr} \leq 0{,}7$	$0{,}1 < r_{corr} \leq 0{,}6$	—
C3	g/(m^2·a)	$200 < r_{corr} \leq 400$	$5 < r_{corr} \leq 15$	$5 < r_{corr} \leq 12$	$0{,}6 < r_{corr} \leq 2$
	µm/a	$25 < r_{corr} \leq 50$	$0{,}7 < r_{corr} \leq 2{,}1$	$0{,}6 < r_{corr} \leq 1{,}3$	—
C4	g(m^2·a)	$400 < r_{corr} \leq 650$	$15 < r_{corr} \leq 30$	$12 < r_{corr} \leq 25$	$2 < r_{corr} \leq 5$
	µm/a	$50 < r_{corr} \leq 80$	$2{,}1 < r_{corr} \leq 4{,}2$	$1{,}3 < r_{corr} \leq 2{,}8$	—
C5	g/(m^2·a)	$650 < r_{corr} \leq 1\,500$	$30 < r_{corr} \leq 60$	$25 < r_{corr} \leq 50$	$5 < r_{corr} \leq 10$
	µm/a	$80 < r_{corr} \leq 200$	$4{,}2 < r_{corr} \leq 8{,}4$	$2{,}8 < r_{corr} \leq 5{,}6$	—
CX	g/(m^2·a)	$1\,500 < r_{corr} \leq 5\,500$	$60 < r_{corr} \leq 180$	$50 < r_{corr} \leq 90$	$r_{corr} > 10$
	µm/a	$200 < r_{corr} \leq 700$	$8{,}4 < r_{corr} \leq 25$	$5{,}6 < r_{corr} \leq 10$	—

NOTE 1 The classification criterion is based on the methods of determination of corrosion rates of standard specimens for the evaluation of corrosivity (see ISO 9226).

NOTE 2 The corrosion rates, expressed in grams per square metre per year [g/(m^2·a)], are recalculated in micrometres per year (µm/a) and rounded.

NOTE 3 The standard metallic materials are characterized in ISO 9226.

NOTE 4 Aluminium experiences uniform and localized corrosion. The corrosion rates shown in this table are calculated as uniform corrosion. Maximum pit depth or number of pits can be a better indicator of potential damage. It depends on the final application. Uniform corrosion and localized corrosion cannot be evaluated after the first year of exposure due to passivation effects and decreasing corrosion rates.

NOTE 5 Corrosion rates exceeding the upper limits in category C5 are considered extreme. Corrosivity category CX refers to specific marine and marine/industrial environments (see Annex C).

Dose-response functions for calculation the first-year corrosion loss of structural metal (ISO9223):

Use Equation (1) for carbon steel:

$$r_{corr} = 1{,}77 \cdot P_d^{0{,}52} \cdot \exp(0{,}020 \cdot RH + f_{St}) + 0{,}102 \cdot S_d^{0{,}62} \cdot \exp(0{,}033 \cdot RH + 0{,}040 \cdot T) \quad (1)$$

f_{St} = 0,150·(T – 10) when $T \leq$ 10 °C; otherwise –0,054·(T – 10)

N = 128, R^2 = 0,85

Use Equation (2) for zinc:

$$r_{corr} = 0{,}012\,9 \cdot P_d^{0{,}44} \cdot \exp(0{,}046 \cdot RH + f_{Zn}) + 0{,}017\,5 \cdot S_d^{0{,}57} \cdot \exp(0{,}008 \cdot RH + 0{,}085 \cdot T) \quad (2)$$

f_{Zn} = 0,038·(T – 10) when $T \leq$ 10 °C; otherwise, –0,071·(T – 10)

N = 114, R^2 = 0,78

Use Equation (3) for copper:

$$r_{corr} = 0{,}005\,3 \cdot P_d^{0{,}26} \cdot \exp(0{,}059 \cdot RH + f_{Cu}) + 0{,}010\,25 \cdot S_d^{0{,}27} \cdot \exp(0{,}036 \cdot RH + 0{,}049 \cdot T) \quad (3)$$

f_{Cu} = 0,126·(T – 10) when $T \leq$ 10 °C; otherwise, –0,080·(T – 10)

N = 121, R^2 = 0,88

Use Equation (4) for aluminium:

$$r_{corr} = 0{,}004\,2 \cdot P_d^{0{,}73} \cdot \exp(0{,}025 \cdot RH + f_{Al}) + 0{,}001\,8 \cdot S_d^{0{,}60} \cdot \exp(0{,}020 \cdot RH + 0{,}094 \cdot T) \quad (4)$$

f_{Al} = 0,009·(T – 10) when $T \leq$ 10 °C; otherwise –0,043·(T – 10)

N = 113, R^2 = 0,65

Table III-3: Parameters used in the derivation of Dose-response functions, including symbols, descriptions, intervals, and units.

Symbol	Description	Interval	Unit
T	Temperature	–17,1 to 28,7	°C
RH	Relative humidity	34 to 93	%
P_d	SO_2 deposition	0,7 to 150,4	mg/(m²·d)
S_d	Cl^- deposition	0,4 to 760,5	mg/(m²·d)
The sulfur dioxide (SO_2) values determined by the deposition method, P_d, and volumetric method, P_c, are equivalent for the purposes of this International Standard. The relationship between measurements using both methods may be approximately expressed as P_d = 0,8 P_c [P_d in mg/(m²·d), P_c in µg/m³].			
NOTE All parameters are expressed as annual averages.			

Appendix IV: Worldwide Atmospheric Corrosion Data

Table IV-1: MICAT Program: Atmospheric corrosion investigation in the Ibero-America [66].

Country	Site	Corrosion Rate (CR)		T	RH	TOW	SO_2	SO_2	Cl^-
		$g/m^2/year$	µm/year	°C	%	h/year	$mg/m^2/day$	$\mu g/m^3$	$mg/m^2/day$
Argentina	Camet	389.1	49.5	14.1	79	5974	0	0	55.1
	Iguazu	115.5	14.7	16.7	75	5063	9.2		0
	San Juan	44.8	5.7	20.6	76	5825	0	0	0
	Jubany	293.2	37.3	-2	84	2689	0	0	
	La Plata	220.9	28.1	17	78	5195	9.8	12.3	0
Brazil	Caratina	87.2	11.1	21.5	74	4222	1.25	1.6	8.92
	Ipatinga	388.3	49.4	23.8	89	4222	23	28.8	6.84
	Arrial do Cabo	1300	165.4	24.8	77	5098	6.39	8	234
	Cubatao	1249.7	159	22.7	73	5072	54.5	68.1	8.14
	Ubatuba	2372.9	301.9	21.9	78	5072	2.56	3.2	113.2
	Sao Paulo	161.9	20.6				57.8	72.3	
	Rio de Janeiro	872.5	111	20.1	80	5238	43.48	54.4	16.4
	Belem	152.5	19.4	26.1	88	5974			
	Fortaleza	929.8	118.3	26.6	72	4380			>300
	Brasilia	101.4	12.9	20.4	69	3872			
	Paulo Afonso	136	17.3	25.9	77	1507			
	Paorto Velho	38.5	4.9	26.6	90				
Colombia	Isla Naval	263.5	33.53	27.6	85	8664	10.3	12.9	60.7
	San Pedro	133.6	17	9.6	98	8760	0.56	0.7	0
	Cotove	154.1	19.6	27	76	2891	0.33	0.4	0
Costa Rica	Puntarenas	263.5	33.53	27.6	85	8664	10.3	12.9	60.7
	Limon	133.6	17	9.6	98	8760	0.56	0.7	0
	Arenal	544.7	69.3	22.9	88	7341	4.05	5.1	20.62
	Sabanilla	130.5	16.6	18.9	83	6088	235	2.9	12.08
Cuba	Ciq	283.7	36.1	25.2	80	5002	29.73	37.2	13
	Conjimar	3074	391.1	25.2	79	5002	23.24	29.1	96.9
	Bauta	265.7	330.8	24	81	5002	18	22.5	7.34

Chile	Cerrillos	285.3	36.3	14.2	71	3469	20	25	4.48
	Valpariaiso	279	35.5	14	82	6675	23.63	29.5	10
	Idiem			12.2	82	6675	43.3	54.1	16.83
	Petrox	1314.2	167.2	12.2	82	6141	65.16	81.5	12.8
	Marsh	189.4	24.1	-2.3	85	4669	6.46	8.1	
	Isla de Pascua	235.8	30	20.5	79		1.15	1.4	
Ecuador	Guayaquil	177.6	22.6	26.1	71	4853	3	3.8	1.49
	Riobamba	66	8.4	12.9	66	3583	1	1.3	0.4
	Salinas	435.4	55.4	23	78	6798	2.27	2.8	4.31
	Esmeraldas	617.8	78.6	26.8	78	6220	16.48	20.6	2.7
	San Cristobal	271.2	34.5	24.6	80		1.05	1.3	25.01
Spain	Leon	163.5	20.8						
	EI Pardo	88.8	11.3						
	Barcelona, E	136.8	17.4						
	Tortosa	158.8	20.2						
	Granada	66.8	8.5						
	Lagoas	221.7	28.2						
	Labastiada	117.9	15						
	Arties	30.7	3.9						
Mexico	Mexico	76.2	9.7	16	62	2523	13.6	17	0
	Cuernavaca	105.3	13.4	21	56	1664	7.9	17	0
	San Luis Potosi	244.4	31.1	18	51	0	18.9	23.6	0
	Acapulco	173.7	22.1	27.6	76	5010	9.6	12	23
Panama	Panama	216.9	27.6	26.9	71	5010	21.7	27.1	9.76
	Colon	848.9	10.8	27	77	6605	47.44	59.3	16.76
	Veraguas	157.2	20	27.2	70	4993	16.54	20.7	14.84
	Chiriqui	180.8	23	27	68	4652	8.21	10.3	8.71
Peru	Piura	143.8	18.3	24.5	67	2400		0	
	Villa Salvador	275.9	35.1	19.1	84	7332	18	22.5	38
	San Borja	242.1	30.8	19.2	84	6666	29	36.3	20
	Arequipa	121	15.4	15.6	34	228	0	0	0
	Cuzco	11	1.4	12.2	67	2847	0	0	0
	Pucallpa	112.4	14.3	25.6	84	5037	0	0	0
Portugal	Leixoes	569.1	72.4						
	Sines	2869.7	365.1						
	Pego	224	28.5						
Uruguay	Trinidad	52.7	6.7	16.8	74	5133	0.7	0.9	1.5
	Prado	261.7	33.3	17	76	4424	12.1	15.1	10.8
	Melo	110.8	14.1	17.4	80	5747	0.4	0.5	2.5
	Artigas	517.2	65.8	-1.7	91	3101	0	0	159.4
	Punta del Este	416.6	53	16.5	78	5580	3.95	4.9	143.5

Venezuela	EI Tablazo	23.03	29.3	27.7	77	4415	6.01	7.5	63.33
	Punto Fijo	168.2	21.4	27.1	78	4958	3.69	4.6	32
	Coro	116.3	14.8	27.4	76	4695	3.82	4.8	29
	Matangas	180.8	23	27.6	78	4721	9.33	4.8	29
	Barcelona, V	145.4	18.5	27	78	4380	2.05	2.6	25.2
	Puerto Cabello	293.2	37.3	27.2	85	5405	0	0	

Table IV-2: ISO CORRAG Program [72]

Country	Sites	Corrosion Rate (CR)		TOW	SO_2	SO_2	Cl^-
		g/m^2/year	µm/year	h/year	mg/m^2/day	$\mu g/m^3$	mg/m^2/day
Belgium	Oostende	780.5	99.3	6084	19.2	24	173
Czech	Kasperske Hory	204.4	26	3622	13.52	16.9	3.3
	Praha	372.6	47.9	2311	53.68	67.1	3.4
	Kopisty	555.7	70.7	2427	71.52	89.4	2.8
Finland	Helsinki	261.7	33.3	3578	15.12	18.9	4
	Otaniemi	201.2	25.6	3409	12.16	15.2	2.8
	Ahtari	100.6	12.8	3105	3.36	4.2	3.2
France	St. Denis	292.4	37.2	4268	38.68	49.6	27.8
	Ponteau Martigues	569.1	72.4	3815	69.6	87	241
	Picherande	126.5	16.1	4171	7.12	8.9	6.5
	St. Remy	338.8	43.1	6310	24.24	30.3	378
	Sain de giraud	573.8	73	3422	31.76	39.7	184
	Paris	327.8	41.7	3189	42.72	53.4	
	Adby	835.5	106.3	4571	127.6	159.5	17.8
	Biarritz	687	87.4				193.5
Germany	Bergisch Gladbach	284.5	36.2	4269	14.8	18.5	1.9
Norway	Oslo	198.1	25.2	2641	10.64	13.3	2.1
	Borregaard	485	61.7	3339	35.36	44.2	9.1
	Birkenes	154.8	19.7	4138	0.992	1.24	1
	Tananger	468.5	59.6	4583	3.2	4	301.3
	Bergen	219.3	27.9	4439	6.96	8.7	7
	Svanvik	158.8	20.2	2653	13.36	16.7	0.5
Spain	Madrid	217.7	27.7	2060	32.4	40.5	
	EI Pardo	121.8	15.5	3223	3.92	4.9	
	Lagoas	211.4	26.9	2840	39.2	49	21.2
	Baracaldo	345.1	43.9	4375	24.56	30.7	29.2
Sweden	Stockholm	191.8	24.4	3116	8.16	10.2	
	Kattesand, Bohus Malmon	276.7	35.2	4027	4.24	5.3	85.5

	Kvarnvik, Bohus Malmion	484.2	61.6	4027	4.24	5.3	667
UK	Stratford	304.2	38.7	5142	15.92	19.9	15.1
	Fleet Hall	306.5	39	4864	13.2	16.5	
	Rye	459.8	58.5		16.96	21.2	300
	Crowthorne	294	37.4	6019	12.88	16.1	5.4
Georgia	Batumi	225.6	28.7	3216	21.04	26.3	1
Russia	Murmansk	246	31.3	3227	4	5	19.9
	Vladivostok	203.6	25.9	3920	21.04	26.3	19.4
	Oymyakon	6.3	0.8	385	4	5	0.8
Japan	Tokyo	310.5	39.5	2173	11.68	14.6	4.8
	Choshi	340.3	43.3	5706	6.16	7.7	66.8
	Okinawa	591.1	75.2	3903	8.88	11.1	130
	Ohigawa-oki	380.4	48.4		26.32	32.9	396
New Zealand	Judgeford	155.6	19.8				
Argentina	Iguazu	45.6	5.8	5626	9.6	12	
	Camet	355.3	45.2	6216	9.6	12	47.2
	Buenos Aires	115.5	14.7	4560	9.44	11.8	
	San Juan	36.2	4.6	912	9.6	12	
	Jubany	299.5	38.1	2791	0.8	1	16.8
Canada	Boucherville	188.6	24	2453	12.64	15.8	59
US	Kure Beach	297.9	37.9	4289	7.68	9.6	184
	Newark	207.5	26.4	2060	26	32.5	
	Point Reyes	289.2	36.8	3905		6.1	
	Los Angeles	168.2	21.4	3690	8.08	10.1	
	Research Triangle Park	181.6	23.1				
	Panama Canal Zone	2931.8	373	7598		51.5	619

Table IV-3: Atmospheric corrosion data in Japan [73]

Prefecture	Corrosion Rate		T (ºC)	RH (%)	TOW	SO_2*	SO_2*	Cl^-*
	g/m²/year	µm/year			h/year	mg/m²/day	µg/m³	mg/m²/day
Asahikawa	127.7	16.2	6.9	77	3658	3.12	3.9	0.56
Kushiro	272.5	34.7	6.6	75	3359	10.95	13.7	18.02
Saporo	155.9	19.8	9.1	68	2635	7.7	9.6	13.65
Akita	252.1	32.1	12.1	73	3744	4.05	5.1	51.01
Yamagata	137	17.4	12	75	4093	2.32	2.9	2.5
Niigata	200.5	25.5	14.2	69	3194	4.92	6.2	24.8
Takaoa	221.3	28.2	14.4	73	3887	3.3	4.1	8.98
Kyoto	114.6	14.6	16.3	63	2363	2.66	3.3	3.82
Yonago	203.4	25.9	15.5	72	3632	2.74	3.4	12.53
Morioka	135	17.2	10.4	72	3233	2.16	2.7	6.1
Sendai	177.4	22.6	12.5	72	3402	1.72	2.2	3.79
Tsukuba	176.8	22.5	15.9	76	4370	3.22	4	1.23
Choshi	316.2	40.2	14.4	78	4629	4.6	5.8	14.96
Tokyo	147.6	18.8	16.6	59	1841	6.03	7.5	4.13
Yamanakako	146.3	18.6	11.1	72	3402	2.01	2.5	0.91
Shimizu	247.9	31.5	16.9	69	2758	5.15	6.4	2.46
Kariya	150.5	19.1	16.3	66	2654	4	5	3.94
Izumi	160.4	20.4	17.4	63	2411	3.43	4.3	2.69
Kochi	194.8	24.8	17.5	68	3020	5.34	6.7	3.68
Fukuyama	159.1	202	15.9	69	3284	4.45	5.6	1.14
Omura	160.5	20.4	17.5	68	3020	4.4	5.5	8.02
Hayato-Cho	217.7	27.7	18.9	67	3020	3.7	4.6	2.79
Nishibara-Machi	376.6	47.9	23.2	70	3444	2.83	3.5	23.46
Miyakochima	981.9	124.9	23.7	79	5409	3.29	4.1	34.4
Miyakochima kaigan	3221.2	409.8	23.7	79	5409	15.68	19.6	113.05

Table IV-4: Atmospheric corrosion of Vietnam [74], [75].

Province	Corrosion Rate		T (°C)	RH (%)	TOW	Cl^-	Exposure Test
	$g/m^2/year$	µm/year			h/year	$mg/m^2/day$	
Hanoi	240.36	30.6	24.1	81.3	4697	0.64	1995
Do Son	290.7	37	23.6	86.1	6359	30.5	1995
Da Nang	264.64	33.7	25.9	83.1	5672	3.08	1995
Nha Trang	254.23	32.3	26.7	80.8	4651	19.3	1995
HCM City	191.92	24.4	27.7	75.6	4205	1.22	1995
Vong Tau	191.23	24.3	27.5	79.3	4495	13.58	1995
Son Tay	289.74	36.9	23.4	86.3	6451	0.56	1995
Do Son	297.74	37.9	23.3	86.1	6081	17.51	2003
Hai Duong	287.52	36.6	23.5	85.9	6226	6.89	2003
Hanoi	249.71	31.8	24.1	79.8	4917	2.24	2003
Thanh Hoa	242.95	30.9	23.9	84.7	6158	3.48	2003
Quang Ninh	255.76	32.5	24.8	82.6	5604	10.28	2003
Hue	247.567	31.5	24.6	85.89	6001	1.33	2003
Da Nang	264.65	33.7	25.8	83.3	5701	4.99	2003
HCM City	190.53	24.2	27.7	75.6	4205	4.58	2003
Vong Tau	205.77	26.2	27.4	79.4	4400	16.5	2003
Tieng Giang	166.05	21.1	27	81	5086	8.9	2002
Tieng Giang	186.35	23.7	27	83	5543	8.9	2005
Hanoi	181.85	23.1	24.7	79	4661	1.8	2002
Hanoi	226.75	28.8	24.5	78	4435	1.76	2005
CHM city	163.65	20.8	28.3	74	3467	3.06	2002
CHM city	138.75	17.7	28	77	4157	2.66	2005